

92
NASA CR-132318

FINAL REPORT

SINK-FLOAT FERROFLUID SEPARATOR
APPLICABLE TO
FULL SCALE NONFERROUS SCRAP SEPARATION

Contract No. NAS 1-11793

Prepared for

National Aeronautics and Space Administration
Langley Research Center
Langley Station
Hampton, Virginia 23365

Prepared by

Avco Systems Division
Lowell Industrial Park
Lowell, Massachusetts 01851



NASA-CR-132318) SINK-FLOAT FERROFLUID
SEPARATOR APPLICABLE TO FULL SCALE
NONFERROUS SCRAP SEPARATION Final
Report, 28 Jun. 1972 - 28 (Avco Corp.,
Lowell, Mass.) 130 p HC \$8.50 CSCL 13H

N74-11303

Unclas
G3/15 22614

FINAL REPORT

SINK-FLOAT FERROFLUID SEPARATOR
APPLICABLE TO
FULL SCALE NONFERROUS SCRAP SEPARATION

Contract No. NAS 1-11793

Prepared for

National Aeronautics and Space Administration
Langley Research Center
Langley Station
Hampton, Virginia 23365

Prepared by

Avco Systems Division
Lowell Industrial Park
Lowell, Massachusetts 01851

TABLE OF CONTENTS

<u>Section</u>	<u>Title</u>	<u>Page No.</u>
	SUMMARY	S-1
I	INTRODUCTION	1
	A. Ferrofluid Levitation	1
	B. Structure of the Car Scrapping Industry	6
	1. Sources of Automobiles for Recycling	6
	2. Processing of Scrap Automobiles	8
	3. Automobile Shredding Process	10
	4. Nonferrous Metal Recovery from Shredded Automobiles	10
	a. Hand-Picking	14
	b. Heavy Media Plants	14
	c. Sweat Separation	15
	5. Economics of Nonferrous Metal Recovery	15
	C. Program Plan	17
II	RESULTS	20
	A. Magnet Construction and Evaluation	20
	B. Materials Handling System (Separator)	21
	C. Behavior of Single Objects and Model Mixture	35
	1. Single Objects	35
	2. Model Mixture Separations	39
	D. Separation of Car Scrap	44
	1. Scrap Properties	44
	2. Scrap Pretreatment	46

TABLE OF CONTENTS (Continued)

<u>Section</u>	<u>Title</u>	<u>Page No.</u>
	3. Scrap Separations	46
	a. Procedures	46
	b. Aluminum-Zinc Separation (Stage A)	47
	c. Zinc-Copper Separation (Stage B)	47
	d. Non-Metal-Aluminum Separation (Stage C). .	51
	e. Copper-Steel Separation (Stage D)	51
	E. Ferrofluid Recovery	56
III	PROCESS DESIGN	57
	A. Basis for the Plant Design	57
	1. Scrap Supply	57
	2. Feed Preparation	58
	a. Reshredder	61
	b. Air Classifier	61
	c. Magnetic Separators	62
	3. Separations to be Made.	62
	4. Separator	64
	5. Ferrofluid Recovery.	64
	B. Basis for the Cost Estimates	67
	1. Capital Cost	67
	a. Magnet Costs	67
	b. Conveyor Costs	67
	c. Feed Bins	69
	d. Ferrofluid Recovery Module	69

TABLE OF CONTENTS (Concluded)

<u>Section</u>	<u>Title</u>	<u>Page No.</u>
	2. Operating Costs	75
	a. Operating Labor	75
	b. Maintenance	75
	c. Supplies	75
	d. Utilities	75
	e. Insurance	76
	3. Profitability	76
	C. Plant Design	76
	1. Batch Plant	76
	2. Continuous Plant	85
	D. Discussion.	85
	E. Ecological Considerations	91
IV	CONCLUSIONS AND RECOMMENDATIONS	93
V	REFERENCES	95
APPENDIX A	THEORETICAL ESTIMATE OF SEPARATION RATE IN FERROFLUID SINK-FLOAT SEPARATOR	A-1
APPENDIX B	MAGNET DESIGN	B-1
APPENDIX C	FACTORS FOR ESTIMATING PLANT CAPITAL COSTS	C-1

LIST OF ILLUSTRATIONS

<u>Figure</u>	<u>Title</u>	<u>Page No.</u>
1	Magnetization Curve of a Kerosene Base Ferrofluid . . .	2
2	Forces on a Non-Magnetic Solid Body Immersed in a Ferrofluid	4
3	Ball of Copper Floating in Ferrofluid Suspended in the Gap of a Magnet	5
4	Flow Diagram for Ferrofluid Sink/Float Solid Separation Process	7
5	Typical Flow of Discarded Automobiles through Automobile Scrap Industry	9
6	Typical Process Flow at Automobile Shredder Plant . . .	11
7	Automobile Shredder Plant and Ferrous Metal Output System	12
8	Automobile Shredder Plant and Nonferrous Metal Output System	13
9	Projected Metal Supply from Automobile Shredding in 1975	18
10	Variation of H_x with Distance from Mirror Plate	22
11	Variation of H_y with Distance from Axis	23
12	Magnetic Field on Vertical Axis of Symmetry of Gap . .	24
13	Vertical Magnetic Gradient on Vertical Axis of Symmetry of Gap	25
14	Model Separator with Cover Plate Removed.	26
15	Model Separator in Laboratory Magnet.	27
16	Sketch of Separator	29
17	Top View of Separator	30
18	Product Removal Conveyors	31
19	Feed Conveyor	32
20	Ferrofluid Separator during Assembly	33

LIST OF ILLUSTRATIONS (Concluded)

<u>Figure</u>	<u>Title</u>	<u>Page No.</u>
21	Modified Floats Conveyor	34
22	Modified Feed Conveyor - Assembled View	36
23	Modified Feed Conveyor - Partly Disassembled	37
24	Separation System	38
25	Magnetization of Ferrofluid FF 1135	40
26	Release Points for Scrap Pieces	42
27	Feed Preparation Sequence	60
28	Nonferrous Metal Separation System Material Balance . .	63
29	Ferrofluid Recovery System	66
30	Estimated Price of Vibratory Conveyors	68
31	Feed Bin Configuration	70
32	Estimated Price of Feed Hoppers	71
33	Estimated Price of Solvent Recovery Stills	73
34	Estimated Price of Entire Ferrofluid Recovery Module . .	74
35	Eight Hour Material Balance - Batch Plant	77
36	Equipment Layout - Batch Plant	78
37	One Hour Material Balance - Continuous Plant	86
38	Equipment Layout - Continuous Plant	87
A-1	Schematic of Separator	A-4
B-1	Hyperbolic Poles	B-2
B-2	Constant Gradient Poles (Front View).	B-3
B-3	Constant Gradient Poles (Side View)	B-4
B-4	Constant Gradient Magnet (Front View)	B-6
B-5	Constant Gradient Magnet (Side View Along Section A-A) .	B-7
B-6	Power Requirements of Magnets	B-10

LIST OF TABLES

<u>Table</u>	<u>Title</u>	<u>Page No.</u>
S-1	Materials in Nonferrous Portion of Car Scrap	S-3
I	Nonferrous Metals Present in Average Automobile as Manufactured and as Processed by Shredder, and Potential Scrap Value	16
II	Effect of Shape	41
III	Effect of Size	43
IV	Effect of Release Point	43
V	Separation of Zinc Alloy and Brass	44
VI	Materials in Nonferrous Portion of Car Scrap	45
VII	Effect of Apparent Density on Zinc Separation	48
VIII	Effect of Fluid Magnetization on Zinc Recovery	49
IX	Effect of Processing Rate on Zinc Purity	50
X	Effect of Processing Rate on Aluminum Purity	52
XI	Effect of Apparent Density on Copper Alloy/Steel Separation	53
XII	Effect of Fluid Magnetization on Copper Alloy/Steel Separation	54
XIII	Separation of "Non-Magnetic" Copper and Steel Alloys	55
XIV	Composition of Non-Magnetic Residue of Automobile Shredding	57
XV	Nonferrous Metal Content of Average Shredded Automobile	58
XVI	Nominal Composition of Mixed Nonferrous Metals	61
XVII	Basis for Process Design-Experimentally Obtained Separation Results	62
XVIII	Capacities of Separators	65

LIST OF TABLES (Concluded)

<u>Table</u>	<u>Title</u>	<u>Page No.</u>
XIX	Size of System Components-Solvent Recovery	65
XX	Costs of Piano Hinge Conveyors	69
XXI	Ferrofluid Recovery Module-Cost of Pumps and Tanks . .	72
XXII	Ferrofluid Recovery Module-Cost of Stills	72
XXIII	List of Feed Bins - Batch Plant	79
XXIV	List of Conveyors - Batch Plant	80
XXV	Capital Costs - Batch Plant	81
XXVI	Operating Costs - Batch Plant One Shift Per Day	82
XXVII	Operating Costs - Batch Plant Two Shifts Per Day . . .	83
XXVIII	Operating Costs - Batch Plant Three Shifts Per Day . . .	84
XXIX	List of Conveyors - Continuous Plant	88
XXX	Capital Costs - Continuous Plant	89
XXXI	Operating Costs - Continuous Plant	90
XXXII	Potential Energy Savings in 1975 Due to Recovery of Nonferrous Metals	92
B-I	Magnetic Characteristics	B-8
C-I	Direct Cost Elements	C-2
C-II	Indirect Cost Elements	C-3
C-III	Plant Building Costs	C-4
C-IV	Comparison of Cost Ratios Derived by Two Cost Estimating Methods	C-5

Symbols Used in Text*

M	- magnetization - emu
M_{sf}	- saturation magnetization of ferrofluid - emu
M_s	- magnetization of object immersed in ferrofluid - emu
M^*	- saturation magnetization of colloidal particles -emu
M_f	- magnetization of ferrofluid - emu
F'_M	- magnetic body force per volume of ferrofluid
F_M	- magnetic body force per volume of immersed object
H	- magnetic field strength - oersted
F_g	- gravitational force per volume on object immersed in ferrofluid
H_x	- horizontal component of magnetic field strength
H_y	- vertical component of magnetic field strength
G	- magnetic field gradient
g	- acceleration of gravity
ϵ	- volume fraction of dispersed phase
ρ_s	- density of object immersed in ferrofluid
ρ_f	- density of ferrofluid
ρ_{af}	- apparent density of ferrofluid
ρ_{as}	- apparent density of object immersed in ferrofluid
Γ	- magnetic field gradient on vertical axis of symmetry of interpole volume

*Symbols used in Appendices are defined where used.

SUMMARY

This report describes the work carried out by Avco under NASA Contract No. NAS 1-11793 to build a ferrofluid levitation separator for recovering nonferrous metals from shredded automobiles, to evaluate the separator and to project the economics of this separation process to industrial scale. This program demonstrates the application of aerospace technology, ferrofluids, to an important problem in solid waste management.

The scrap separator consists of:

1. An electromagnet designed to generate a region of constant apparent density within a pool of ferrofluid held between the magnet poles, over a working volume of 20 cm x 20 cm x 20 cm. A kerosene base ferrofluid, with 500 gauss saturation magnetization, will have an apparent density of nearly 12 g/cm³ when the magnet is operated at a maximum power input 63 KW which generates a field gradient of 250 oe/cm. This density level is sufficient to float all common industrial metals of interest.
2. Conveyors for introducing into the ferrofluid the scrap to be separated. Objects less dense than the apparent density of the ferrofluid float to the top of the ferrofluid pool where they are removed by an upper conveyor while those more dense sink and are removed by a lower conveyor. The separation process is thus continuous. Since magnetic forces also retain the ferrofluid in the gap of the magnet, conveyors can be introduced directly into the pool without fluid leakage or sealing problems. The conveyors of the materials handling system have been found capable of moving typical automobile scrap at rates over 5000 lb/hr.

The behavior of the non-magnetic objects within the separator has been found to be essentially a function of density and independent of the size or shape of the objects. There was close agreement (better than 10%) between the density of an object and the apparent density of the ferrofluid required to float it, for objects ranging in size from 5 cm to 0.6 cm on a side, and of widely different shapes.

The separation of well characterized scrap mixtures was evaluated in the separator in order to obtain information on the effects of operating parameters on the purity of the recovered fractions. Mixed pieces of a zinc alloy ($\rho = 6.6 \text{ g/cm}^3$) and of brass ($\rho = 8.5 \text{ g/cm}^3$) fed, at a rate of 3700 lbs/hr, into a ferrofluid pool with an average apparent density of 7.9 g/cm³ were completely separated into two pure metal fractions. An increase in feed rate to 5100 lbs/hr resulted in only a slight decrease in product purity. These test results demonstrate conclusively that very high separation rates are achievable by ferrofluid sink-float separation. With optimal adjustment of operating parameters, the separation is virtually error free.

The principal materials present in the "nonferrous" portion of car scrap, and their physical properties are listed in Table I which also lists the range of potential values for the pure recovered nonferrous metals. Zinc has the highest potential total value, followed by copper and aluminum, and stainless steel has the lowest total value. In this program most emphasis was accordingly placed on zinc separation and least on the separation of stainless steel.

Mixed nonferrous scrap, reshredded to a size of 3 inches or less, and containing less than 10% non-metals and magnetic metals, as typically produced by an air classifier or by water elutriation, was found to be a suitable feed for the ferrofluid separator. The most effective method of processing this scrap by the ferrofluid method is first to separate aluminum and non-metals from zinc and heavier metals. Zinc is then removed from the heavier metals (copper and stainless steel) and aluminum from the non-metals.

It was possible to recover a high yield of essentially pure aluminum and zinc alloys from mixed, reshredded automobile scrap. When the separator was operated at its nominal design capacity of 1 ton/hour, over 91% of the zinc was recovered as a product that contained 99.7% zinc alloy and over 95% of the aluminum was recovered as a product that contained 99.7% aluminum alloy. In each instance, the major impurity was copper wire which is not harmful. Samples of these materials have been sent to smelters for analysis, and each fraction has been reported to be well within specification limits and of a purity which can command a premium price on the secondary metals market.

The recycling of solid wastes, in general, is a formidable problem largely because of the low intrinsic value of the discarded material, which makes its processing economically unattractive. Junk automobiles, however, are high value solid waste because of their high metals content. The 8 million cars discarded annually contain about 650,000 tons of nonferrous metals which are not now being fully recovered and recycled, for lack of an efficient process to do so. The potential worth of the discarded nonferrous metals ranges for \$6 to \$11 per car, depending on the market price of the metals.

Based upon the separation test data obtained during the experimental phase of the program, as well as the successful recycling of ferrofluid recovered from scrap, the recovery of nonferrous metals from automobile scrap promises to be a profitable process. The effect of the method of operation (batch versus continuous) and plant capacity on capital and operating costs was analyzed. A small batch plant capable of processing 2,000 tons of scrap per year (equivalent to 300 cars/day), would require a capital investment of about \$360,000 and payout time of 2.8 years, assuming a conservative added value of \$150/ton to the processed material. A continuous plant capable of processing 25,000 tons/yr of scrap per year would require a capital investment of \$925,000, but would have an extremely attractive payout time of only 0.6 years.

The ferrofluid separation process for nonferrous metal scrap described above has important ecological impact. There would be greater economic incentive to recover abandoned automobiles. Recycling of the recovered metals would result in a net reduction in the electrical energy requirements of the Nation by over five billion kwh/yr. The process should also be applicable to the recovery of nonferrous metals from municipal waste and should be able to defray in part the costs of the overall process.

TABLE S-1

MATERIALS IN NONFERROUS PORTION OF CAR SCRAP*

<u>Material</u>	<u>Approximate Range of Physical Densities g/cm³</u>	<u>Estimated Content of Avg Shredded Auto (lbs)</u>	<u>Potential Value Per Car</u>	
			<u>Min</u>	<u>Max</u>
Non-metals	1.00 to 2.60	6	-	-
Aluminum Alloys	2.65 to 2.75	10	1.00	1.40
Zinc Alloys	6.60 to 6.70	40	2.80	7.20
Copper Alloys	8.30 to 8.90	5	1.50	2.00
Stainless Steel	7.80 to 8.00	<u>2</u>	<u>0.20</u>	<u>0.36</u>
		Total 63 lbs	\$5.50	\$10.96

Weighed average value of mixed metals \$0.096 to \$0.192 - per lb
 \$192 to \$384 - per ton

*Data summarized from Table I.

I. INTRODUCTION

This report describes the work carried out by Avco under NASA Contract No. NAS 1-11793 to build a ferrofluid levitation separator for recovering nonferrous metals from shredded automobiles, to evaluate the separator and to project the economics of this separation process to industrial scale. This project was carried out in the period June 28, 1972 to June 28, 1973 by the Avco Systems Division at Lowell, Massachusetts.

A. Ferrofluid Levitation

The separation of nonferrous metals by the ferrofluid levitation process uses these magnetic liquids in a suitable magnetic field to float or levitate non-magnetic objects having a higher density than the ferrofluid. By opposing the normal gravitational force on an object with this levitating force, it is possible to separate objects of different densities; the less dense objects float in the ferrofluid pool while the denser objects sink. By this method it is possible to separate nonferrous metals of different densities from each other.

In search of a simple means of simulating the effect of reduced gravity on nucleate boiling of a liquid, Papell of NASA Lewis Research Center observed that he could suspend an oleic acid stabilized dispersion of subdomain magnetite in the gap of an electromagnet. While colloidal magnetic materials have been known for a long time, this was the first time that these colloidal suspensions were considered as an apparently magnetically responsive liquid continuum^{(1, 2)*}. The impact of Papell's work is that while it is theoretically possible to consider the existence of a homogeneous ferromagnetic liquid⁽³⁾, no such liquid is known to exist in spite of extensive attempts at its preparation^(4, 5). These colloidal dispersions also known as ferrofluids are, therefore, a unique class of liquids in which it is possible to induce substantial magnetic forces resulting in liquid motion⁽⁶⁾.

Ferrofluids are very stable suspensions of single domain magnetic particles. The suspended particles are so small (typically less than 150 Å) that they do not settle under gravity or interact even in the presence of a strong magnetic field. The magnetic response of a ferrofluid results from the coupling of individual particles with a substantial volume of the bulk liquid. This coupling is facilitated by a stabilizing agent which adsorbs on the particle surface and is also solvated by the surrounding liquid.

The magnetic properties of a ferrofluid can best be described by considering the particles in a ferrofluid to behave as an assembly of non-interacting magnets⁽⁷⁾. In the absence of a magnetic field their moments are randomly oriented and the ferrofluid has no net magnetization. In a magnetic field, the particle moments tend to align with the field resulting in a net induced fluid magnetization, M . The magnetization increases with increasing field until a saturation value is observed as shown in Figure 1. Under these conditions the particle moments are all aligned in the direction of this applied field. The saturation magnetization of the ferrofluid, M_{sf} , is given by

$$M_{sf} = \epsilon M^* \quad (1)$$

*Superscripts refer to References listed on page 95.

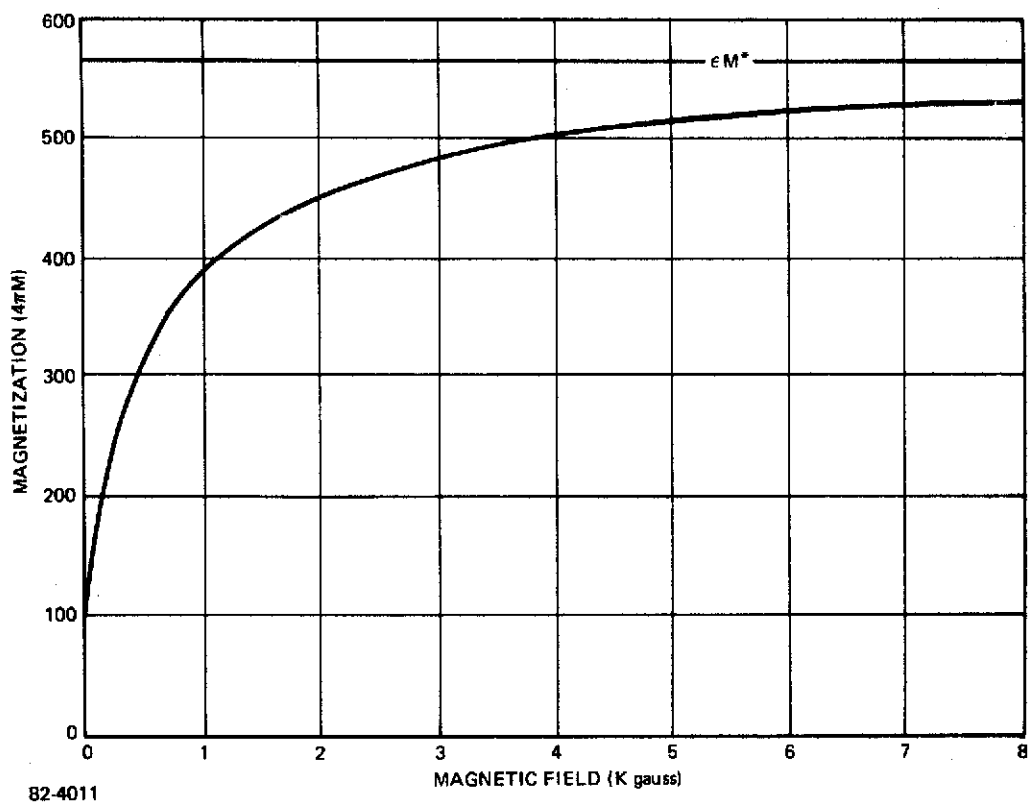


Figure 1 MAGNETIZATION CURVE OF A FERROFLUID

where ϵ is the volumetric concentration of magnetic colloid and M^* is the effective saturation magnetization of the colloidal particles. As soon as the magnetic field is removed, the particle moments become randomly oriented again because of thermal motion. The ferrofluid, therefore, has no residual magnetization and does not exhibit hysteresis.

Because the particles do not interact, a ferrofluid remains a liquid in a magnetic field. A minor increase in viscosity (which can be made as small as desired) is noted because of the interaction of the particles with the field. It is to be emphasized that ferrofluids are very different from classical magnetic clutch fluids which become solid in a magnetic field, because they are composed of micron size particles which do interact when aligned by the field.

A ferrofluid placed in a non-homogeneous magnetic field experiences a net magnetic force which tends to drive it, like all magnetizable objects, towards regions of highest magnetic field intensity. The magnetic body force, F'_M , per unit volume of fluid, V , is proportional to the induced magnetic dipole moment, M , and to the applied field gradient ∇H (6):

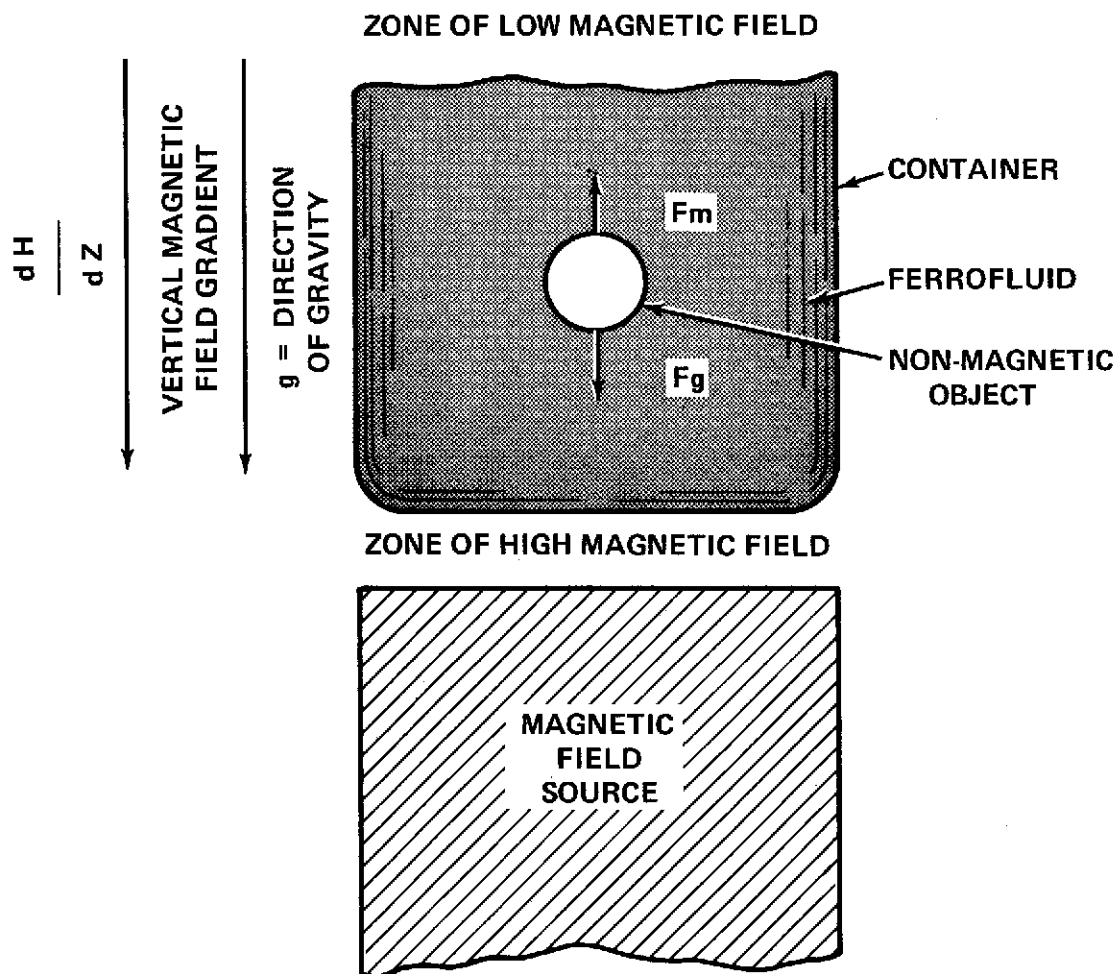
$$F'_M = M \nabla H \text{ dynes/cm}^3 \quad (2)$$

When a non-magnetic object is immersed in a ferrofluid in the presence of a magnetic field gradient, as shown in Figure 2, there is a magnetic force, F_M , on the object which tends to expel it to a region of minimum field. This magnetic body force is equal to, but opposite in sign to F'_M defined above(8). If the magnetic field gradient is parallel to the direction of gravity, the magnetic body force can be used to cancel the gravitational body force, F_g , on a non-magnetic object immersed in a ferrofluid. Consequently an object of high density can float in a ferrofluid of low density when $F_M > F_g$. F_g is given by Archimedes' Law:

$$F_g = (\rho_s - \rho_f) g \quad (3)$$

This effect is shown in Figure 3 where a copper ball with a density, ρ_s of 8.90 gr/cm³, floats on a ferrofluid with a density ρ_f of 1.14 gr/cm³, placed in a gradient field of 1500 oe/cm, established by the tapered poles of a permanent magnet. The fluid magnetization, $4\pi M$, is 200 gauss. In this case, the product $M \nabla H$ (24,000 dynes/cm³) is high enough to float even the densest metal, osmium, which has a density of 22.48 gr/cm³.

When the object immersed in the ferrofluid is not totally non-magnetic the above treatment needs to be modified somewhat. The details of this modification are discussed in Appendix A. If the magnetic dipole moment of this object is smaller than that of the ferrofluid, it is still forced from the region of high field to the region of low field. The magnitude of the force is smaller, however, than it would have been, had the object been completely non-magnetic. If the magnitude of the objects' magnetic dipole moment is greater than that of the ferrofluid, it will move to the region of high magnetic field and force the ferrofluid to the region of low field.



71-534

Figure 2 FORCES ON A NON-MAGNETIC SOLID BODY IMMERSED IN A FERROFLUID

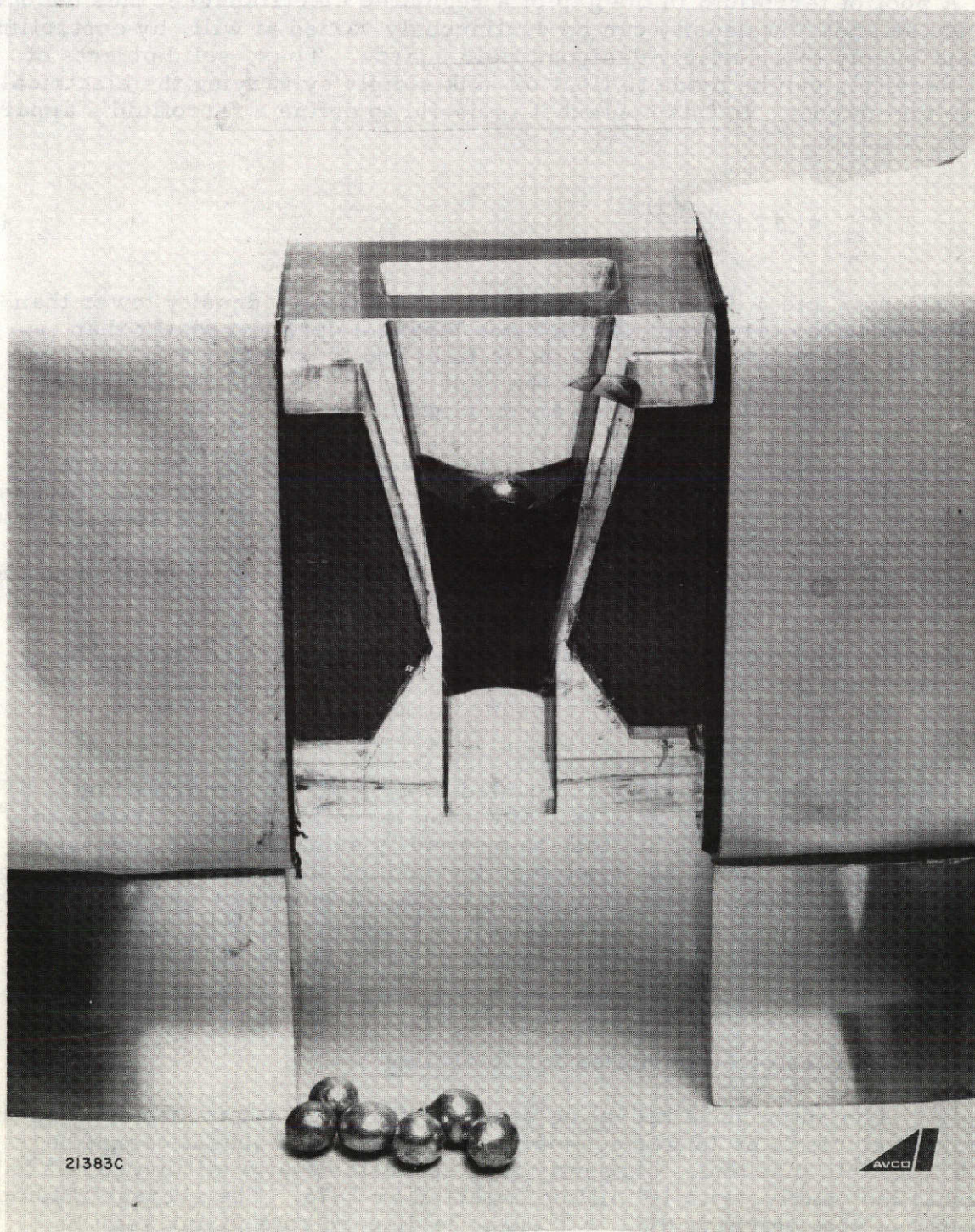


Figure 3 BALL OF COPPER FLOATING IN FERROFLUID SUSPENDED IN THE GAP OF A MAGNET

A pool of ferrofluid in the gap of a regulated electromagnet thus becomes a liquid whose apparent density can be continuously varied at will, by controlling the current supply to a suitably designed field source. Thus, solid objects of different densities can be made to float or sink simply by varying the electrical current to the magnet. In this context it is useful to define a ferrofluid's apparent density, ρ_{af} , as:

$$\rho_{af} = \rho_f + \frac{M \nabla H}{g} \quad (4)$$

From Equations 2 and 3 it can be seen that objects having a density lower than ρ_{af} , will float in the ferrofluid, while those having a density greater than ρ_{af} , will sink in it. By controlling the magnetic field and thus M and ∇H , ρ_{af} can be set to a value intermediate between the densities of the objects immersed in the pool, and their separation thus accomplished.

The ferrofluids which Avco anticipates will be used for the separation of scrap metals have a kerosene base. They are made by a continuous process involving precipitation of magnetic iron oxide particles and their dispersion into the base liquid. Economic studies indicate that the cost of ferrofluid made by this process will be about \$30 per gallon when demand rises to several thousand gallons per year.

Because the major component of these ferrofluids is kerosene, their flammability characteristics will be similar to kerosene and accordingly the precautions used when dealing with kerosene must also be applied to these ferrofluids.

This separation technique is coupled to a means of removing the ferrofluid from the separated objects. Since the ferrofluid is too valuable to discard and the scrap must be oil free to be readily saleable. For kerosene based ferrofluids this can be accomplished by washing the objects with a chlorinated hydrocarbon solvent or a hydrocarbon solvent which has a lower boiling point than the kerosene. The ferrofluid is recoverable by boiling away the solvent. A schematic of such a complete process is shown in Figure 4.

B. Structure of the Car Scrapping Industry

1. Sources of Automobiles for Recycling

The automobile recycling process starts when someone decides that a particular vehicle is no longer economical to repair, and that it cannot be sold as a workable machine. Currently it is estimated that 8 million cars are being discarded yearly, with 10 million expected by 1975. The average automobile in use today is about 6 years old. Although the discard rate in any year is perhaps more closely related to the rate of manufacturing 6 years prior, it has been found that the rate for any year falls quite consistently between 7% and 10% of the total registrations for that year^(9,10). Thus, the availability of discarded cars can be estimated for any year quite accurately.

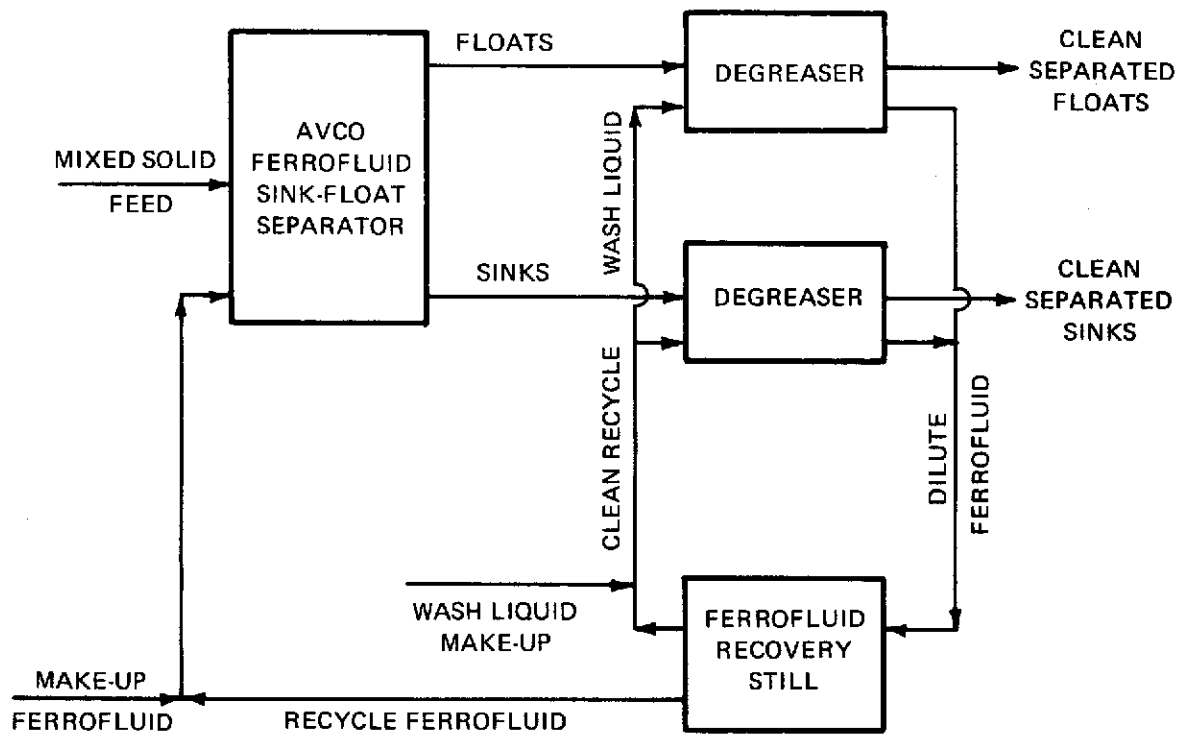


Figure 4 FLOW DIAGRAM FOR FERROFLUID SINK/FLOAT
SOLID SEPARATION PROCESS

Currently, about 7 million discarded automobiles enter the recycling process, and the great bulk of them, around 5 to 6 million at present, eventually end up as shredded metals. The remaining 1 million are simply abandoned by their owners in their backyards, in the country, or on city streets, creating a major disposal problem for the communities. They not only represent a large wastage of needed metal resources but also spoil the appearance of the landscape for the public as a whole. It has been variously estimated that there are between 5 and 20 million such abandoned automobiles around the countryside, with about 9 million appearing the most probable value⁽¹¹⁾.

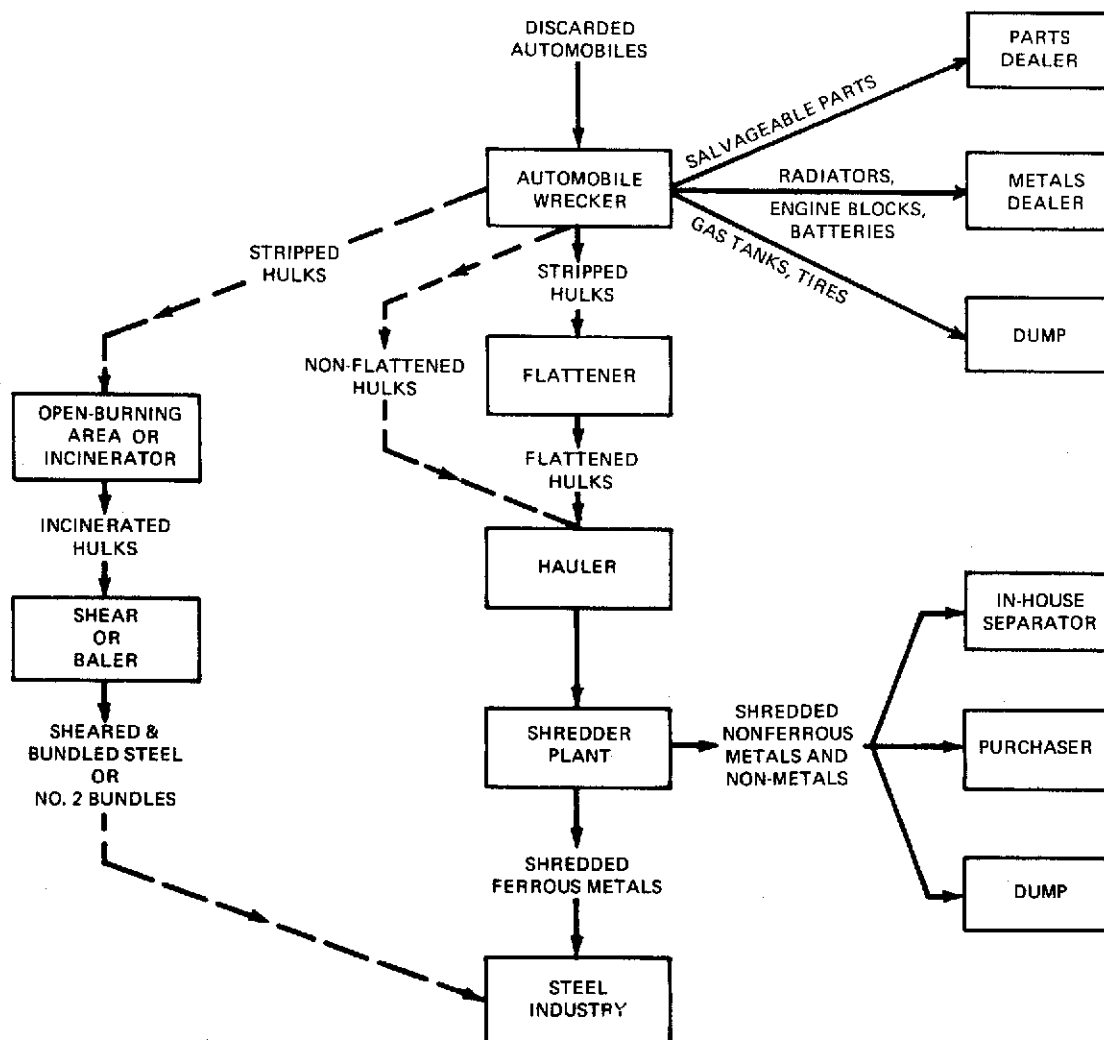
2. Processing of Scrap Automobiles

The typical flow of scrap automobiles through the recycling process is shown in Figure 5. Normally the cycle starts at an auto wrecker or dismantler, to which the automobile is driven, towed or trucked. There are an estimated 7,000 to 10,000 such concerns⁽¹¹⁾, most of which are small operations, and many constitute spare-time occupations of their owners. The wrecker will remove valuable parts himself for sale directly to users or rebuilders, or leave the hulk in his yard for customers to scavenge. Almost always the wrecker will remove the radiators and batteries, which he will collect and ultimately sell by the truckload to established scrap metal dealers. Most also remove the engines and transmissions, which they may break apart themselves for sale as scrap, or they may sell by the truckload to a scrap specialist. For safety, most also remove the gasoline tank.

Ultimately the wrecker must dispose of the old hulks in order to bring in new ones. Most wreckers sell their hulks to a shredder plant either directly or through an intermediary. A few still cut up the hulks with torches and sell the resulting steel to a dealer. Some have large shears in which they cut up the hulks for sale as sheared stock. Some sell the hulk to dealers who have such large shears, or have equipment for pressing the hulk into the dense block commonly called the "No. 2 Bundle". The latter application requires that the hulk first be burned to rid it of combustible material. The No. 2 bundle is disappearing as a means of recycling automobiles both because open burning is no longer acceptable to most communities and because technology changes in the steelmaking process have made this relatively contaminated form of steel scrap less desirable. It is being replaced by the shredded product.

Shredder operators pay for the hulks on the basis of their net weight as offloaded at their plant. Thus, the wrecker or his intermediary must pay the costs of transportation. Wreckers located 100 miles or less from a shredder may simply load four to ten hulks onto an old truck or automobile carrier and take the load to the shredder. For longer distance this is uneconomical, and more hulks must be taken at a time. For this purpose, the hulks are flattened to a thickness of 18 to 24 inches. Twenty to thirty such hulks can be stacked on a flatbed trailer, and larger wreckers may ship 40 to 50 in a railroad flatcar.

Flattened hulks can now be brought in economically from distances up to 400 miles away from a shredder. Even a small increase in the amount a shredder could pay for the hulk would extend this range substantially further, since additional mileage is relatively inexpensive compared to the fixed costs of preparation, loading and offloading. The Avco ferrofluid nonferrous metals separation system promises to increase the yield a shredder operator receives for his processed scrap, and thereby permit an increase in the price he pays for hulks. Hulks now too far away, then should begin to appear at the shredders, with beneficial results accruing to the nation's economy, its countryside, and its people.



82-4025

Figure 5 TYPICAL FLOW OF DISCARDED AUTOMOBILES THROUGH AUTOMOBILE SCRAP INDUSTRY

3. Automobile Shredding Process

A landmark development in the recycling of automobiles was the advent of the automobile shredder in the late 1950's. In this process, the entire automobile, stripped of its valuable parts and often the engine and transmission, is broken up into fist-sized pieces in giant hammermills. The automobile enters the shredder as a recognizable hulk; it leaves the shredder as a mixture of fist-size pieces of steel, iron, dirt, rubber, fabric, and the nonferrous metals -- copper, zinc, aluminum, etc., -- on a conveyor belt. As of 1970, there were in the United States nearly 100 such plants, with capacities ranging from 12,000 cars/year to up to 300,000 cars/year, processing an estimated 5.4 million discarded automobiles per year⁽¹²⁾. It has been projected that by 1980 there may be up to 200 such plants, processing 10 million automobiles/year⁽¹⁰⁾.

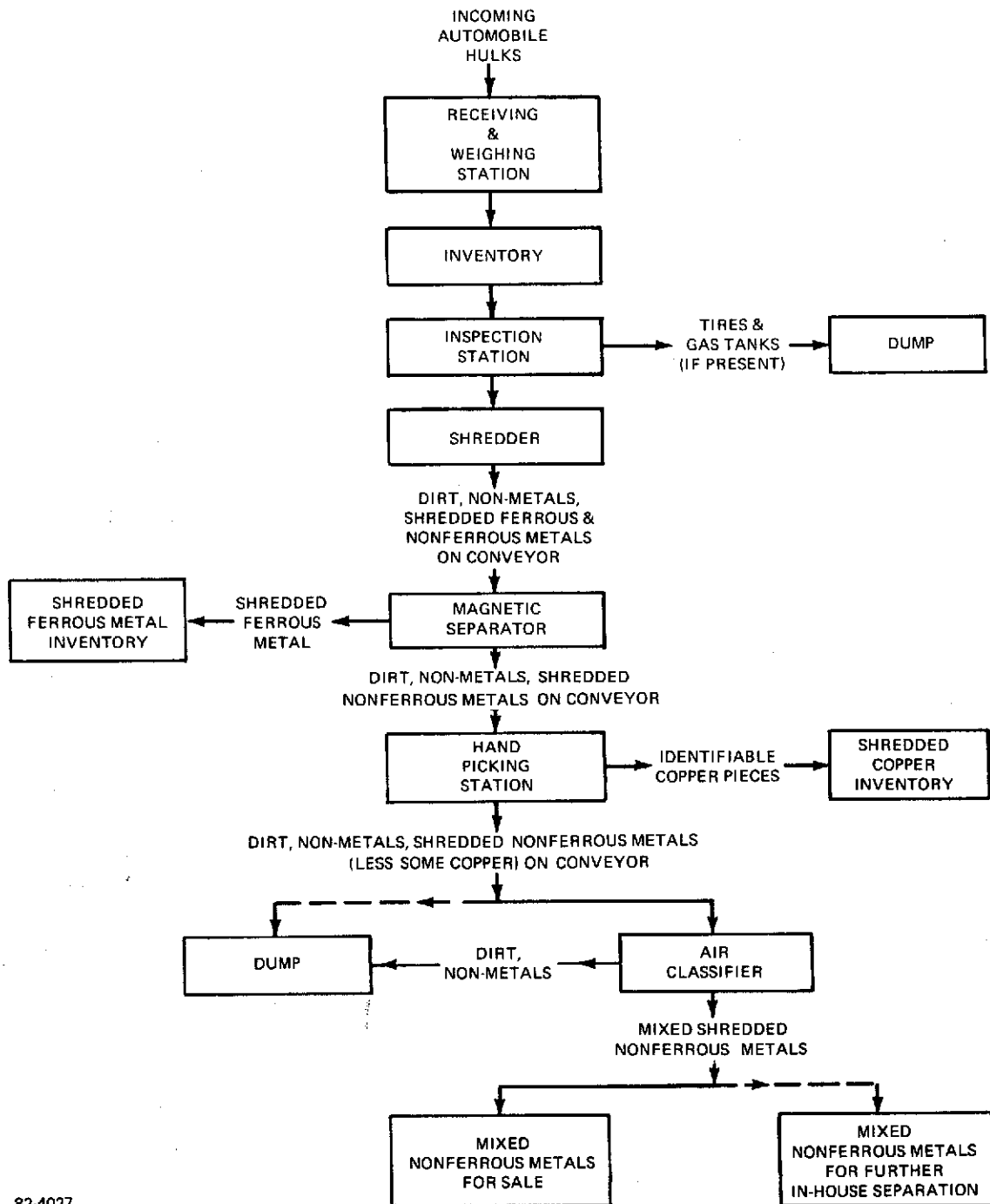
As shown in Figure 6, the scrap metal from the shredders first undergoes magnetic separation, which diverts most of the ferromagnetic material into a separate stream where it is collected for shipment directly to the smelters without further processing. The residual stream, commonly called the "dirt stream" contains a mixture of dirt, fabrics, rubber, plastics, and, of interest to this work most of the nonferrous metals. The processes now used for separation and recovery of these metals, and the application of the Avco process to this task, will be described in later sections.

Shredding plants are large capital-intensive operations, with installed costs ranging from around \$300,000 for the smallest plants to several million dollars for the largest⁽¹⁰⁾. Because of the high fixed costs of plant ownership, the operator is under great pressure to keep the plant working steadily, and to recover every possible dollar from its products. When running near to capacity, however, such plants offer a lower total cost per pound of metal produced than the older technique, while delivering a more saleable product⁽¹⁰⁾. The economies from their operation, coupled with a product price equal to or greater than that of the older forms of scrap, means that they can support a higher price for the hulks delivered to them.

A typical automobile shredding plant, that of Tewksbury Metals Company, Tewksbury, Mass., is shown in Figures 7 and 8. This plant shreds 250-300 hulks per day. In Figure 7 a hulk is shown being lifted into the input hopper of the shredder. In Figure 7 is shown the ferrous metal system, with a magnetic separator picking up only ferrous metals which are then transported by a series of conveyors to rail cars waiting in the background. In Figure 8, the "dirt" and nonferrous metals are diverted to a side stream at the magnetic separator. After an air classifier which removes most of the dirt and fluff, the mixed nonferrous metals are stored awaiting sale or further processing.

4. Nonferrous Metal Recovery From Shredded Automobiles

The principal product of the shredder plant is shredded steel, of which there is approximately a ton for each hulk processed. The secondary product, recovered in part by some operators, and potentially recoverable in its entirety by all operators, is the nonferrous metal -- zinc, aluminum, copper and stainless steel -- of which there is 50-60 lbs in each hulk as it is processed by a shredder.



82-4027

Figure 6 TYPICAL PROCESS FLOW AT AUTOMOBILE SHREDDER PLANT

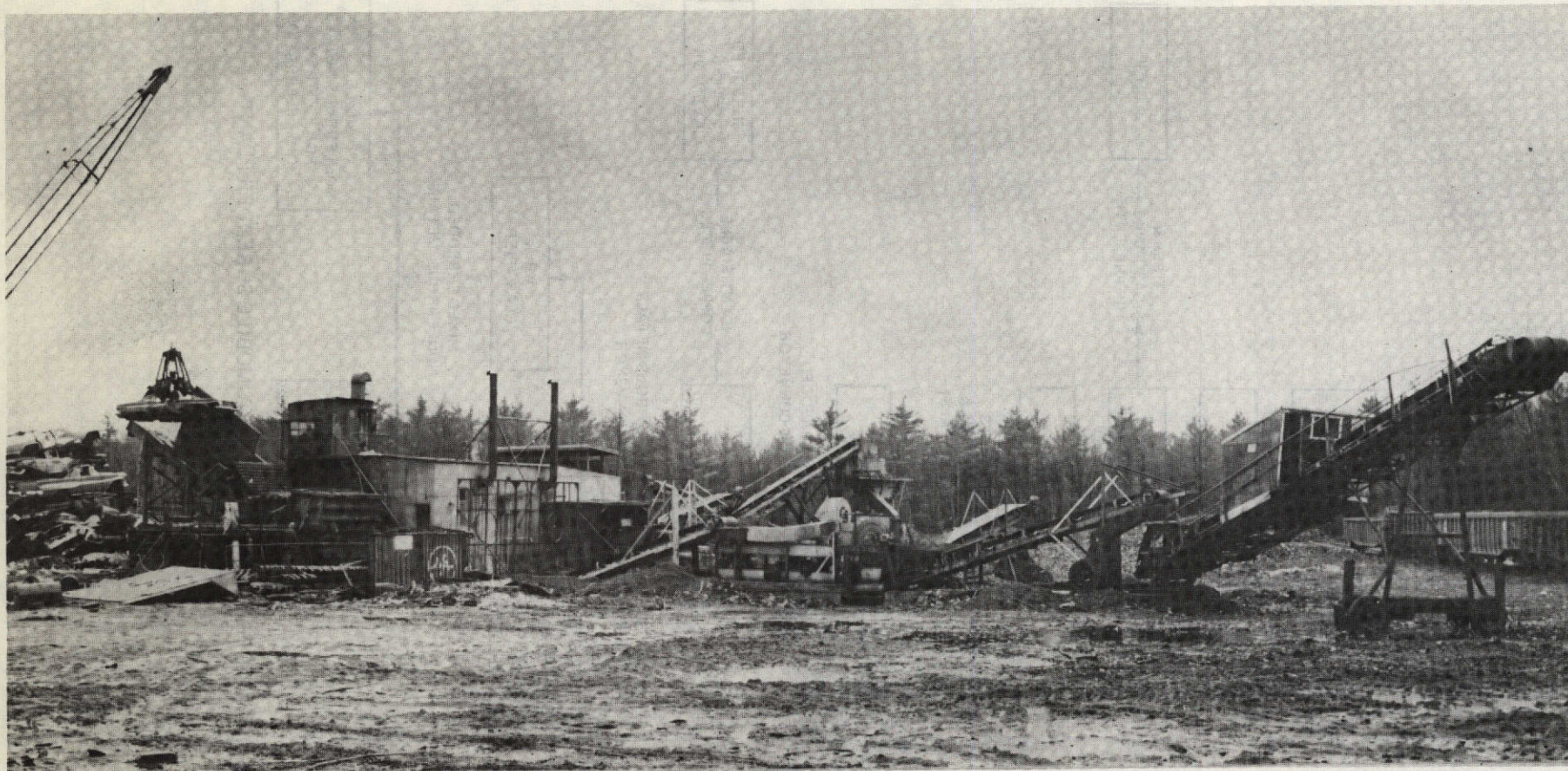


Figure 7 AUTOMOBILE SHREDDER PLANT AND FERROUS METAL OUTPUT SYSTEM

Photo courtesy of
Tewksbury Metals Co.
Tewksbury, Mass.

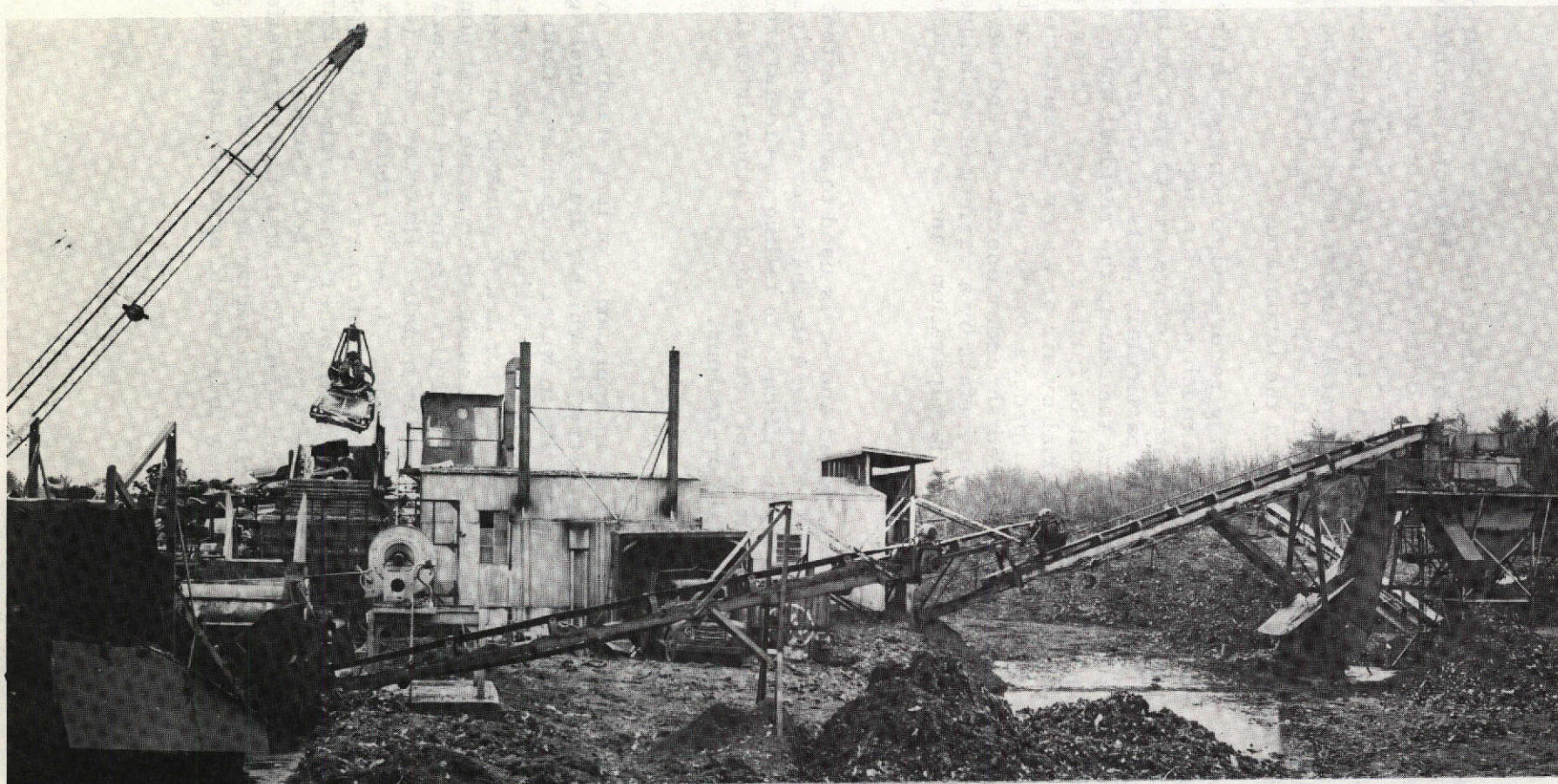


Figure 8 AUTOMOBILE SHREDDER PLANT AND NONFERROUS METAL OUTPUT SYSTEM

Photo courtesy of
Tewksbury Metals Co.
Tewksbury, Mass.

None of the existing commercial techniques, nor a combination of them, is a fully satisfactory solution to the problem. Ferrofluid nonferrous metals separation system promises to be less costly than combination of presently available processes, to be far more versatile, and to produce separated products of greater purity and sales value. By increasing the profitability of automobile shredding operations, it will ultimately lead to the processing of still larger quantities of abandoned automobiles with the resultant added yield of needed metals and concomitant clearing of the landscape.

The nonferrous metals are being recovered to some extent by shredder operators now, but there remains much room for improvement. Almost all, station one or more men on the "dirt stream" conveyors to pick out the recognizable nonferrous metal parts -- in particular, parts of copper heater and air conditioner cores. Many operators then dump the residual material, considering its value to be less than the cost of further recovery. Others attempt to remove much of the non-metallic material by air or water classification then sell the residual mixed metals to a central processor, of which there are two or three in the country. The most advanced shredder operators, and the central processors, attempt to separate the mixed metals by a variety of techniques, including further hand-picking, heavy media separation, and selective melting.

a. Hand-Picking

Hand-picking as described above, is used to some extent by nearly all shredder operators. However, it permits the recovery of only 25% or less of the available metals due to the difficulty of telling one metal from another visually at high flow rates. It is, of course, highly labor-intensive, and therefore unsuitable for large-scale operations.

b. Heavy Media Plants

Heavy media plants are an application of long standing mineral beneficiation technology to the scrap industry, in which a slurry of finely ground material, typically silicon-iron or magnetite in water, comprises a fluid medium of a density well above that of water, permitting a sink-float separation based on density. Normally such slurries are limited to a maximum specific gravity of about 3. With these systems it is possible to separate most non-metallics, such as plastics and rubber, from a dirt stream, and to separate aluminum (specific gravity 2.7) from the other metals. However, zinc (s.g. 7.1), stainless steel (s.g. 7.9), brass and copper (s.g. 8.3-8.9) remain as mixed metals in the sink product. The major drawback, of course, is that the process can remove only the aluminum, while leaving all other metals mixed. Furthermore, the process is troublesome to run, and all its products, both "sinks" and "floats", are coated with the medium, which is difficult to remove and affects the purity of the metals if left on. Therefore, an additional cleaning process is required. A typical plant purchased new today would have an installed cost in excess of \$300,000.

c. Sweat Separation

Sweat separation, or selective melting, permits the separation of the metals on the basis of their different melting points. It is used by some shredder operators and central processors to recover zinc from the mixed metals, and at least one operator is known to be using this technique to separate aluminum as well. In a typical case, the sink product from a heavy media plant, is run through a furnace just hot enough to melt the zinc (melting point 420°C) but not the residual aluminum (m.p. 660°C); copper (m.p. 1083°C). The zinc pours out and is cast into ingots, while the "non-meltables" are collected and either disposed of or subjected to further manual separation.

The major problem with this process is the cross-contamination of one metal with the others, adversely affecting the value of all. For instance, some lead (m.p. 327°C) from body fillers, if not also from batteries, will be present in the mixtures and will melt into the zinc, seriously affecting its purity. Temperature control is imperfect, and therefore some copper or aluminum from hot spots is likely to melt into the zinc, again affecting its purity. Zamac, a premium grade of zinc alloy commonly used in automobile die castings, costs significantly more than most "pure" zinc grades. Once it has gone through the sweat separation process it is degraded to a secondary zinc value whereas if it could be recovered intact, it would still command a premium price. The residual non-melting metals -- aluminum, if present, copper, and stainless steel -- are coated with zinc, making further visual separation virtually impossible and degrading their values even if they could be separated.

There is yet another potential by-product of the sweat separation process, albeit quite undesirable -- smoke and air pollution. The metals processed in the ovens are likely to be somewhat dirty, and they may be oil-contaminated. Modern installations of such ovens must have elaborate stack-cleaning systems, further adding to their costs and operating difficulties. A typical plant purchased new today would have an installed cost, including the air-pollution equipment, in excess of \$100,000, and would be capable of performing one metal separation at a time.

The ferrofluid levitation process by contrast, is capable of separating all the nonferrous metals, and producing each of them in a more pure form. In the process, it contributes no environmental pollution of its own.

5. Economics of Nonferrous Metal Recovery

The nonferrous metal content of scrapped automobiles and its value is given in Table I. The price ranges for the various metals reflect fluctuations in the market demand for these metals. The historical trend in recent years has been for scrap metal prices to rise, it is therefore probable that the upper values rather than the lower one will prevail in the future. The value of the steel recovered from a typical automobile has ranged in recent years from about \$35 to \$60 per ton. Although the value of the recoverable nonferrous metals is much smaller than the value of the steel, the profitability of nonferrous metal recovery promises to be much higher. The recovery of these metals should therefore have a significant impact on the profitability of automobile scrapping, and thus provide additional incentives for procuring abandoned cars.

TABLE I
NONFERROUS METALS PRESENT IN AVERAGE AUTOMOBILE
AS MANUFACTURED AND AS PROCESSED BY SHREDDER,
AND POTENTIAL SCRAP VALUE

<u>Metal</u>	<u>Average Content/Car as Manufactured(1)</u>	<u>Average Content/Hulk as Shredded(2)</u>	<u>Price Range as Separated Scrap(2)</u>		<u>Potential Scrap Value Per Hulk</u>	
			<u>Min.</u>	<u>Max.</u>	<u>Min.</u>	<u>Max.</u>
Zinc	54 lb	40 lb	\$.07/lb	\$.18/lb	\$2.80	\$ 7.20
Aluminum	51 lb	10 lb	\$.10/lb	\$.14/lb	1.00	1.40
Copper	32 lb	5 lb	\$.30/lb	\$.40/lb	1.50	2.00
Stainless Steel	<u>2 lb</u>	<u>2 lb</u>	\$.10/lb	\$.18/lb	<u>.20</u>	<u>.36</u>
TOTAL	139 lb	57 lb			\$5.50	\$10.96

Weighted Average Value of Mix: Per lb -	\$.096	\$.192
Per ton -	\$192	\$384

Conservative Nominal Value as Separated	\$250/ton
Maximum Value as Mixed Metals(2)	<u>\$100/ton</u>

Minimum Probable Increment from Separation \$150/ton

Sources:

- (1) Zinc, Copper, Aluminum per Karl Dean, Bureau of Mines, "Dismantling a Typical Junk Automobile to Produce Quality Scrap", RI No. 7350, December, 1969.
Stainless Steel, Avco Conservative Estimate.
- (2) Avco Estimates based upon interviews with personnel from four leading automobile shredding plants.

Figure 9 projects a material balance for the car scrapping industry, and the probable range of values for the recovered ferrous and nonferrous metals. The ecological and economic implications of these numbers will be evaluated in a later section of this report.

C. Program Plan

The theory of ferrofluid levitation as previously described and an approximate analysis of the motion of non-magnetic objects in a ferrofluid pool, given in Appendix A, suggested that the important metal alloys found in car scrap aluminum, zinc, and copper could be separated from each at commercially attractive rates by ferrofluid levitation. There were however two important uncertainties in applying these projections to the separation of automobile scrap. The first centered on the rates of separation that could be achieved. Because automobile scrap consists of irregular, jagged metal fragments the entanglement of dissimilar metal pieces at high processing rates could lead to mis-sorting. If this phenomenon were frequent enough, uneconomically low processing rates might have resulted. Although Avco had constructed prior to this program, a scale model of the magnet that was to be built in the course of this program, this model was too small to accept automobile scrap. The possibility of entanglement could therefore not be checked on this model.

The second uncertainty centered on those properties of individual scrap fragments that could result in low separation rates or inadequate purities. The fragments produced by an automobile shredder range in size up to about 8 inches. This size would require an uneconomically large magnet. It was therefore decided to precede the separation process by reshredding the nonferrous metals to a size no larger than about 3 inches. This size reduction carried the possibility of producing very small fragments that could seriously reduce the capacity of the process. A converse of this possibility was that the scrap might contain a large fraction of fragments consisting of mechanically joined dissimilar pieces of metal. Such fragments would range in density between the densities of their constituents and could therefore not be separated accurately according to density. Since these uncertainties were critical to the workability of the process, the principal objective of the program was to resolve them by determining the separation characteristics of automobile scrap that had been reshredded on commercial reshredding equipment. In order to carry out these separation tests a magnet and ancillary materials handling equipment had to be constructed, which would be capable of separating scrap up to 2 to 3 inches in size at rate of about 2000 pounds per hour. The construction of this separator and its use to separate the principal nonferrous metals of car scrap was therefore the principal goal of the program.

As mentioned previously, the recovery of ferrofluid from the separated scrap is an essential part of the process. Prior to this program it had been demonstrated that kerosene based ferrofluid could be washed off metal fragments by hydrocarbon or chlorinated hydrocarbon solvents such as heptane, trichloroethane and perchloroethylene. It had also been demonstrated that the ferrofluid could be recovered from a ferrofluid-solvent solution by boiling away these low boiling solvents. A second order objective of this program was to check the efficiency of this two step ferrofluid recovery process when dealing with substantial quantities of real automobile scrap.

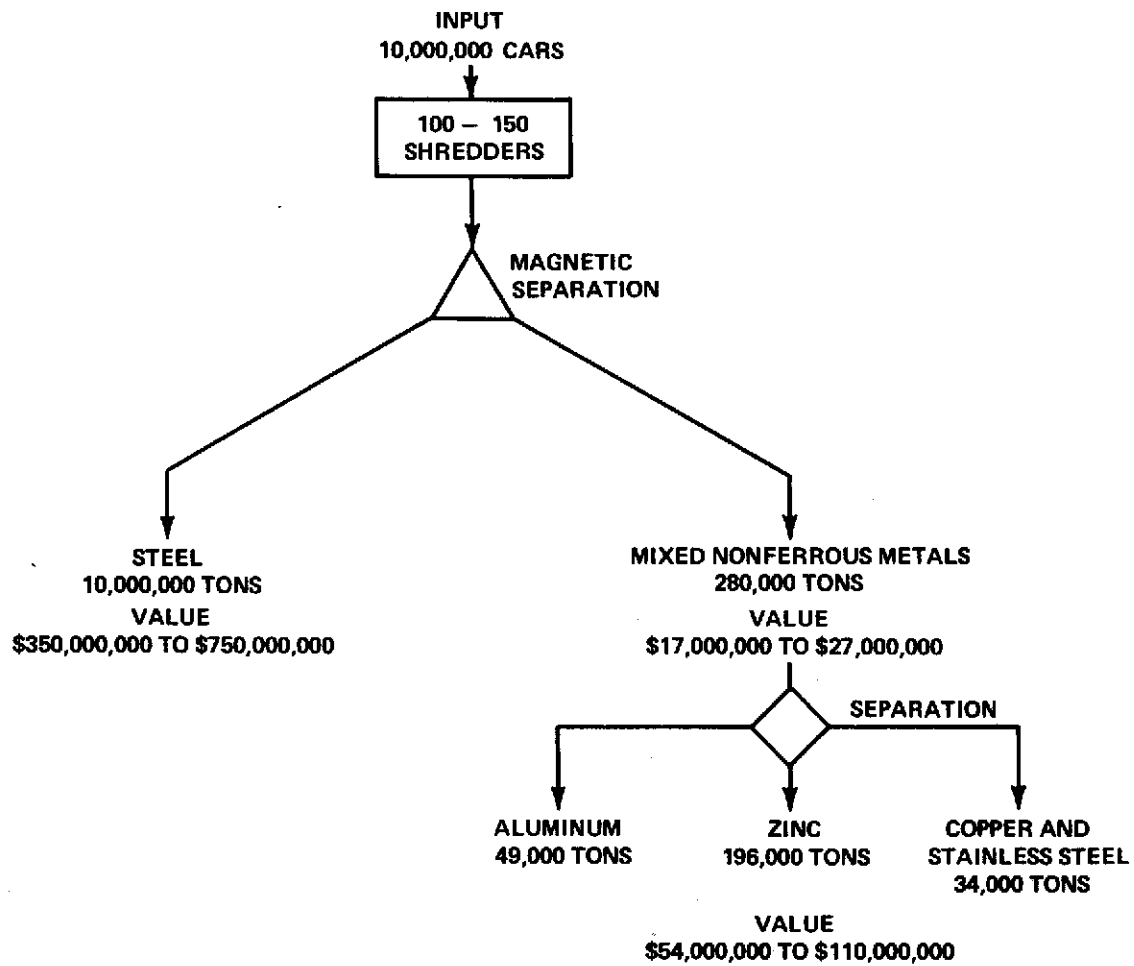


Figure 9 PROJECTED METAL SUPPLY FROM AUTOMOBILE SHREDDING IN 1975

The information on permissible processing rates, the purities of the various metal fractions and the extent of ferrofluid recovery was to provide the data base for an economic analysis of commercial recovery of these metals. The preliminary design of a ferrofluid levitation process and its economic analysis was the second major goal of the program.

The program was structured into three major tasks.

Task 1

The goal of this task was to design, develop and construct the magnet and its ancillary scrap handling equipment.

Task 2

The goal of this task was to verify the accuracy of the magnet design and to carry out the various separations of interest. Although it was fully expected from ferrofluid theory that this separator could separate individual metal pieces differing in density by 10%, with essentially 100% accuracy, it was decided to incorporate as a sub-task the separation of metal fragments differing widely in size and shape in order to prove conclusively the independence of the separation on these factors and thus its dependence only on density. Likewise a sub-task to separate model mixture of non-entangling scrap was incorporated, to verify the expected high separation rates in the absence of entanglement. Having verified the separability of individual scrap pieces and the separability of non-entangling mixtures, any deviations observed with actual car scrap could then be safely attributed to peculiarities of the scrap rather than to deviations from the expected accuracy of the process. The final and most important objective of this task was to study the separation of nonferrous reshredded scrap from automobiles to determine processing rate, degrees of separation, and ferrofluid removal.

Task 3

Based on the results of Task 2, the preliminary design of a complete plant for separating the nonferrous metals of car scrap, was to be carried out. An economic and ecological analysis of the plant was a part of this design.

II. RESULTS

A. Magnet Construction and Evaluation

The general objective of this task was to design and construct a magnet which could accommodate and magnetize a body of ferrofluid sufficiently large, to carry out the separation of 2-3 inch scrap fragments. The design goals required to meet this objective were to construct a magnet that could magnetize a cubic region of space (the working volume) no less than 6" on a side, with a constant magnetic field gradient sufficiently large to produce an apparent density in a ferrofluid of up to 8 g/cm^3 . In order to provide a margin of safety, the "working volume" was actually designed to be 8" on a side. Part of this extra space, as will be seen later, was used to accommodate the scrap handling mechanisms. Equation (4) shows that for ferrofluids approaching saturation, the apparent density of a ferrofluid varies linearly with the imposed magnetic field gradient. In order to sort objects accurately, the apparent density variations in a ferrofluid pool must be considerably smaller than the density differences among the objects. For separating the nonferrous metals of car scrap this implied that the imposed magnetic field gradient throughout the ferrofluid pool would have to be constant to within 10%. With available ferrofluids a gradient of 250 oe/cm would be large enough to create an apparent density of 8 g/cm^3 in the ferrofluid pool. These were the specific objectives of the design.

The design of the magnet was based on hyperbolic pole pieces described in detail in Appendix B. The magnet was constructed by Industrial Coils, Inc. and the blueprints of its constituent parts are being supplied as Attachment 1 to this report. The design of the pole pieces of this magnet (Attachment 1, drawing 3132) was a direct scale up of pole pieces that Avco had constructed and tested prior to the initiation of this program. Based on these tests it was expected that the large magnet constructed for this program would have a cubic region 8 inches on a side in which the vertical magnetic field gradient was constant to 10%. Figure B-2 shows a front view of the magnet and the region of constant gradient, the working volume. The width of this square region, K, is 8".

Figure B-3 shows a side view of the pole with the central region of constant gradient marked by the "10%" lines. The distance between these lines is also 8".

To demonstrate the constancy of the magnetic field gradient in this region, it is sufficient to show that the field in this region satisfies Equation (1) of Appendix B. The theory developed in Appendix B shows that this can be demonstrated by proving that in the working volume, the x component of the field, H_x , varies linearly with y, and that the y component, H_y , varies linearly with x; and that the proportionality constant, Γ , is the same in both cases. The gap of this magnet has a planes of symmetry at $x = 0 \text{ cm}$ and at $z = 20 \text{ cm}$ as can be seen from Figures B-2 and B-3. It is therefore sufficient to verify the correctness of the above relations in only one quadrant of the working volume because the working volume is centered on the intersection of these planes of symmetry. A suitable quadrant could be $0 < x < 10$, $19 < y < 39$, $10 < z < 20$. As will seem however, these relations were verified over almost all of the working volume, to provide checks.

This was demonstrated by measuring H_x and H_y by means of a Hall probe gaussmeter. Figures 10 and 11 show that this relation indeed holds to better than 5%. The practical implication of having met the constancy of gradient design criterion in this working volume, is that the constancy of the apparent density of a ferrofluid pool occupying this volume would not be impaired by non-constant gradients.

In addition to these magnetic field measurements, the magnetic field was measured as a function of the coil energizing current, at the top of the working volume (19 cm, 7.5 inches below the mirror plate), and at the bottom of the working volume (39 cm, 15.5 inches below the mirror plate). The gradient was calculated from these values as a function of current. These data, shown in Figures 12 and 13, will be used in conjunction with measured properties of the ferrofluid to calculate the apparent density of the ferrofluid pool as a function of the energizing current. It will be shown in a later section of this report that with the maximum measured gradient of 250 oersted/cm at 690 amperes, and the ferrofluid used throughout most of the program, an apparent density of about 10 g/cm³ could be generated. With a higher magnetization ferrofluid used in the course of some of the work an apparent density of about 15 g/cm³ could be generated.

In summary the magnet design was successful both in terms of the constancy of the gradients, and in terms of the maximum apparent density of the ferrofluid that could be generated.

B. Materials Handling System (Separator)

For the sake of shortness the materials handling subsystem will be referred to as the "separator" in this section. In later sections, the combination of magnet and materials handling system will however be called the separator.

The function of the separator is to confine the ferrofluid pool and to provide means for introducing the mixed solids and for removing the separated products. The design of the separator to accomplish these objectives was based on a model that had been used with the small laboratory magnet Avco had constructed to verify the pole design. Figure 14 shows an uncovered top view of this model separator (inch scale superimposed) and identifies its key features. Figure 15 shows the separator in position between the poles of the laboratory magnet. Several features of this design deserve comment. The central "well" is centered on the region of constant gradient, and is entirely within the working volume of the magnet. Most of the ferrofluid is confined to this region, although some penetrates into the feed and product removal channels. These channels extend well beyond the poles in order to prevent the ferrofluid which penetrates into them from running out of the apparatus onto the poles themselves. Objects were introduced into the ferrofluid by pushing them in with a rake through the central channel (the feed channel), which is half way between the top and bottom of the working volume. The floats were removed by raking the portion of the ferrofluid pool which extended above the floor of the upper channel. The top of ferrofluid is somewhat above the working volume.

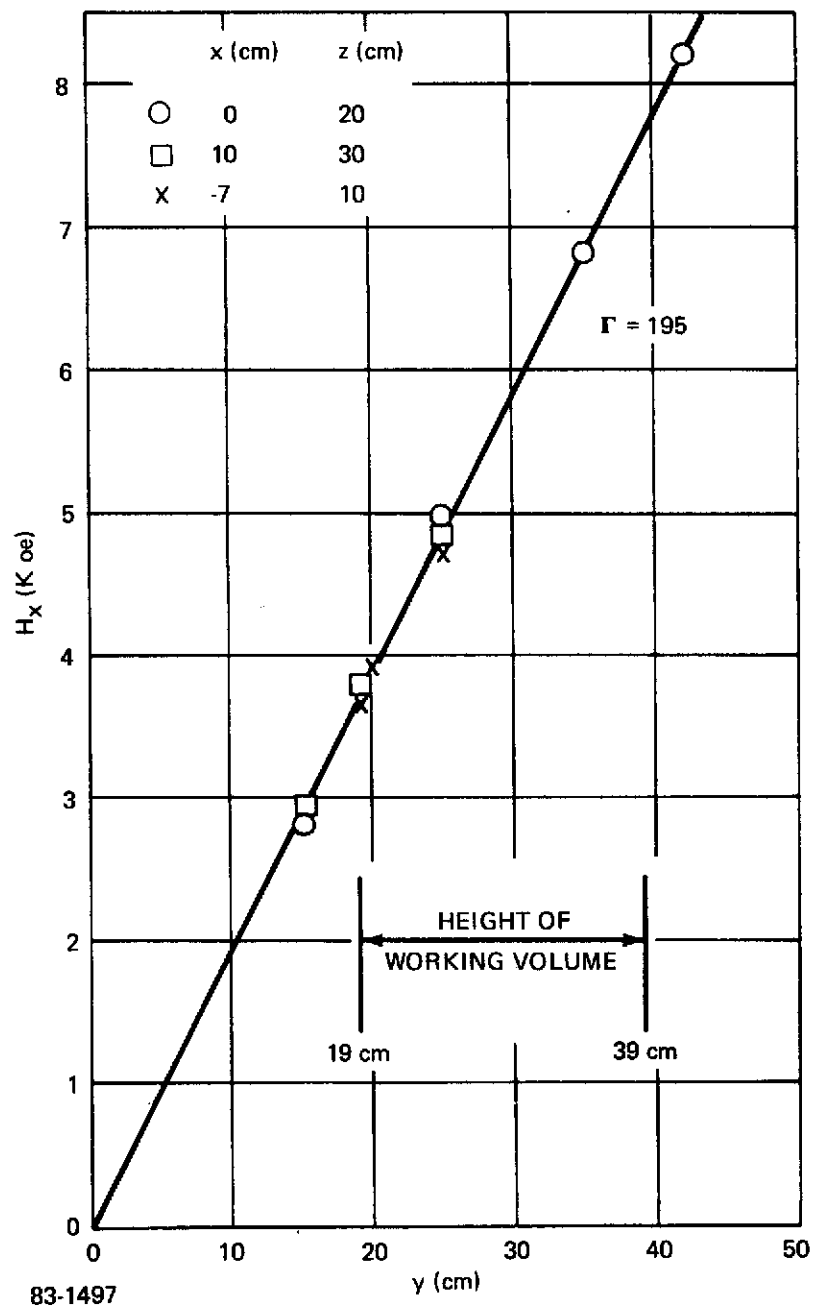
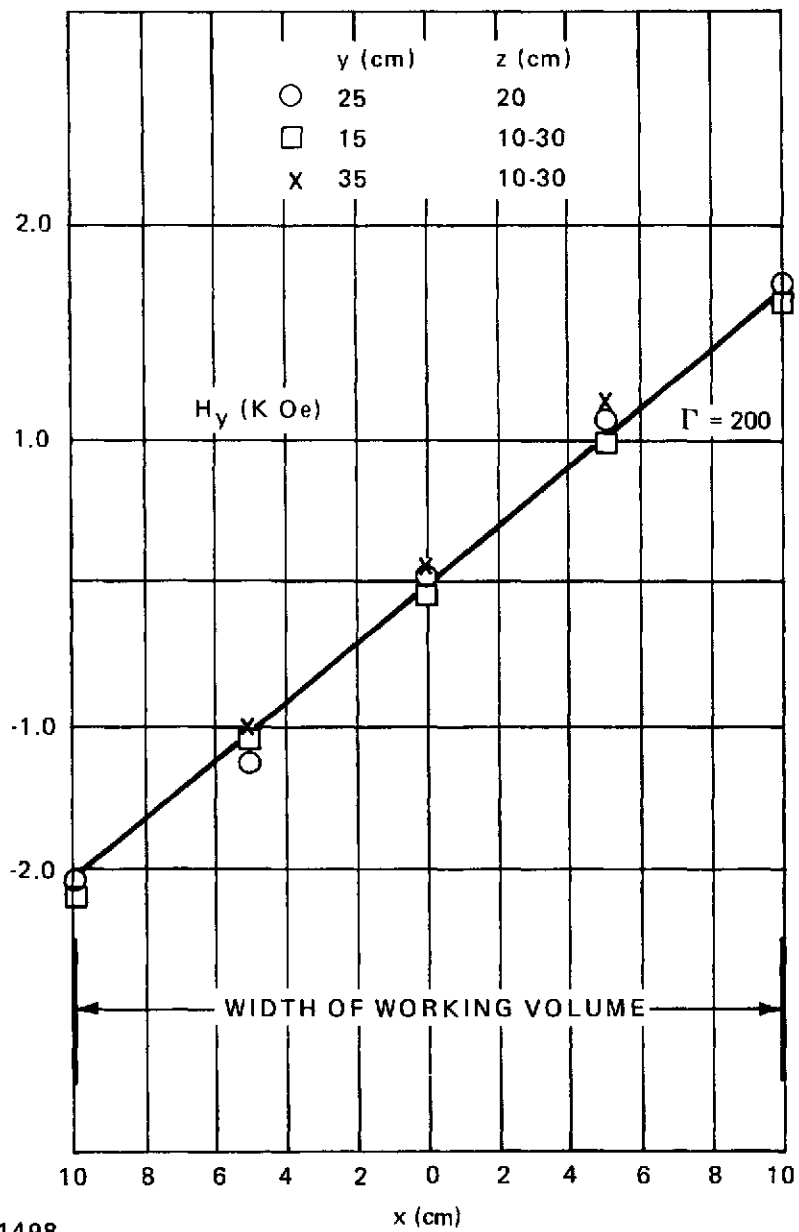


Figure 10 VARIATION OF H_x WITH DISTANCE FROM MIRROR PLATE



83-1498

Figure 11 VARIATION OF H_y WITH DISTANCE FROM AXIS

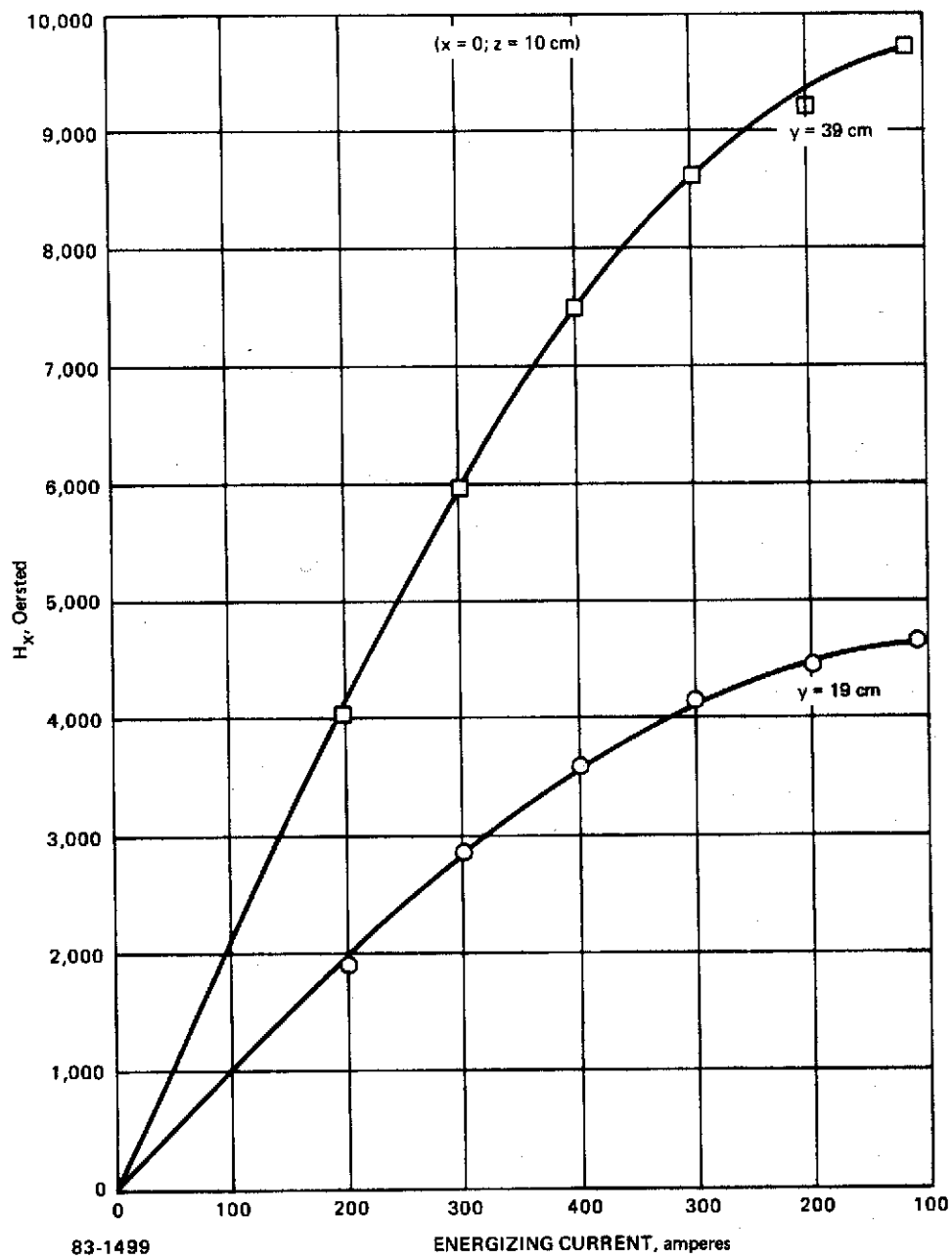


Figure 12 MAGNETIC FIELD ON AXIS OF GAP

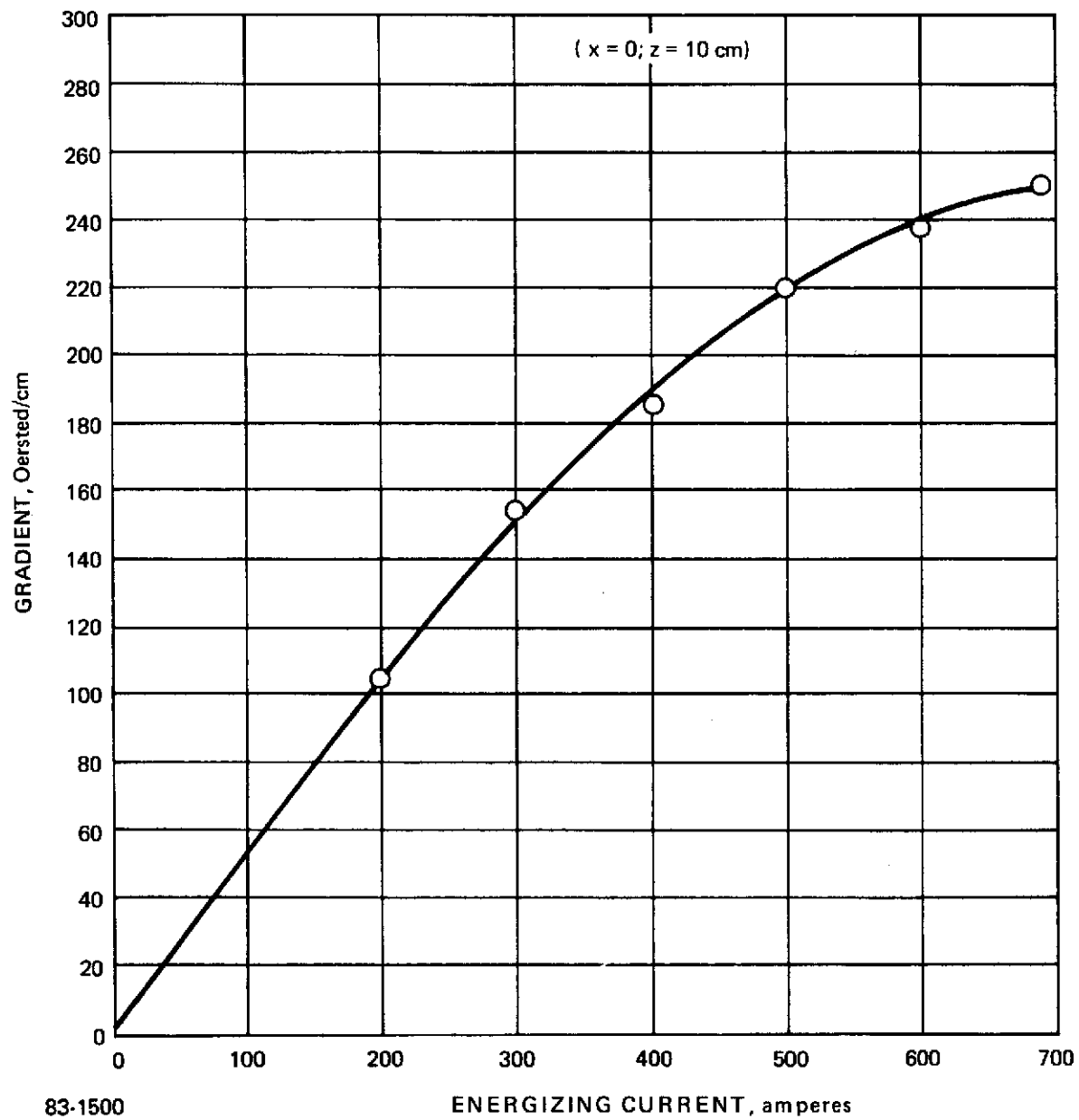


Figure 13 VERTICAL MAGNETIC GRADIENT ON AXIS OF GAP

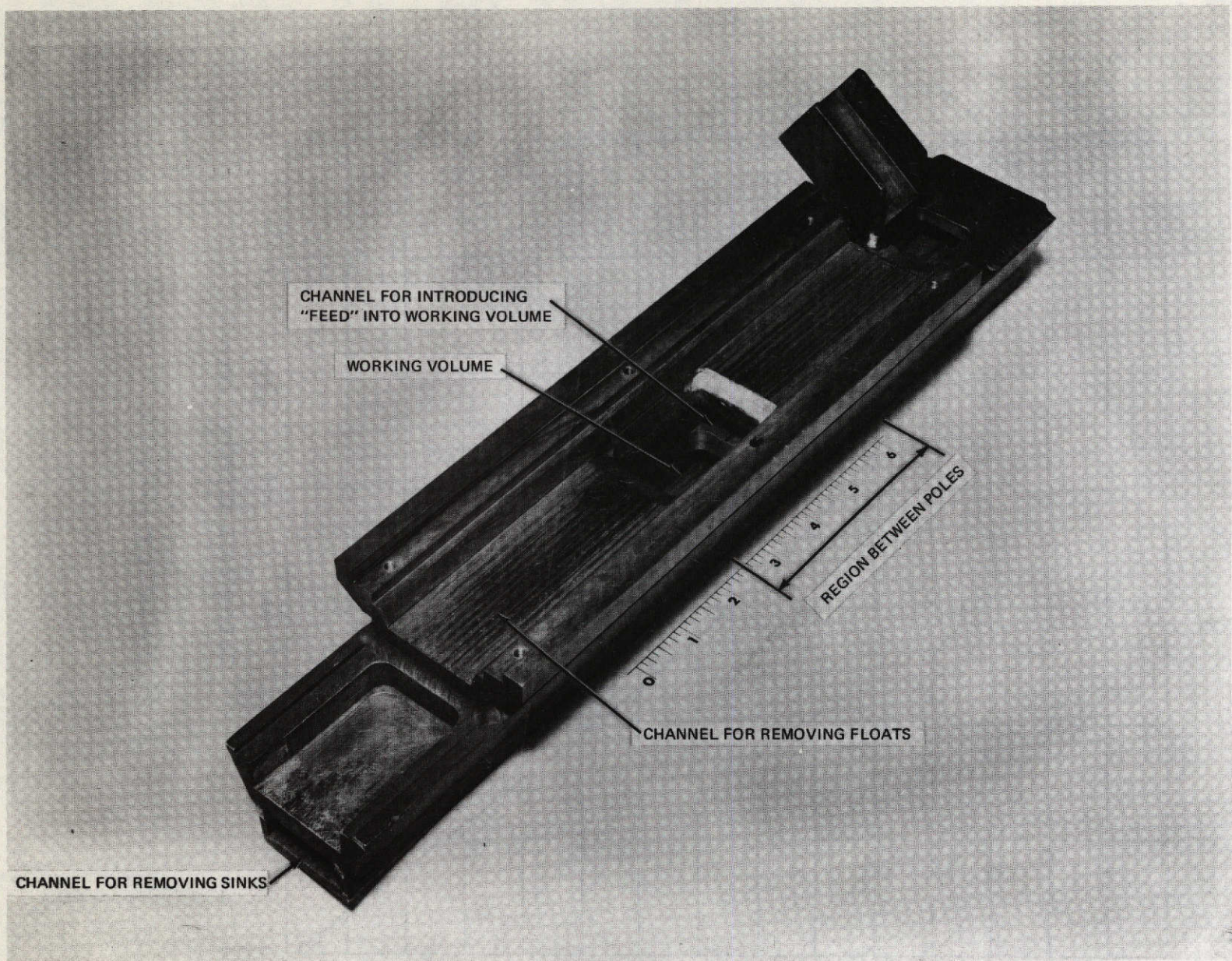


Figure 14 MODEL SEPARATOR WITH COVER PLATE REMOVED

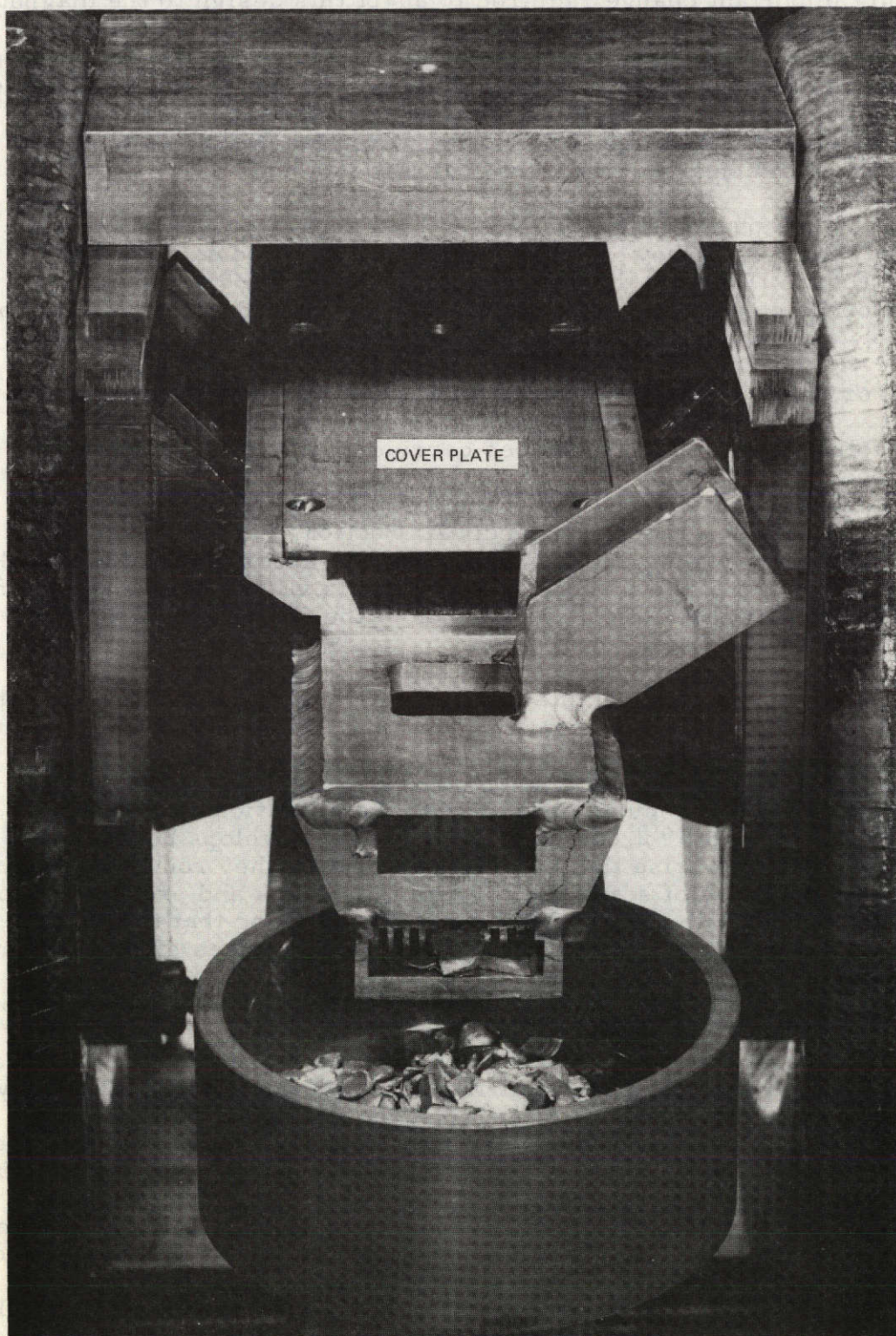


Figure 15 MODEL SEPARATOR IN LABORATORY MAGNET

The only important change required to adapt this design to the magnet constructed for this program were to replace the manual raking process by suitable conveyors and to increase the scale by about a factor of 4. An illustrator's sketch of this separator based on blueprints and a partly assembled portion is shown in Figure 16. The close similarity to the model separator is obvious. The conveyors were designed to carry scrap fragments up to about 2-3 inches in largest dimension at rates of over a ton an hour.

Figure 17 is a photograph of the assembled separator, identifying the key components. Figure 18 shows a close up view of the product removal conveyors, and Figure 19 shows the feed conveyor. Figure 20 shows the separator positioned between the poles of the electromagnet during the assembly of the system.

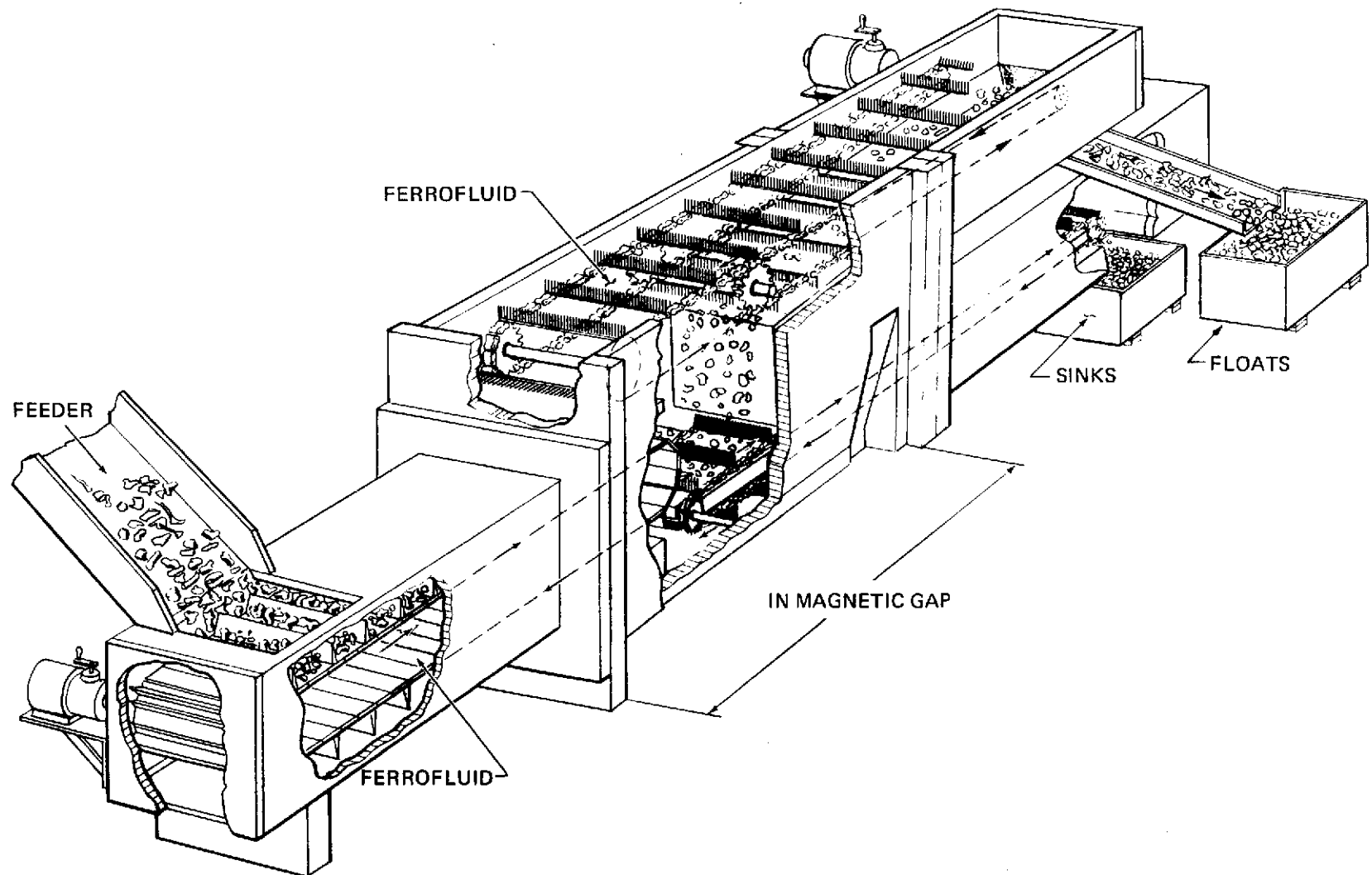
The floor onto which the sinks fall coincides with the bottom of the working volume. The top of the feed conveyor is slightly below the mid point of the working volume, so that scrap pieces carried by it enter at about the midpoint of the working volume. This entry point equalizes the transit times of sinks and floats to the bottom and top of the ferrofluid pool, and is thus conducive to high separation rates, (Appendix A, Section 2). The rakes of the upper (floats) conveyor protrude about 1 inch below the upper plane of the working volume, and since the top of the ferrofluid pool extends slightly above this plane, the rakes sweep through a little more than 1 inch of the ferrofluid to remove the floats.

After the system was assembled, filled with ferrofluid and tested with scrap, a number of difficulties with conveyor operation showed up, which required correction.

The most serious difficulty showed up in the operation of the feed conveyor. In Figures 17 and 19 it can be seen that a gap develops between the interlocking plates that comprise the feed conveyor, when they round the driving and idling sprockets. Pieces of scrap got through these gaps and prevented proper meshing of the sprockets with the driving chain. It was found that the flights attached to the plates were not high enough to force scrap pieces effectively into the ferrofluid pool. This resulted in pile up of scrap at the interface of the ferrofluid within the feed channel, and occasional jamming of the feed conveyor.

Similar, although far less severe problems were encountered with the product removal conveyors. The rakes or flights of the floats removal conveyor occasionally jammed thin pieces of scrap against the floor of the floats outlet channel. On somewhat rarer occasions very small pieces of scrap got into the links of the chain carrying the flights of the drag conveyor that removed the sinks.

The floats conveyor problem was overcome by replacing the aluminum rakes with rubber flaps. These flaps had enough rigidity to remove floating scrap pieces from the ferrofluid and to drag them along the floor of the channel, yet they were sufficiently flexible to pass over any scrap pieces caught temporarily against the channel floor. A view of this modified conveyor is shown in Figure 21.



83-1270

Figure 16 SKETCH OF SEPARATOR

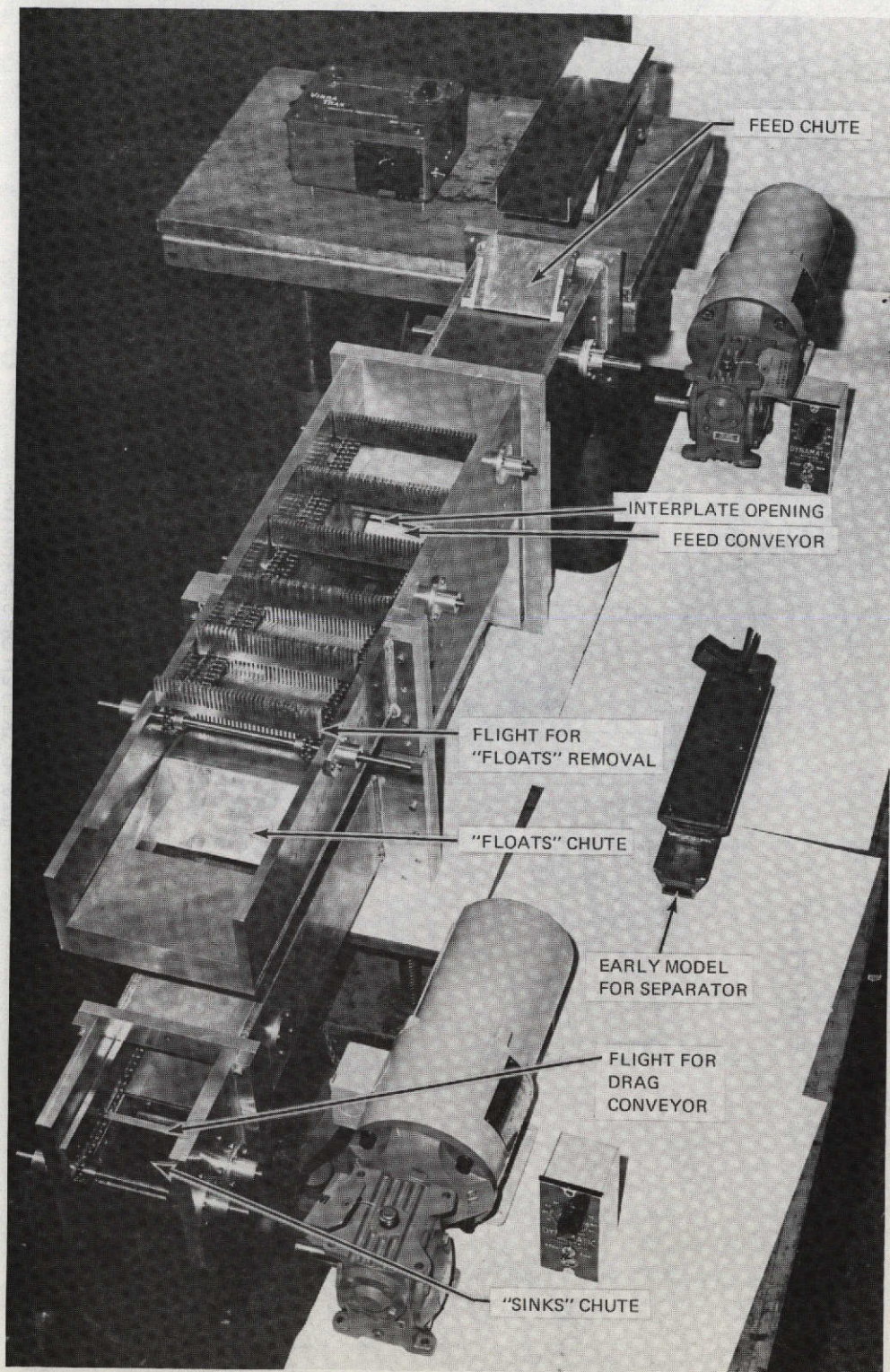


Figure 17 TOP VIEW OF SEPARATOR

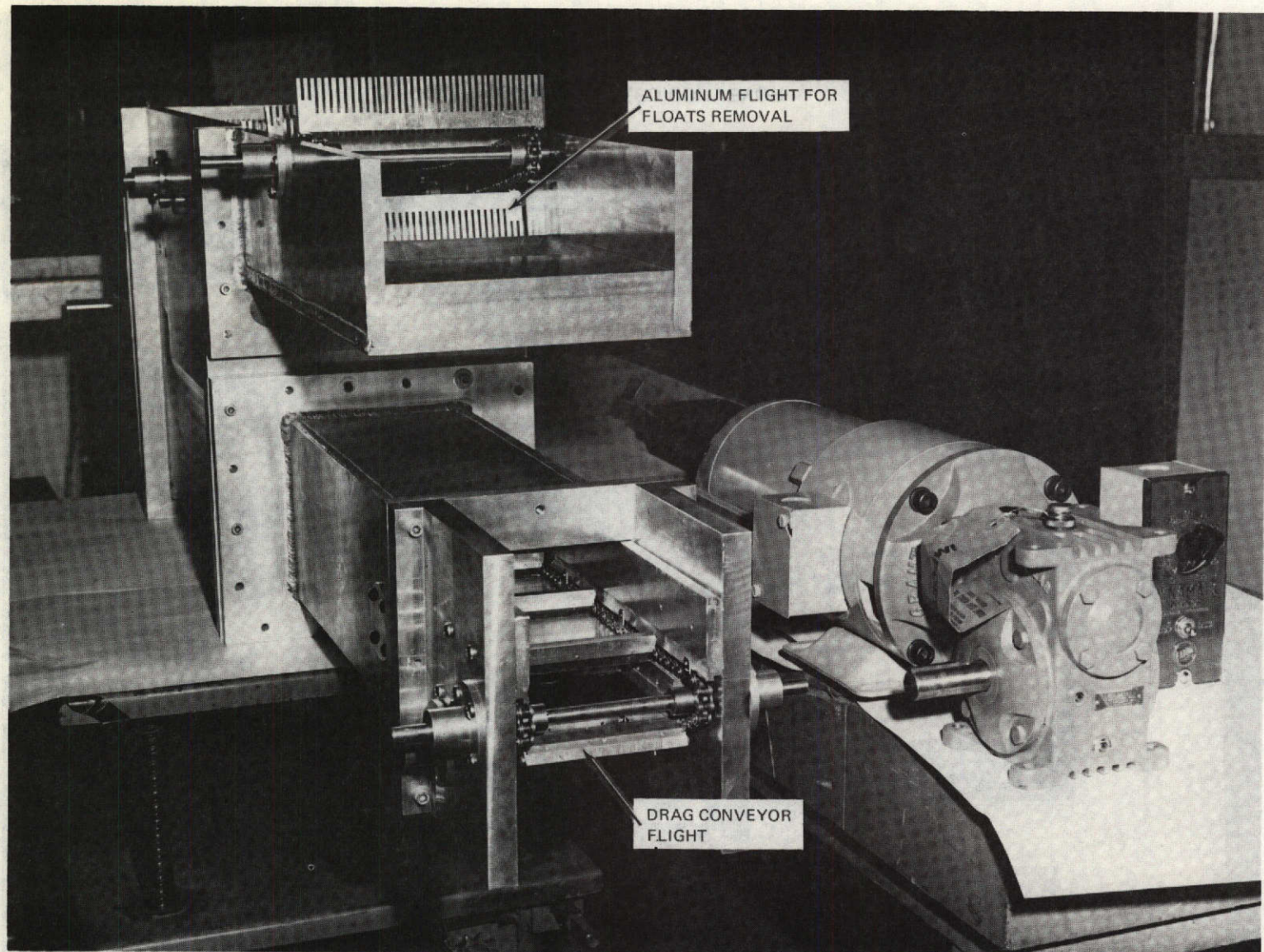


Figure 18 PRODUCT REMOVAL CONVEYORS

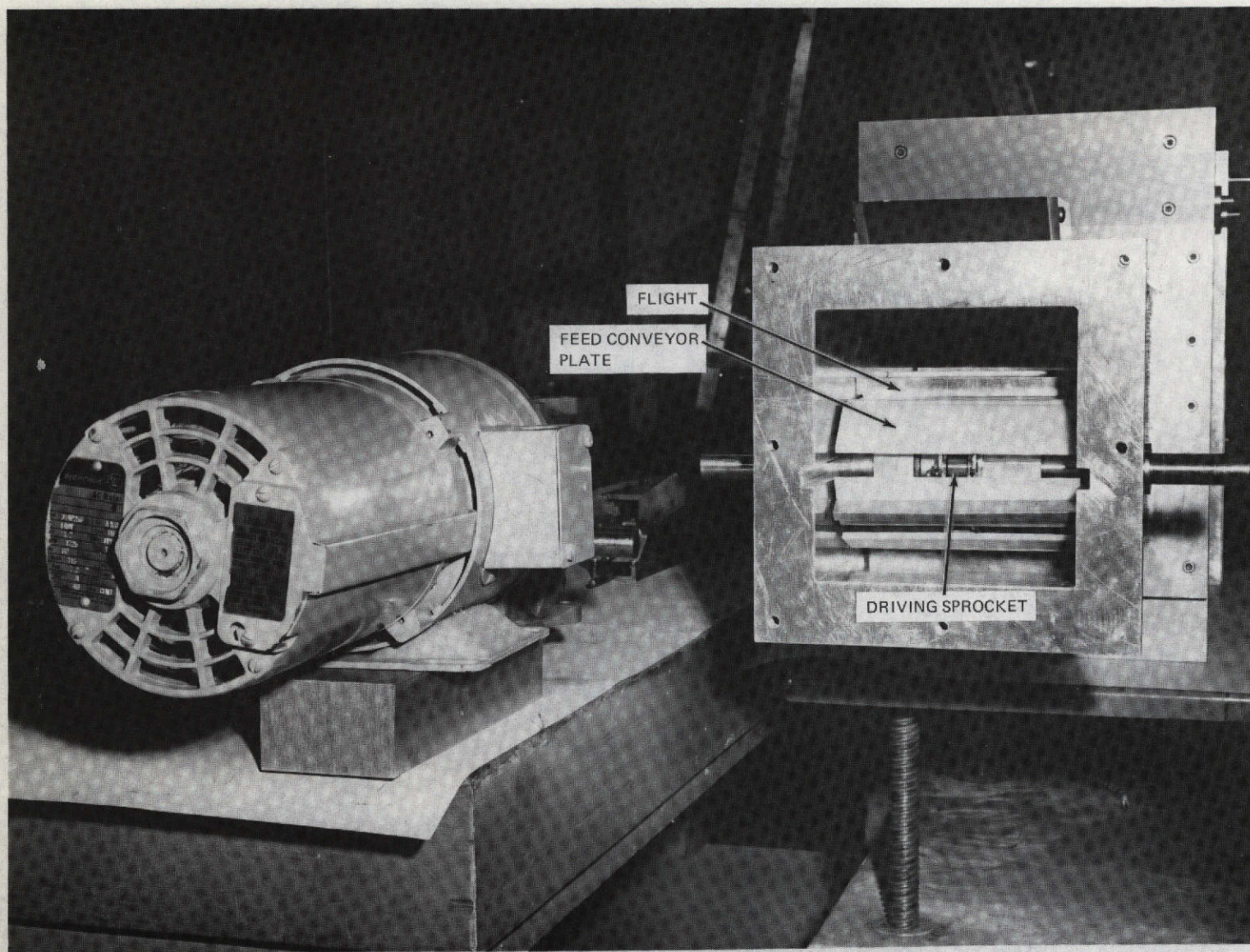


Figure 19 FEED CONVEYOR

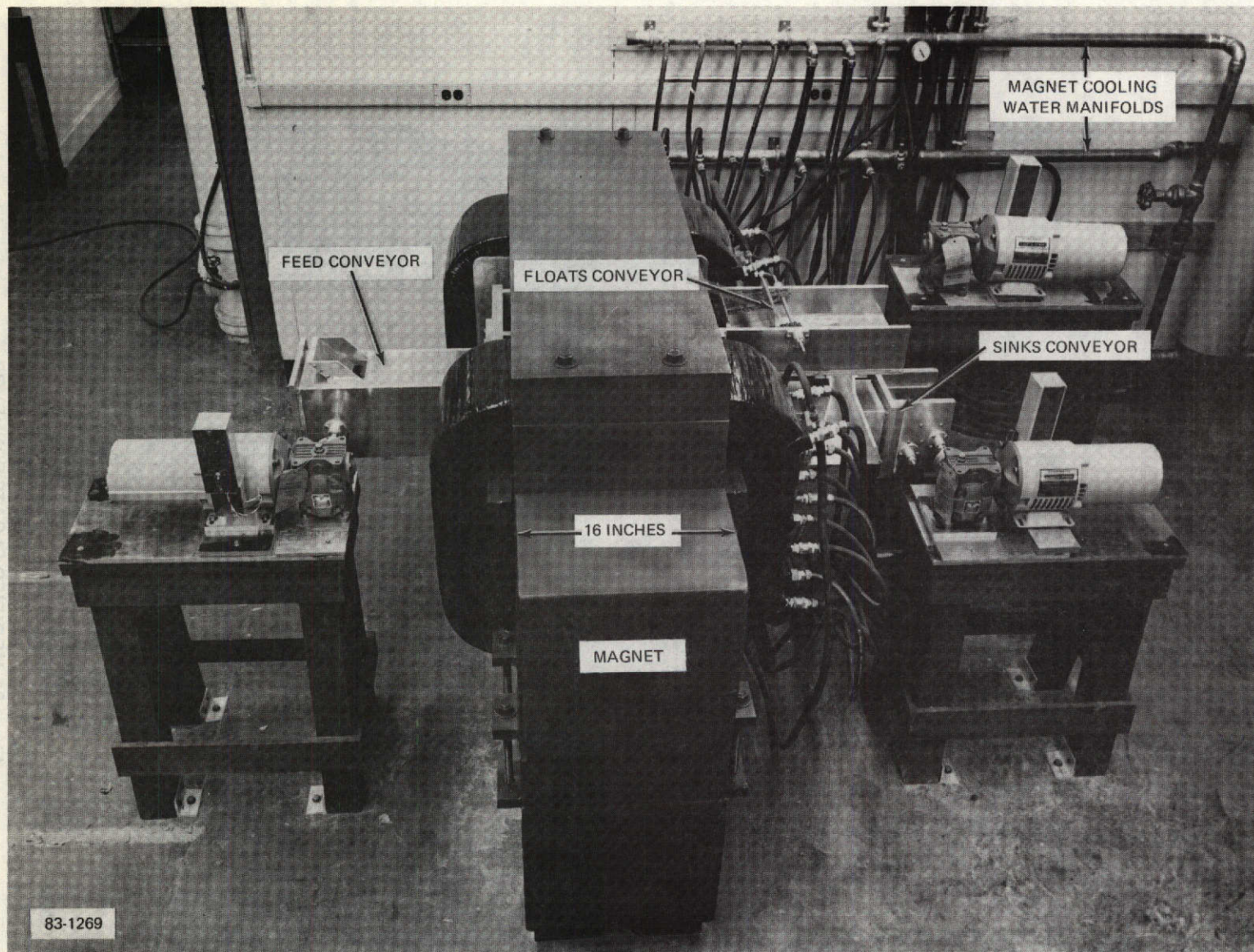


Figure 20 FERROFLUID SEPARATOR DURING ASSEMBLY

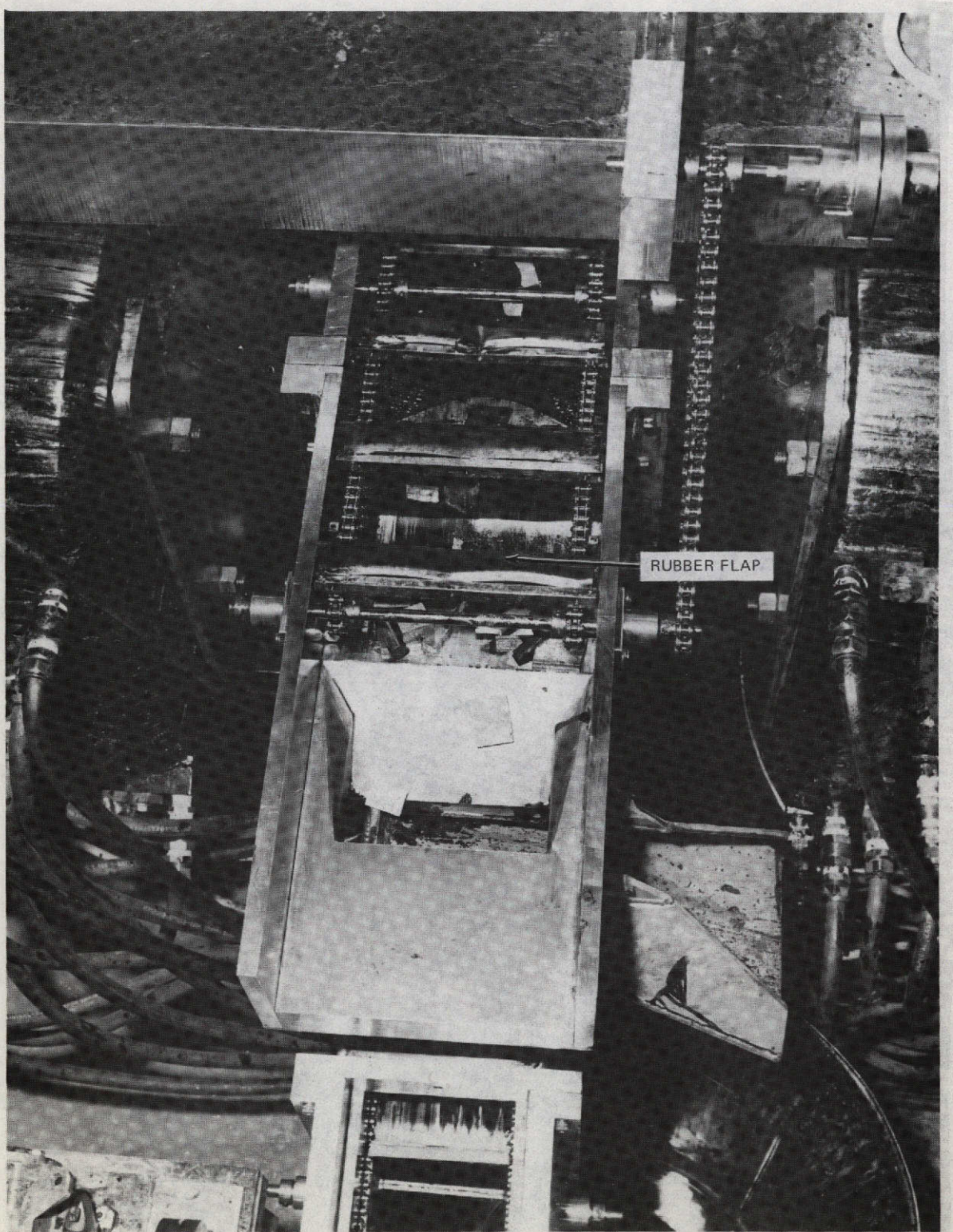


Figure 21 MODIFIED FLOATS CONVEYOR

The sinks conveyor and the feed conveyor were both replaced with belt conveyors of Buna-N reinforced with cotton. The sinks conveyor had no flights while the feed conveyor was equipped with 2 inch high flights as shown in Figures 22 and 23. The rough sides of both belts rides against the knurled driving and idling pulleys in order to prevent slippage. Small pieces of scrap are prevented from getting under the belts by having the belt edges positioned inside a slot in the side wall of the channel. The rubber flights on the feed belt sweep the entire height of the feed channel and thus prevents pile up of scrap at the ferrofluid interface. In commercial models of this separator these flights would be vulcanized to the belt rather than being attached to it by metal bars.

After the above changes had been made the conveyor belts functioned satisfactorily. Scrap metal could be fed to the separator and removed after separation at over 2 tons per hour. The blueprints of the separator's components after these modifications had been made, are supplied as Attachment 2 to this report. An overall view of the separation system showing the driving motors mounted on top of the magnet mirror plate and baskets for the scrap is shown in Figure 24.

C. Behavior of Single Objects and Model Mixtures

The principal objective of this work was to provide background information which would aid in understanding the results that might be obtained with the complex metal mixtures encountered with car scrap. On the basis of ferrofluid theory, experiments on the small laboratory magnet and the constancy of the gradient in the working volume of the large magnet it was felt that the behavior of single particles would follow theoretical predictions with respect to sink-float behavior and that model mixtures at low feed rates would separate cleanly. This work was carried out with the expectation that these results would be realized and thus to enable us to attribute deviation from these results, when processing actual car scrap, to the nature of car scrap itself.

1. Single Objects

In this experiment the behavior of metal fragments was studied as a function of density, shape, size and release point into the ferrofluid pool. The procedure used was to operate only the lower (sinks) conveyor while adjusting the current to the coils to the minimum value required to prevent the test object from sinking and being carried out by this conveyor. At this current value, the apparent density at the lower conveyor (which is at the bottom of the working volume) should just about equal or exceeds slightly the density of the test object. Equation (4) for the apparent density may be rewritten to show its explicit dependence on the coil current.

$$\rho_{af} = \rho_f + M [H(I)]_B \frac{\nabla H(I)}{g} \quad (5)$$

$M [H(I)]_B$ - Magnetic dipole moment per cm^3 of ferrofluid
(which is a function of H which in turn is a
function of I) at the bottom of the working volume.

I - Coil current.

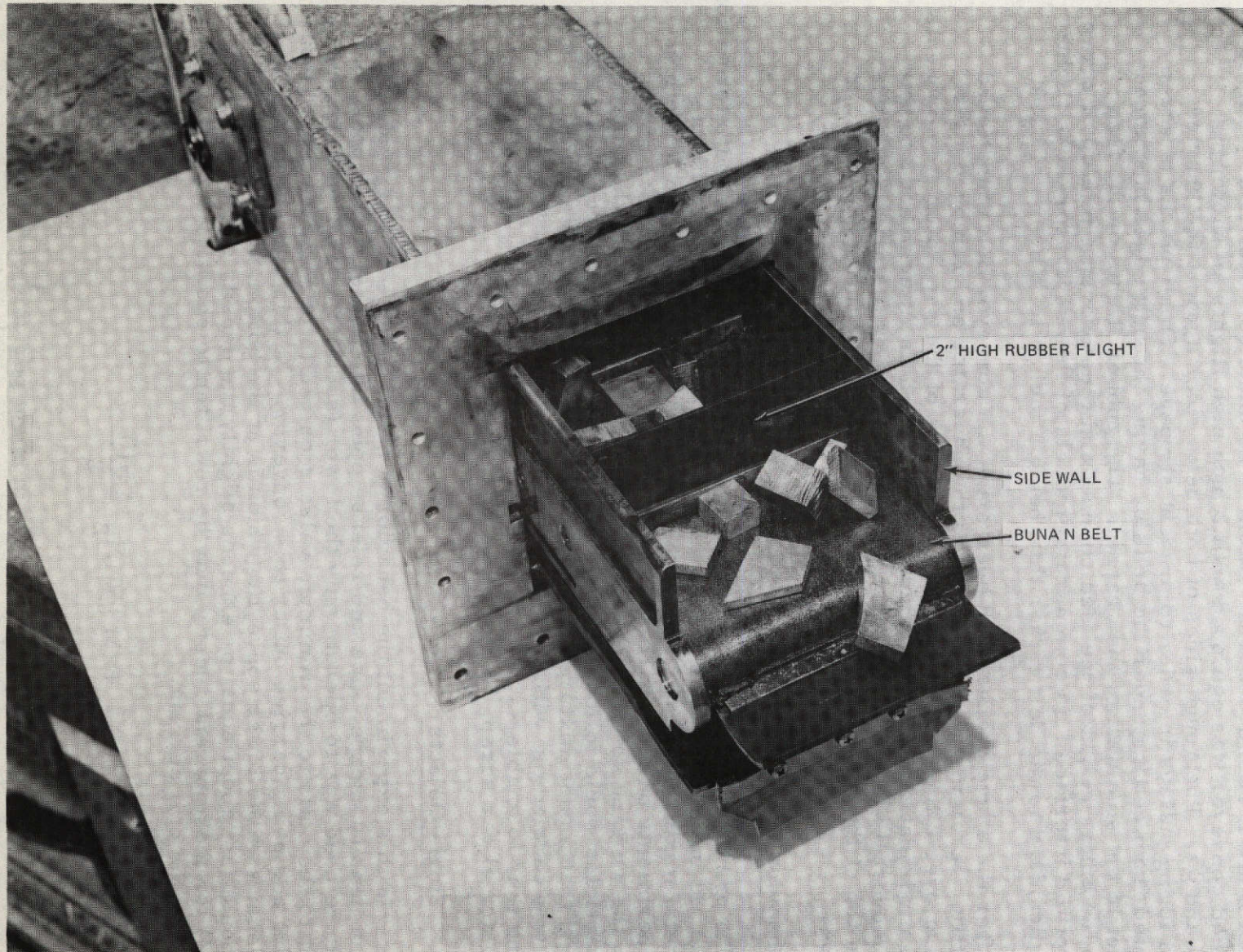


Figure 22 MODIFIED FEED CONVEYOR — ASSEMBLED VIEW

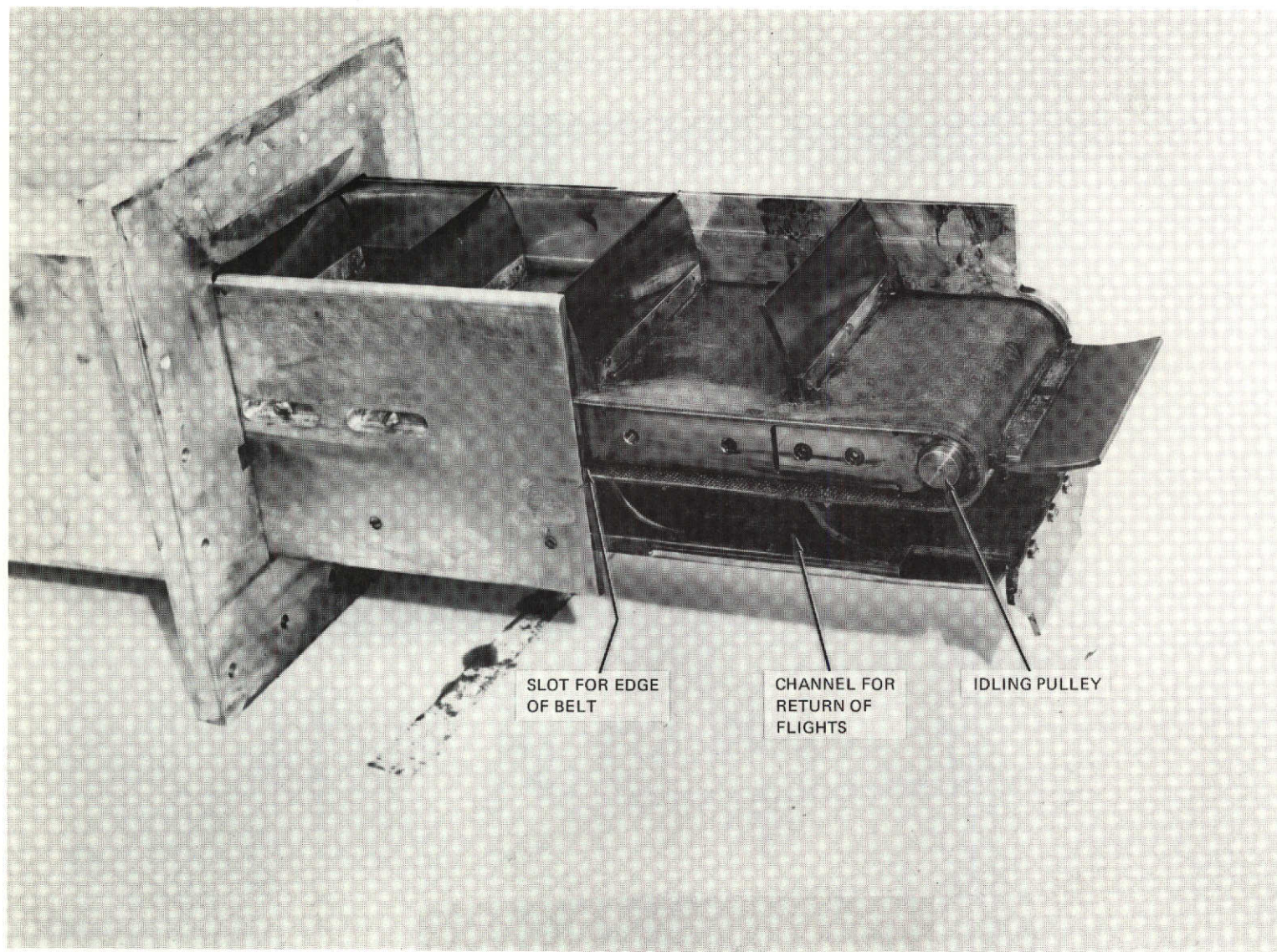


Figure 23 MODIFIED FEED CONVEYOR – PARTLY DISASSEMBLED

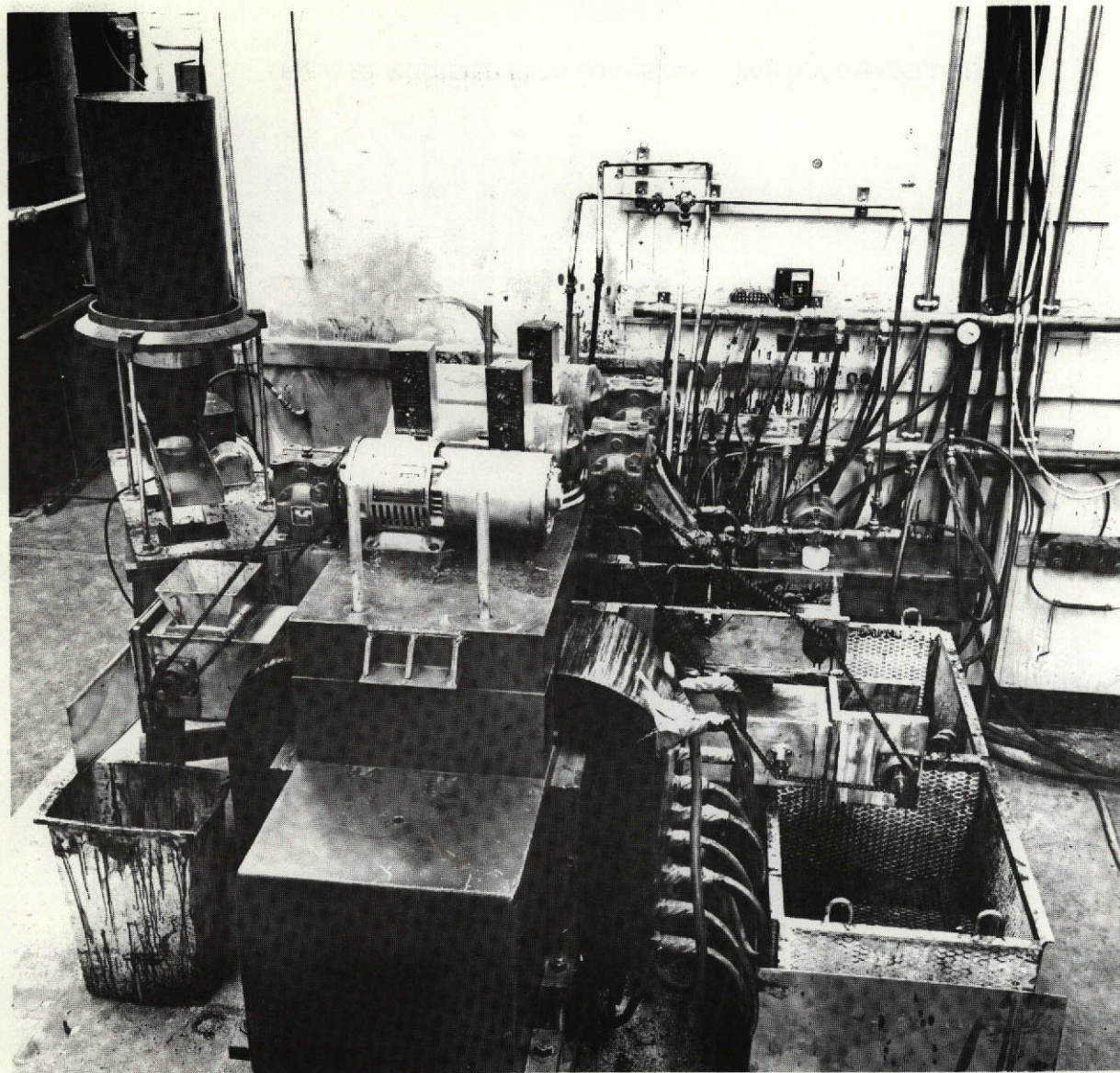


Figure 24 SEPARATION SYSTEM

The upper curve in Figure 12 shows the dependence of H at the lower conveyor on I , and Figure 13 shows the dependence of the magnetic field gradient on I . Figure 25 shows the dependence of M on H for the ferrofluid used. Therefore by knowing I , all factors on the right side of Equation (5) may be obtained, and ρ_{af} the apparent density required to prevent the test object's sinking may be calculated and compared with the object's physical density. This comparison is shown in Table II for shapes typically encountered in car scrap when the test objects were released at the "central release point" (Figure 26). These data show the expected close agreement between the apparent density of the pool and the physical density of the test object, and the lack of dependence on object shape. The average deviation is less than 5%.

In view of this agreement with theory, the study of the effects of object size was limited to brass cubes. The results are summarized in Table III, and as expected show no dependence on size over an eightfold variation in length and a 500 fold variation in volume.

The effects of the release point were studied for the three off center release points shown in Figure 26. The results shown in Table IV show no effect of release point. This was of course to be expected in view of the constancy of the magnetic field gradient over the working volume.

2. Model Mixture Separations

The scrap for these studies was prepared by cutting up plates and bars into pieces between 2 inches and 1/4 inch in size. This size range reflected the expected size range of reshredded nonferrous metals from automobile scrap. The metals used were those to be found in largest amounts in car scrap; various alloys of aluminum (density 2.65-2.75), zinc die cast (density 6.6), and brass (density 8.5). Some preliminary experiments were carried out on separating aluminum-brass mixtures. The separation at a feed rate of about 3,600 lb/hr was 100% accurate. It was therefore decided to confine the balance of these studies to the most difficult of the separations, zinc from brass. The results of these tests are shown in Table V.

In the first test some zinc contaminated the brass fraction. This was probably caused by large brass pieces resting on top of small zinc pieces. When the combined density of such a "sandwich" is greater than 7.4, it sinks. To alleviate this situation, test 2 was carried out at an apparent density of 8.4. This density was too high and resulted in rather substantial contamination of the zinc fraction by brass, probably by the inverse of the mechanism proposed explain the results of test 1. In test 3 the apparent density was adjusted to an intermediate value, 7.9, and complete separation resulted. In test 4 the higher feed rate resulted in minor contamination of the zinc fraction by brass.

In summary, the results of single object studies and the separations of the model mixtures demonstrated good agreement with the predictions of ferrofluid theory.

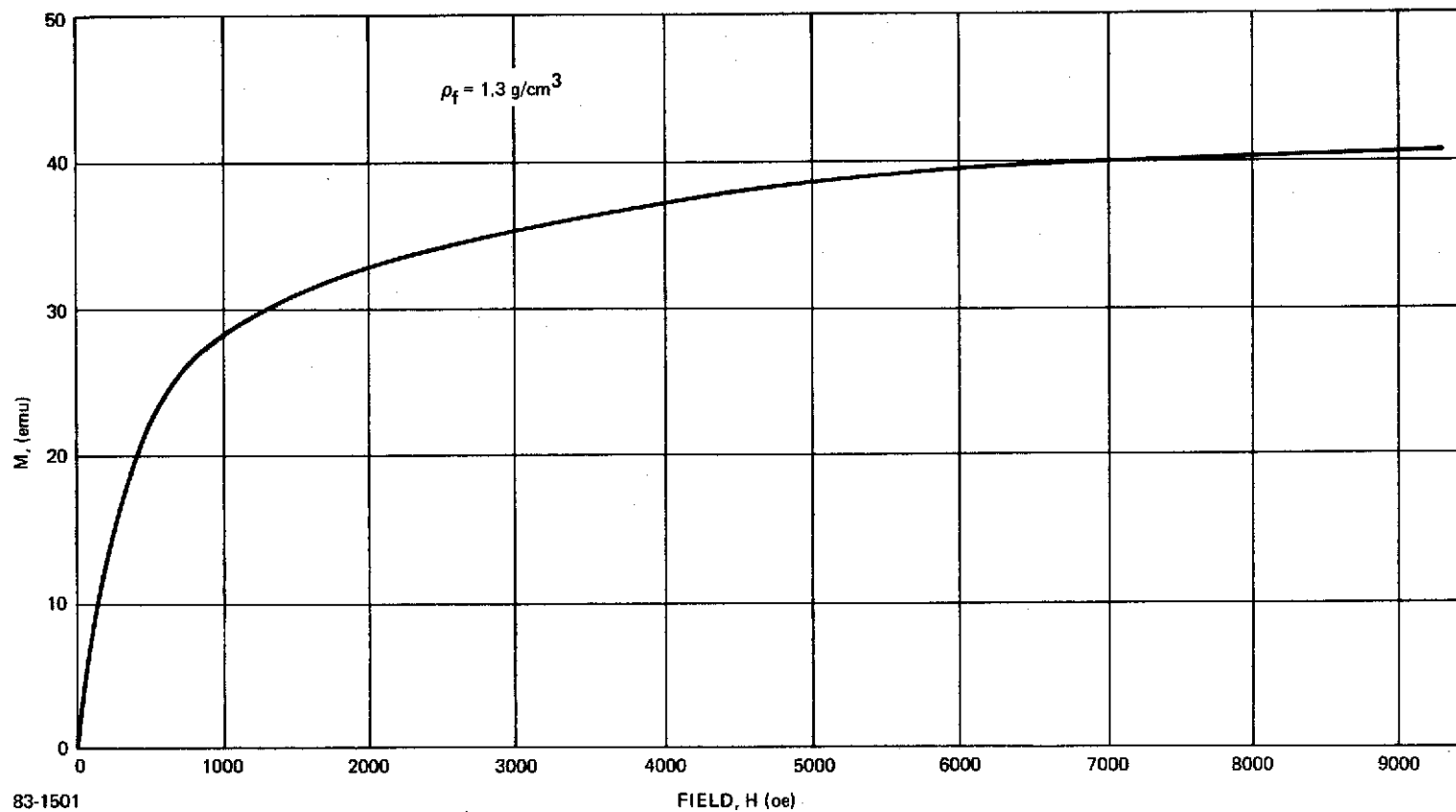


Figure 25 MAGNETIZATION OF FERROFLUID FF1135

TABLE II
EFFECT OF SHAPE

<u>Material</u>	<u>Object Shape</u>	<u>Measured Density</u>	<u>Apparent Density of Ferrofluid Object</u>
Brass	Cube	8.5	8.3
	Plate	8.6	8.0
	Needle	8.6	7.9
Tin	Cube	7.3	6.9
	Plate	7.1	6.7
	Needle	7.4	6.6
Gallium	Cube	6.0	5.7
	Plate	6.7	6.2
Zinc	Cube	6.8	6.0
	Plate	6.7	6.2
Lead-Tin Alloy	Cube	10.5	10.5
	Plate	10.7	10.6
	Needle	10.8	10.6
Stainless Steel	Plate	8.2	8.0
	Needle	8.2	7.8
Lead-Tin Alloy	Plate	9.5	9.2
	Needle	9.5	9.3
Zinc-Aluminum Alloy	Cube	4.2	4.3
	Plate	4.2	3.9
	Needle	4.2	3.9

Cubes: About 3 cm on a side.

Plates: About 6 cm by 3 cm by 0.3 cm.

Needles: About 6 cm long and 0.4 cm in diameter.

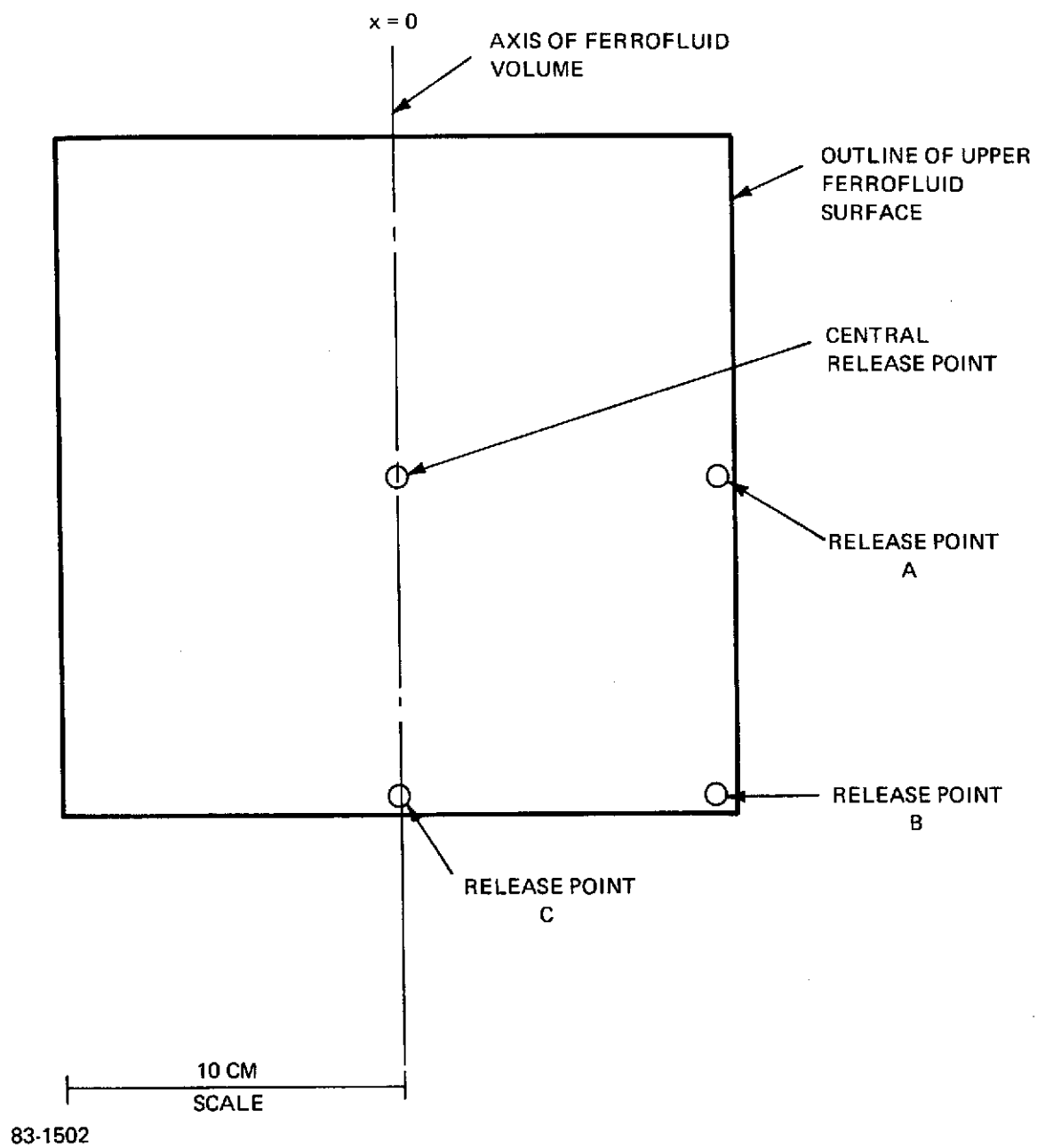


Figure 26 RELEASE POINTS FOR SCRAP PIECES

TABLE III
EFFECT OF SIZE*

<u>Length of Cube Side</u> <u>cm</u>	<u>Volume of Cube</u> <u>cm³</u>	<u>Measured</u> <u>Density</u> <u>g/cm³</u>	<u>Apparent Density of</u> <u>Ferrofluid to</u> <u>Float Object</u>
5	125	8.5	8.2
2.5	15.7	8.5	8.2
1.2	1.73	8.5	8.2
0.63	0.25	8.5	8.2

*Cubes released at "central release point".

TABLE IV
EFFECTS OF RELEASE POINT

<u>Material</u>	<u>Object</u> <u>Shape</u>	<u>Release</u> <u>Point</u>	<u>Apparent Density of</u> <u>Ferrofluid to Float Object</u>
Brass	Cube	A	8.2
		B	8.3
		C	8.2
Gallium	Cube	A	5.7
		B	5.7
		C	5.7
Lead-Tin Alloy	Cube	A	10.5
		B	10.5
		C	10.5
Brass	Plate	A	8.1
		B	8.1
		C	8.1

TABLE V
SEPARATION OF ZINC ALLOY AND BRASS

<u>Test No.</u>	<u>Feed Rate to Separator lb/hr</u>	<u>Average Apparent Density of Ferrofluid g/cm³</u>	<u>Purity of Zinc Fraction</u>	<u>Purity of Brass Fraction</u>
1	2,600	7.4	100.0%	99.5%
2	3,100	8.4	98.7%	100.0%
3	3,700	7.9	100.0%	100.0%
4	5,100	7.9	99.6%	100.0%

D. Separation of Car Scrap

1. Scrap Properties

The principal materials present in the "nonferrous" portion of car scrap, and their physical properties are listed in Table VI. The detailed quantitative composition of car scrap is discussed in a later section of this report. In Table I the range of potential values for the pure recovered nonferrous metals is shown. Zinc has the highest potential total value, followed by copper and aluminum, and stainless steel has the lowest total value. In this phase of the program most emphasis was accordingly placed on zinc separation and least on the separation of stainless steel. The separation of the four valuable metals can be carried out in twelve different sequences. The first step in the sequence chosen, in this work was the separation of aluminum and non-metals from zinc and heavier. This is followed by the removal of zinc from the heavier metals, the separation of copper from steel and the separation of non-metals from aluminum. This particular sequence was chosen because it first does the easiest separations, those having the widest density differences between sinks and floats. This reduces the amount of material to be treated in the subsequent more difficult separations such as non-metals from aluminum and therefore minimizes the size of the separator.

TABLE VI
MATERIALS IN NONFERROUS PORTION OF CAR SCRAP

<u>Material</u>	<u>Approximate Range of Physical Densities</u>	<u>Magnetic Properties</u>
Non-Metals	1 to 2.6	Non-Magnetic
Aluminum Alloys	2.65 to 2.75	Non-Magnetic
Zinc Alloys	6.6 to 6.7	Non-Magnetic to Slightly Magnetic
Copper Alloys	8.3 to 8.9	Non-Magnetic
Stainless Steels	7.8 to 8.0	Weakly Magnetic to Strongly Magnetic
Steel	7.8	Strongly Magnetic

The materials in the nonferrous portion of car scrap have a number of intrinsic and shape related properties that complicate the separations involved. First, some of these metals have magnetic properties. The theory of scrap behavior in a ferrofluid outlined in Appendix A shows that an object that has a magnetic dipole moment acts in the separator as though it had an apparent density higher than its true density (Equation (4b)). This has to be taken into account when adjusting the apparent density of the ferrofluid to a value intermediate between the densities of the materials to be separated. Table VI shows that zinc alloys and stainless steels can be magnetic. The magnetism of the zinc alloys is due to a nickel coating used beneath the outer chromium coating. The stainless steels usually found in car scrap are rendered magnetic by cold working during manufacture or during the shredding process. The magnetism of these two classes of metals does not influence significantly the first step of the separation sequence; aluminum and non-metals from zinc and denser metals, because the rate of separation is controlled by the density difference between the densest of the floats (aluminum) and the least dense of the sinks (non-magnetic zinc). In the second step the magnetism of the zinc does however reduce the density difference between the densest of the floats (slightly magnetic zinc) and the least dense of the sinks (brass). As a matter of fact, it will be seen that the apparent density of a small fraction of the zinc is higher than that of copper alloys, and it therefore contaminates the copper alloy fraction. The situation is more serious when separating the copper alloys from stainless steel because the physical density difference between these classes of metals is quite small, and the magnetic dipole moment of stainless steel can easily raise its apparent density to a higher level than the density of some copper alloys. This could make the separation difficult or impossible.

The principal scrap properties with a potential for harming the completeness of separation are bimaterial fragments, closed shapes with trapped air pockets and loose, non-compact, shapes with a propensity for entanglement. Bimaterial fragments have a density intermediate between the two components and may therefore wind up in either of the fractions involved, depending on the ratio of the two components in the fragment. A frequent bimaterial fragment is a piece of carburetor body (zinc) with an imbedded brass fitting. Insulated copper wire is also frequently found. Nonferrous metal fragments with attached iron fasteners have very high apparent densities because of the iron, and generally wind up in the densest fraction.

Closed shapes with trapped air pockets have lower apparent densities than the density of the material itself; the precise density depends of course on the ratio of solid to gas. Typical fragments having this property are pieces of tubing with crimped ends and pieces of radiator or heater cores.

Fragments having a special propensity for entanglement are frayed multibraid copper wire and fabric swatches.

In a very real sense the objective of the separation studies described in the following sections was to determine to what extent these scrap properties would harm the quality of the separation expected on the basis of the results obtained with the model scrap separations.

2. Scrap Pretreatment

The scrap used in this study was largely obtained from Tewksbury Metals, Inc. This company operates a shredding plant in Tewksbury, Massachusetts, with a separation system very similar to that given in Figure 5 for a "typical" plant. The nonferrous metals are cleaned of most of the accompanying non-metals by air classification. A sample of this classified nonferrous metal stream was reshredded by Tewksbury Metals for Avco's use on a small shredder. Before being subjected to separation, fragments larger than 3 inches as well as large pieces of magnetic steel were removed. This was done in order to simulate more closely the properties of reshredded scrap that would be produced by a process specifically designed to carry out nonferrous scrap pretreatment. This process is described in detail in a later section of this report.

3. Scrap Separations

a. Procedures

In most of the experiments described in this section between 100 and 200 pounds of scrap were separated. The amount of material separated per run was limited by two factors; a) lack of automated ferrofluid recovery equipment, which necessitated hand washing of the separated scrap fractions; a very time consuming process; b) need to hand pick impurities from the separated fractions as one step in the analytical procedure. Handpicking much larger quantities of scrap is impractical.

The scrap was introduced into the separator by means of a vibratory feeder (Figure 24). In the initial phase of the work a laboratory vibratory feeder was used which had inadequate capacity and whose feed rate was controllable to about 30%. Toward the end of the program an industrial vibratory feeder was procured; it had ample capacity and was controllable to within about 15%.

The purity of the aluminum, zinc and copper fractions was estimated by a two step procedure. The first step as mentioned above was to pick out obvious impurities such as pieces of wire and rubber or brass from the "white" metals and "white" metals from the copper alloy fraction. This was followed by measuring the density of the residual metal. Since the range of aluminum alloy and zinc alloy densities in car scrap is very small, the density is a fairly sensitive measure of contamination. This density method does not however apply to the copper alloy fraction because the density range of copper alloys is large. The densities were determined on two pound samples of the scrap by the liquid displacement technique.

b. Aluminum-Zinc Separation (Stage A)

The first step in the separation procedure was the separation of aluminum and non-metals from zinc and the denser metals. This separation was carried out with the apparent density of the ferrofluid (FF 1135, Figure 25) set at 4.5. The feed rate in various runs varied from 2000 to 3000 lb/hr. Since no pure fractions are produced in this separation, the goodness of the separation could be most easily gauged by the purity of products produced in subsequent runs. For example; if rubber fragments showed up in the zinc fraction produced in the course of the zinc-copper split, this would be a clear indication that the first step was responsible for this contamination. Accordingly no attempt was made to measure the purities of the fractions produced in the first step. These fractions were used as feed to the subsequent steps in the process.

c. Zinc-Copper Separation (Stage B)

As mentioned previously, the separation of the zinc alloys is the most important of the separation to be made because these alloys are the largest component of the scrap. In view of the previously noted effect of ferrofluid apparent density on the separation of the model zinc/brass mixture, the first step in this study was to determine the affect of this operating variable. A low feed rate was used in order not to confound the effects of apparent density by variations in the feed rate. The results are shown in Table VII. As expected the contamination of the zinc fraction (floats) increases with increasing apparent density of the ferrofluid. The level of contamination is however quite low. The contamination of the copper fraction (sinks) by zinc alloys is much greater. All of the zinc alloy fragments found in the sinks were magnetic, either due to the nickel undercoat or due to attached iron screws. This made their apparent density much greater than their physical density and accounts for most of this contamination.

TABLE VII
EFFECT OF APPARENT DENSITY ON ZINC SEPARATION

Feed Material: Automobile scrap from which
aluminum and lighter components
had been floated off.

Feed Rate: 300 lb/hr

Ferrofluid: FF 1135

Average Apparent Density of Ferrofluid g/cm ³	<u>Floats</u>		<u>Sinks</u>	
		<u>Percent of Output</u>		
7.1	Zinc Alloys	85.80%	Zinc Alloys	3.34%
	Copper Alloys	0.27%	Copper Alloys & Denser	10.64%
8.1	Zinc Alloys	87.20%	Zinc Alloys	2.72%
	Copper Alloys	0.28%	Copper Alloys & Denser	9.92%

This effect can be minimized by using stronger ferrofluids and a weaker gradient to maintain a constant apparent density level in the ferrofluid pool. The rationale behind this approach can be seen from the following analysis. The apparent density of a slightly magnetic metal in the separator is given by Equation (4b) of Appendix A.

$$\rho_{as} = \rho_s + \frac{M_s G}{g}$$

M_s is nearly constant at the field strengths used in the zinc-copper split.

When the apparent density of the pool is constant while changing the ferrofluid strength, Equation (4a) of Appendix A, shows that the gradient, G , has to vary as shown below.

$$G = (\rho_{af} - \rho_f) \frac{g}{M_f}$$

On substituting this equation into the first one, one obtains;

$$\rho_{as} = \rho_s + (\rho_{af} - \rho_f) \frac{M_s}{M_f} \quad (6)$$

This equation shows that as the magnetic dipole moment (M_f) of the ferrofluid is increased while maintaining ρ_{af} constant (by reducing G), the apparent density of a magnetic solid (ρ_{as}) approaches its physical density (ρ_s).

The effect of this operating change was tested by using a ferrofluid (FF 1147) having a 40% higher magnetization than ferrofluid FF 1135. The results are shown in Table VIII, and are compared to runs at roughly equal feed rates, using FF 1135, shown in Table IX. About 45% of the slightly magnetic zinc fragments found in the copper fractions of runs P79A and P79B have been transferred to the zinc fraction in runs P91 and P92. The untransferred zinc fragments were largely pieces with attached iron screws, which have too high a magnetization to be overcome by this technique. These experiments demonstrate the technical validity of this technique. In commercial practice the benefits of using stronger ferrofluids will have to be weighed against their somewhat higher cost. Since the economic incentives are not very large, direct operating experience will be required to choose the best fluid.

TABLE VIII
EFFECT OF FLUID MAGNETIZATION ON ZINC RECOVERY

Feed Material:	Remixed sinks and floats from Run P79A (Table IX) for Run P91.
	Remixed sinks and floats from Run P79B (Table IX) for Run P92.
Ferrofluid:	FF 1147
Feed Rate:	About 1000 lb/hr
Apparent Ferrofluid Density:	$7.1 \pm 0.1 \text{ g/cm}^3$

<u>Run No.</u>	<u>Floats</u>	<u>Percent of Output</u>	<u>Sinks</u>	
P91	Zinc Alloys	85.60%	Zinc Alloys	2.55%
	Copper Alloys	0.40%	Copper Alloys & Denser	11.53%
P92	Zinc Alloys	85.70%	Zinc Alloys	3.91%
	Copper Alloys	0.25%	Copper Alloys & Denser	10.40%

TABLE IX
EFFECT OF PROCESSING RATE ON ZINC PURITY

Feed Material: Automobile scrap from which
 aluminum and lighter components
 had been removed at about
 2000 lb/hr.

Ferrofluid: FF 135

Apparent Ferrofluid Density: $7.1 \pm 0.1 \text{ g/cm}^3$

<u>Run No.</u>	<u>Feed Rate</u> <u>lb/hr</u>	<u>Floats</u>	<u>Percent of Output</u> <u>Density</u>		<u>Sinks</u>	
P79A	740	Zinc Alloys	84.00%	6.49	Zinc Alloys	5.48%
		Copper Alloys	0.24%		Copper Alloys & Denser	10.30%
P79B	740	Zinc Alloys	83.30%	6.48	Zinc Alloys	5.89%
		Copper Alloys	0.15%		Copper Alloys & Denser	10.80%
P81	2600	Zinc Alloys	82.50%	6.45	Zinc Alloys	8.26%
		Copper Alloys	0.24%		Copper Alloys & Denser	9.20%

The runs in Table IX show the effects of processing rate on product purities. The copper alloy content of the zinc fraction is not significantly affected by the increase in feed rate. The higher zinc alloy content in the copper fraction of the high feed rate run was due to an unusually large number of zinc fragments with attached iron screws. An attempt was made to characterize the copper alloy fragments contaminating the zinc fractions of some of these runs. These copper alloy fragments were largely small pieces of partly insulated wire and pieces having trapped air bubbles such as sintered bearings, crimped tubing and carburetor float bowls. It therefore appears that "mistakes" due to physical entanglement are rare, most "mistakes" are caused by the presence of bimaterial pieces. This suggests that a somewhat greater degree of reshredding would be beneficial.

The densities of the zinc alloys (after copper alloy removal) were somewhat lower than the expected density range (6.6-6.7). This discrepancy may be due to air bubbles trapped between scrap fragments in the liquid displacement column used to measure the density, or it may be due to the presence of aluminum. The latter would indicate that Stage A of the separation was at fault. If it is assumed that the density discrepancy is due to the presence of aluminum, then the aluminum alloy content would be about 1%. This amount of aluminum would not detract from the value of the zinc fraction because the zinc die casting alloys contain over 4% aluminum as a normal ingredient.

d. Non-Metal-Aluminum Separation (Stage C)

The "floats" fraction from the Stage A separation is separated in Stage C into non-metals and the aluminum alloys. This separation was carried out at an apparent density (2.6) very close to that of aluminum in order to minimize the contamination of aluminum by glass fragments which can have densities very close to that of aluminum. The results are shown in Table X. The purity of the aluminum fractions is well in excess of 99.5% as gauged by the non-metals and copper wire content. After these impurities were picked out, the density indicated that the residue was essentially pure aluminum alloy. Most of the non-metals that were picked out were pieces of rubber, glass was found infrequently. The copper wire was partly insulated, and its density was therefore probably close to that of aluminum.

At the higher processing rate about 5% of the aluminum was lost to the non-metals fraction. This loss could be reduced by operating at a somewhat lower apparent density, at the expense of decreased purity of the aluminum fraction. The best strategy to use can only be found from full-scale plant operation, where sufficient material would be produced to determine its value to secondary aluminum smelters as a function of purity.

e. Copper-Steel Separation (Stage D)

The sample of scrap was prepared for this study by floating off all components less dense than 7.8 g/cm^3 , which included zinc, aluminum and the non-metals. The balance of the sample consisted of copper alloys, stainless steel alloys and minor amounts of lead and small pieces of iron attached to large non-magnetic pieces of scrap.

The separation of stainless steel from the copper alloys of automobile scrap presents considerable difficulties. The physical density of stainless steel ranges from about 7.8 to 8.0 g/cm^3 , while the density of copper alloys ranges from 8.9 down to about 8.3 g/cm^3 . The separation of the least dense copper alloys from the densest stainless steels is therefore reasonably difficult. An even greater source of difficulty was the magnetism of the stainless steels. Although most of the stainless steels used in automobiles are classified as "non-magnetic", they do become magnetic on being subjected to cold working during their manufacture and during shredding.

TABLE X
EFFECT OF PROCESSING RATE ON ALUMINUM PURITY

Feed Material: Aluminum and "lighter"
fraction of automobile
scrap from which zinc and
heavier had been removed
at about 2000 lb/hr.

Ferrofluid: FF 1135

Apparent Ferrofluid Density: $2.6 \pm 0.1 \text{ g/cm}^3$

<u>Run No.</u>	<u>Feed Rate</u> <u>lb/hr</u>	<u>Floats</u>	<u>Percent of Output</u>		<u>Sinks</u>	<u>Density</u>
P85	1800	Aluminum Alloys	5.24%	Aluminum Alloys	91.10%	2.74
		Non-Metals	3.41%	Non-Metals	0.12%	
				Copper Wire	0.16%	
P87	1300	Aluminum Alloys	2.74%	Aluminum Alloys	93.20%	2.74
		Non-Metals	3.70%	Non-Metals	0.22%	
				Copper Wire	0.17%	

The situation is therefore very similar to that encountered with the slightly magnetic zinc, and the use of a stronger ferrofluid was accordingly thought to be appropriate. As a preliminary step the separation was studied with the weaker ferrofluid, with the results shown in Table XI.

The stainless steel was divided into magnetic and non-magnetic categories by holding individual pieces near a magnet and determining their response. This procedure while useful, clearly under estimates the amount of magnetic steel, because some of the steel may be too weakly magnetic for its response to be felt.

TABLE XI
EFFECT OF APPARENT DENSITY ON
COPPER ALLOY/STEEL SEPARATION

Ferrofluid: FF 1135
Average Apparent Density: 8.85 g/cm³

	<u>Percent of Output</u>	
	<u>Floats</u>	<u>Sinks</u>
<u>Copper Alloys</u>	22.2	45.0
<u>Stainless Steel</u>		
Non-Magnetic	8.9	3.3
Magnetic	<u>0.0</u>	<u>20.6</u>
	31.1	68.9

Ferrofluid: FF 1135
Average Apparent Density: 8.55 g/cm³

	<u>Percent of Output</u>	
	<u>Floats</u>	<u>Sinks</u>
<u>Copper Alloys</u>	15.8	49.6
<u>Stainless Steel</u>		
Non-Magnetic	9.1	13.3
Magnetic	<u>0.0</u>	<u>12.1</u>
	24.9	75.0

It is apparent that only the non-magnetic steel could be floated, while the sinking stainless steel has a substantial amount of magnetic matter. At the 8.85 g/cm^3 density level, which is well above the physical density of steel, almost all of the steel in the sink fraction is magnetic. In an attempt to reduce the apparent density of stainless steel the separation was repeated, using the stronger ferrofluid, FF 1147. The results are presented in Table XII. A comparison of these results with those obtained in the second run of Table XII, clearly demonstrates the effect of the higher magnetization. There is no longer any non-magnetic stainless steel in the sink fraction, suggesting that most of the non-magnetic steel was in fact slightly magnetic. Another interesting outcome of this experiment was the increase in the fraction of copper in the floats. This immediately suggested that the copper was slightly magnetic! When brought near a magnet a majority of the copper fragments did indeed exhibit a slight magnetic response. Since these copper fragments were largely pieces of radiators and heater cores, we attribute this response to an internal coating of magnetic iron oxides picked up from the engine coolants.

TABLE XII
EFFECT OF FLUID MAGNETIZATION ON
COPPER ALLOY/STEEL SEPARATION

Ferrofluid: FF 1147

Average Apparent Density: 8.61 g/cm³

	<u>Percent of Output</u>	
	<u>Floats</u>	<u>Sinks</u>
<u>Copper Alloys</u>	43.1	15.5
<u>Stainless Steel</u>		
Non-Magnetic	11.6	0.0
Magnetic	<u>15.5</u>	<u>14.2</u>
	70.2	29.7

As a check on these hypotheses, the "non-magnetic" portions of the sinks and floats were handpicked and their separation was carried out under the conditions shown in Table XIII. The separation of the stainless steel from the copper alloys is virtually complete; the sinks contain only 2.5% stainless steel. Unfortunately the stainless steel fraction (the floats) was heavily contaminated with copper. The contaminating copper consisted almost entirely of pieces of radiator. Radiators are made of pure copper having a density of 8.9 g/cm^3 , it was therefore hypothesized that the floating of these pieces was due to sealed off air voids, which caused them to have an apparent density considerably lower than 8.9 g/cm^3 . When these pieces were cut open, these air voids were found.

TABLE XIII
SEPARATION OF "NON-MAGNETIC"
COPPER AND STEEL ALLOYS

Ferrofluid: FF 1135
Average Apparent Density: 8.35 g/cm^3

	<u>Percent of Output</u>	
	<u>Floats</u>	<u>Sinks</u>
<u>Copper Alloys</u>	13.8	71.5
<u>Stainless Steel</u>	<u>12.9</u>	<u>1.8</u>
	26.7	72.3

On the basis of these results it is apparent that the separation of the copper alloys from stainless steel in automobile scrap presents formidable difficulties. The magnetism of the steels makes their apparent densities overlap that of the copper alloys, and the closed air voids in some of the copper fragments which makes their densities overlap that of the stainless steels. It is therefore not possible to recover a pure copper alloy or a pure stainless steel fraction. It may be possible to recover some of the strongly magnetic stainless steels by using low magnetization ferrofluids and high gradients, in order to float the copper and low magnetization steels while sinking the strongly magnetic steels. Perhaps reshredding this fraction to a smaller size may open up the air voids of the radiator fragments to access by ferrofluid. In view however of the small amount of stainless steel in the "non-magnetic" fraction of car scrap ($< 2\%$), and the low economic incentive for its recovery, no further work was carried out on this separation.

E. Ferrofluid Recovery

The recovery of ferrofluid that coats scrap leaving the separator consists of two steps; washing the scrap with a suitable solvent and boiling away the solvent, to recover the ferrofluid. In the course of this program, more attention was paid to the second step than to the first, because it was felt that commercial degreasing equipment would be reasonably well suited for the first step. In the laboratory, heptane was used as the solvent because it was more compatible with the ventilation facilities. In commercial practice, a solvent such as trichloroethane would be used because it presents no fire hazard. The actual washing of the scrap was carried out by placing it in 5 gallon, perforated bottom, pails and pouring room temperature heptane onto the top of the scrap. This procedure required about 2 to 3 gallons of heptane to clean 4 to 5 gallons of scrap. This is about equivalent to 83 gallons per ton.

The amount of ferrofluid coating the scrap was difficult to estimate accurately from these studies because only about 100 pounds of scrap could be washed at a time. A rough estimate obtained from these experiments is that 2.5 pounds of ferrofluid were removed from the separator per 100 pounds of scrap.

The second step of ferrofluid recovery, boiling the solvent from the ferrofluid-solvent solution was carried out in a batch 12 liter glass still. The evaporation of the solvent was continued until the vapor temperature reached 140°C. At this point the ferrofluid was effectively reconcentrated to its initial magnetization. If trichloroethane (B.P. 74°C) were used as the solvent rather than heptane (B.P. 98°C) a final temperature of 120°C would probably suffice to reconcentrate the fluid. The most careful record of ferrofluid recovery was kept from late February to late March. During this period about 1500 pounds of scrap were separated, about 100 pounds of ferrofluid were recovered and recycled and 6.0 pounds of ferrofluid had to be added to the ferrofluid reservoir to make up for ferrofluid losses. The reason that 100 pounds of ferrofluid had to be recovered for only 1500 pounds of scrap (6.67 lb ferrofluid per 100 lb scrap), is that the separator was washed with solvent at the conclusion of each day, and no attempt was made to segregate these washings from the scrap washings. The average magnetization of the recycled ferrofluid was 434 gauss at 3.5 kilo oersted, whereas, the initial magnetization of the ferrofluid was 416 gauss at the same field level. The higher average magnetization of the recovered ferrofluid was due to overheating of two batches and evaporation of a portion of the kerosene which is the base of this ferrofluid. The ferrofluid loss experienced during this monitoring period, 6 pounds, or 8 pounds per ton, was due largely to accidental spills. There was no indication of ferrofluid decomposition in the solvent recovery still; during the entire period no buildup of sludge or caking on the inside of the still pot occurred. Likewise, the amount of ferrofluid left on the scrap after washing was insignificant.

III. PROCESS DESIGN

A. Basis for the Plant Design

1. Scrap Supply

The objective of automobile shredding is the recovery of uncontaminated steel fragments of a high bulk density. The shredders achieve this objective when operated to produce fragments no larger than about 8 inches. This degree of fragmentation effectively frees the steel from contaminants such as copper. The freed steel is separated from the non-magnetic material by magnetic separators suspended over the conveyor that carries the shredded material.

The residual "non-magnetic" material is, however, contaminated with some small iron pieces, because the objective of the steel recovery is to obtain relatively clean steel even if it does result in minor losses of magnetic material. A Bureau of Mines study of the non-magnetic residue from three shredders found their material to be of the average composition shown in Table XIV. The combustible fraction consisted largely of rubber and the non-metallic non-combustibles consisted largely of glass and dirt.

TABLE XIV
COMPOSITION OF NON-MAGNETIC RESIDUE
OF AUTOMOBILE SHREDDING

<u>Component</u>	<u>Percent</u>
Nonferrous	21.4
Ferrous Metals	11.9
Combustibles	24.4
Non-metallic Non-combustibles	<u>42.3</u>
	100.0

Source: Bureau of Mines Technical Progress Report

TPR 31

Recovery of the Nonferrous Metals from
Auto Shredder Rejects by Air Classification
by C.J. Chingren, K.C. Dean and LeRoy Peterson.

The same Bureau of Mines study also estimates the distribution of metals in the nonferrous metals fraction. A comparison of this estimate with Avco's estimate is shown in Table XV. Avco's estimate is based on interviews with shredder operators as well as Bureau of Mines studies. Neither estimate is complete, but the agreement for the important metals, zinc, aluminum and copper is satisfactory.

TABLE XV
NONFERROUS METAL CONTENT OF AVERAGE SHREDDED AUTOMOBILE

<u>Metal</u>	<u>Bureau of Mines Estimate (lb)</u>	<u>Avco Estimate (lb)</u>
Zinc	45	40
Aluminum	9	10
Copper	5	5
Stainless Steel	-	2
Lead	2	-

2. Feed Preparation

In order to transform this material into an economically attractive feed to the ferrofluid nonferrous metal separation process, it must be subjected to three processing steps:

- size reduction
- removal of non-metallic material
- removal of magnetic or ferrous material

The chief objective of further size reduction is to reduce the size of the scrap pieces to a size no larger than 2 to 3 inches. This is required in order to process the material in a magnetic separator having a gap of about 8 inches. It is possible to build separators having a larger gap, and thus to process larger scrap pieces. However, the weight of the magnet is proportional to the gap width cubed and the electrical power to run it is proportional to the gap width to the fourth power. Because these relations imply very rapid increases in capital and operating costs with increasing gap width, the overall cost of the separation system is lowest when using magnets of about an 8 inch gap and reshredding the scrap to a size separable in such a magnet.

The reshredding step has certain ancillary benefits. It frees mechanically linked fragments of dissimilar metals, iron screws attached to pieces of zinc trim for example, and thus makes the subsequent separation steps more accurate. The size reduction step also minimizes the size range of the material and thus makes the subsequent air classification step for removal of non-metallics more efficient. The size reduction also increases the bulk density of the metals; a high bulk density is desirable for shipping economies.

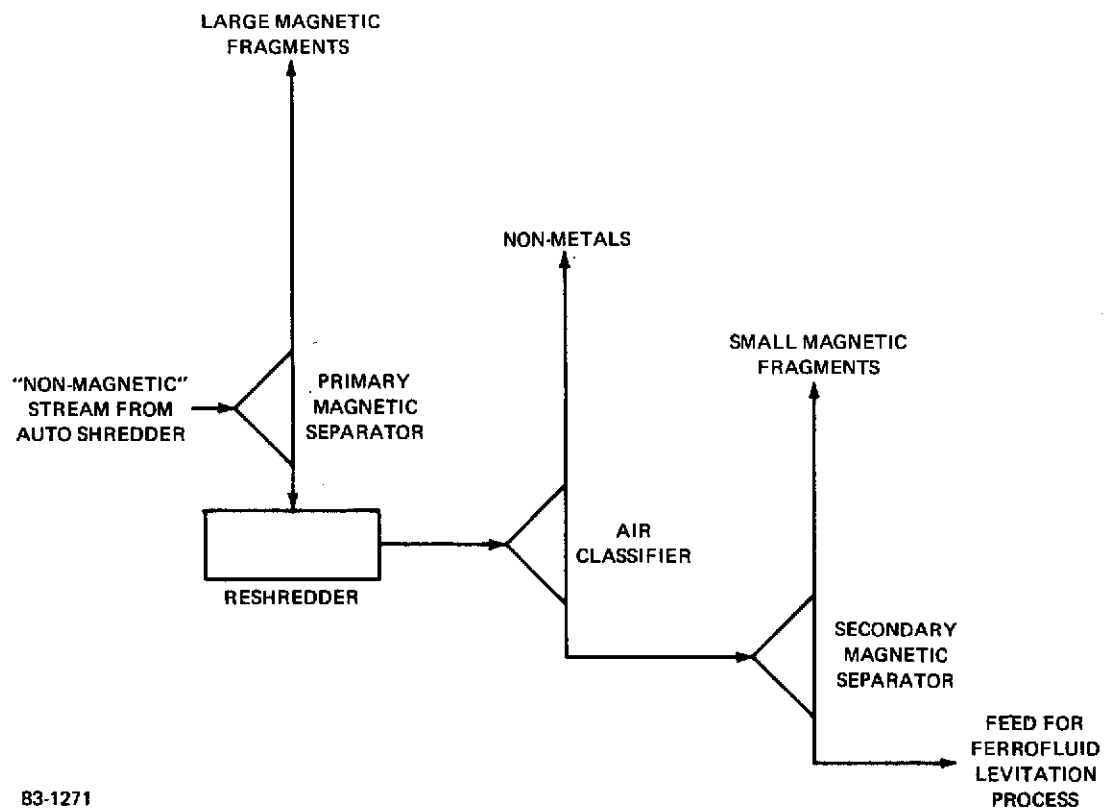
Removal of most of the non-metals prior to ferrofluid separation is desirable for two reasons. The non-metals such as upholstery and foam rubber absorb ferrofluid readily and its recovery by a degreasing solvent is difficult. Prior removal of these absorptive materials is therefore desirable in order to reduce ferrofluid losses. A Bureau of Mines study has shown that about 80% of the non-metals can be removed by a simple air classification step. It appears that this method of removing the bulk of the non-metals is more economical than ferrofluid levitation. It is therefore proposed to use it as part of the feed pretreatment sequence.

The removal of the residual magnetic material is required in order to protect the reshredder from damage by relatively large iron pieces that occasionally slip through the steel recovery magnetic separator, and to reduce the volume of metal that is separated by ferrofluid levitation.

A feed preparation sequence meeting these requirements is shown in Figure 27. In addition to the primary magnetic separator ahead of the reshredder, a second magnetic separator is placed after the air classifier to recover small magnetic fragments freed during the reshredding process. This step is extremely inexpensive and increases the purity of the copper alloys recovered in the subsequent steps.

In this feed preparation process the air classifier for removal of non-metals is placed after the reshredder. This relative placement of these two units is expected to have two important advantages over the reverse placement. The first is that the reshredding step will free mechanically linked metal-non-metal fragments. The second is that reshredding reduces the size range of the material fed to the air classifier, thus making the air classification step more accurate. The reason for this is that air classification depends both on the size of the objects to be separated and on their density. Consequently a reduction in size variation, makes the separation more dependent on density difference. Since the objective of this air classification is to separate low density non-metals from high density metals, a decrease in size variance makes the separation more accurate. It is expected that this increased accuracy will reduce the non-metal content of the metals fraction to about 10% from the 25% value obtained by the Bureau of Mines investigators when using unreshredded scrap.

Based on this assumption and the estimate of nonferrous metal composition shown in Table XV, an estimate of the overall composition of the feed to the ferrofluid separation portion of the plant is shown in Table XVI. It is to be emphasized that this is an estimate of an average composition. In actual practice the composition will vary considerably, depending on the operation of the car shredder and the efficiency of the feed preparation equipment.



83-1271

Figure 27 FEED PREPARATION SEQUENCE

TABLE XVI
NOMINAL COMPOSITION OF MIXED NONFERROUS METALS

<u>Material</u>	<u>Weight Fraction</u>	<u>Pounds Per Car</u>	<u>Pounds Per Ton of Feed</u>	<u>Pounds Per Ton of Metal</u>
Zinc	0.635	40.0	1270	1403
Aluminum	0.159	10.0	318	351
Copper	0.079	5.0	158	175
Stainless Steel	0.032	2.0	64	71
Non-Metals	<u>0.095</u>	<u>6.0</u>	<u>190</u>	<u>210</u>
	1.000	63.0	2000	2210

It is the intent of this report to concentrate almost exclusively on the ferrofluid separation portion of the separation process, because it is felt that feed preparation involves established technology, and the equipment design would be the responsibility of the shredder operator. It is nevertheless interesting to analyze the important economic and technical trade offs made in designing the feed preparation system.

a. Reshredder

The most important piece of equipment used in feed preparation is the shredder. For a nonferrous metal plant having a capacity of less than 5 tons per hour the size of the shredder is controlled by the size of the scrap pieces to be reshredded rather than the weight of material. The minimum capacity of a shredder suited for this application is therefore about 5 tons per hour. The cost of such a machine with the ancillaries is about \$21,000. Thus a small automobile shredding plant generating 8 tons of nonferrous metal scrap per day would operate the secondary shredder for less than two hours per day. It is therefore apparent that the reshredding process is less expensive in a large plant where the reshredder can be used more hours each day.

b. Air Classifier

The air classifier removes most of the non-metals from the reshredded stream. Most commercially available equipment should be capable of processing at least 5 tons per hour of this material. The same economics of scale that hold for the reshredder also apply to this equipment. The air classifier actually consists of three subsystems. The separator is a vertical chamber with an upward moving air stream into which the reshredder scrap is dropped. The metals fall out of the bottom of the chamber, while the non-metals are conveyed out through the top into a cyclone. In the cyclone the pieces of scrap are disengaged from the air stream, which is drawn by a fan into the dust collection system. The dust collection system is generally the bag house type. For a 5 ton per hour processing rate, the purchased cost of the air classification system is estimated to be about \$7,000.

c. Magnetic Separators

The primary magnetic separator must remove, with very high probability, large iron pieces that could seriously damage the reshredder. A magnetic belt separator hung over the conveyor which feeds the reshredder appears most suited for this purpose. The secondary magnetic separator, can be a simpler magnetic pulley type. The cost of both separators is about \$12,000.

On the basis of discussion with shredder operators, it is estimated that the cost of feed preparation at this 5 ton per hour rate will be about \$12 per ton.

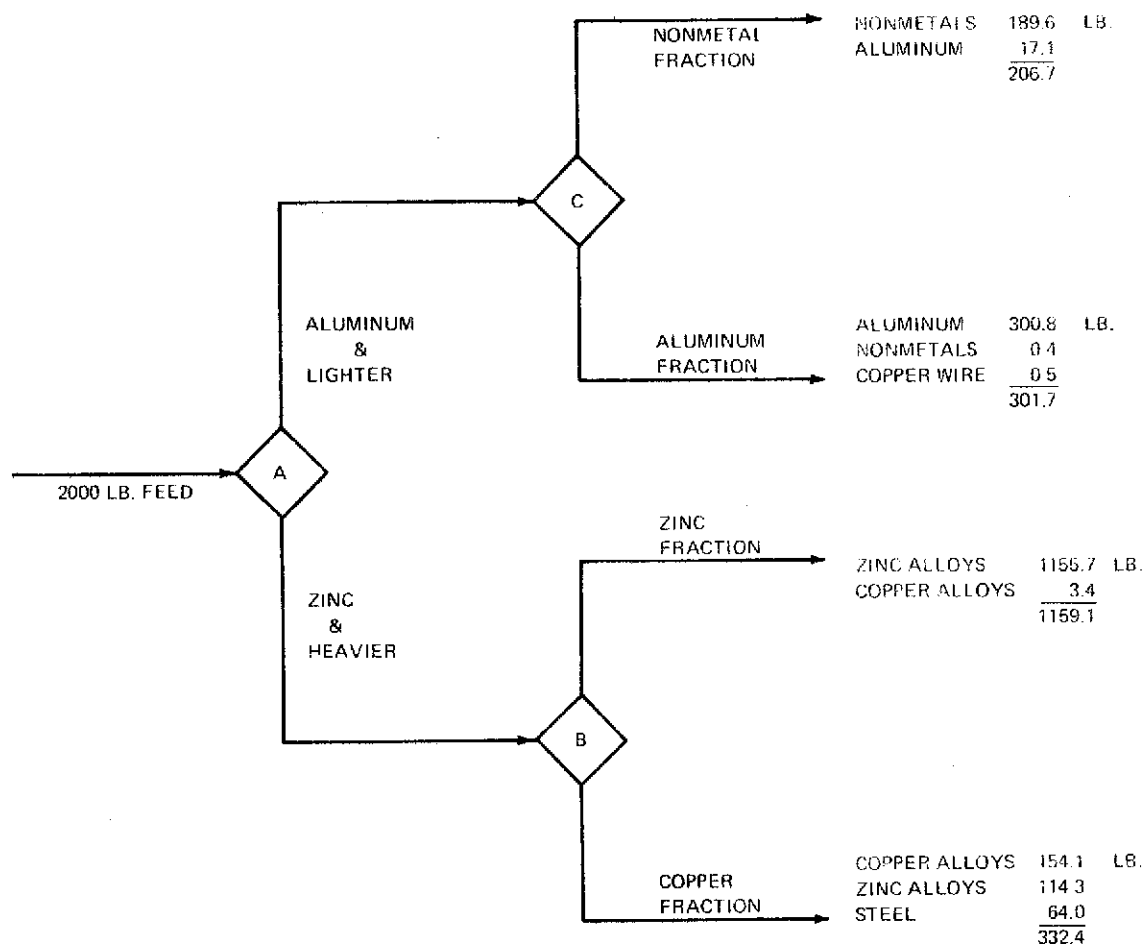
3. Separations to be Made

In the course of the experimental portion of this program, it has been shown that good quality aluminum and zinc fractions could be recovered from reshredded automobile scrap at high processing rates. The separation of copper from stainless steel did not prove practical for reasons previously discussed. The experimental purities obtained will be assumed to apply also to the larger separators that would be used industrially. Table XVII summarizes these experimental results. Again it must be realized that these processing rates are only typical values. Higher rates are possible, with perhaps some loss in purity. Lower rates may be required with particularly entangled scrap. The same caution must be applied to the purities and recoveries.

TABLE XVII
BASIS FOR PROCESS DESIGN-EXPERIMENTALLY
OBTAINED SEPARATION RESULTS

<u>Separation</u>	<u>Feed Rate</u>	<u>Results</u>
Aluminum and lighter from zinc and heavier	2700 lb/hr	The separated fractions were used as feed to the subsequent separation stages.
Aluminum from rubber and lighter	1800 lb/hr	94.6% of the aluminum recovered in 99.8% purity. 5.4% of the aluminum lost with non-metals.
Zinc from copper and heavier	2600 lb/hr	91% of the zinc recovered in 99.6% purity. 9% of the zinc wound up in copper fraction.

Using the scrap composition of Table XVI and the separation results of Table XVII a material balance for a nonferrous metal separation system is calculated and shown in Figure 28. This material balance will be assumed to hold for the plant design to be presented below.



83-1503

Figure 28 NONFERROUS METAL SEPARATION SYSTEM MATERIAL BALANCE

4. Separator

The separation rates and purities obtained on the separator constructed for the current program are shown in Table XVII of the previous section. This separator can process up to about 3000 pounds per hour of scrap. In commercial separation of automobile scrap a separation rate about twice as high is desirable. The analysis of ferrofluid levitation presented in Appendix A predicts that the separation rate is proportional to the horizontal cross-section of the ferrofluid pool. It is therefore possible to double the capacity by doubling the length of the pool. The analysis in Section 3 of Appendix A predicts that scrap can reach this extra length from the inlet of the separator if the feed conveyor velocity is doubled. Doubling the velocity presents no technical problems. A magnet designed to accommodate a ferrofluid pool 16 inches (40.8 cm) long is presented in Appendix B.

In this design, only the central 16 inches of the "z" dimension are used to accommodate the ferrofluid pool, leaving 7 inches of unused interpole distance between the working volume and the edge of the poles, whereas in the present magnet only 4 inches were left on either side of the ferrofluid pool. It is probable that only 4 inches would also be required in the large magnet, but an extra 3 inches were allowed between the pole edge and the working volume, in order to reduce the risk of having a varying magnetic field gradient at the edge of the working volume.

In the present separator the width of the working volume (dimension k of Figure B3) is 8 inches. The ferrofluid pool occupies, however, only the central 6.1 inches of this working volume. About 1 inch of working volume on each side is taken up by the separator walls. This simplifies the design of the materials handling system, at the expense of a 25% reduction in system capacity. In the larger commercial separator, the materials handling system would be designed so that the entire working volume width of 8 inches would be occupied by the ferrofluid pool. The resulting horizontal cross-section of the ferrofluid pool would be 16 x 8 inches, compared to the present 8 x 6 inches; the capacity of this large separator would therefore be about 2.6 times as large on the present one.

The comparison made in Appendix B between the present magnet and the proposed large magnet shows very clearly the economics of scale obtained with the larger design. Although the large magnet is expected to have 2.6 times the capacity of the small magnet it weighs only 1.8 times as much and consumes only 1.33 times as much power.

Table XVIII lists the capacity of the present separator and the proposed larger separator for the three separations to be made by this plant. These capacities will be used as the basis for the plant design.

5. Ferrofluid Recovery

As previously discussed, ferrofluid losses under laboratory conditions were about 8 pounds per ton of scrap. Most of this loss being apparently due to the manual handling of the scrap and the solvent ferrofluid solutions.

TABLE XVIII
CAPACITIES OF SEPARATORS

<u>Separation</u>	<u>Capacity (lb/hr)</u>	
	<u>Present Separator</u>	<u>Proposed Separator</u>
Aluminum and lighter from zinc and heavier	2,700	7,100
Zinc from copper and heavier	2,600	6,800
Aluminum from non-metals	1,800	4,700

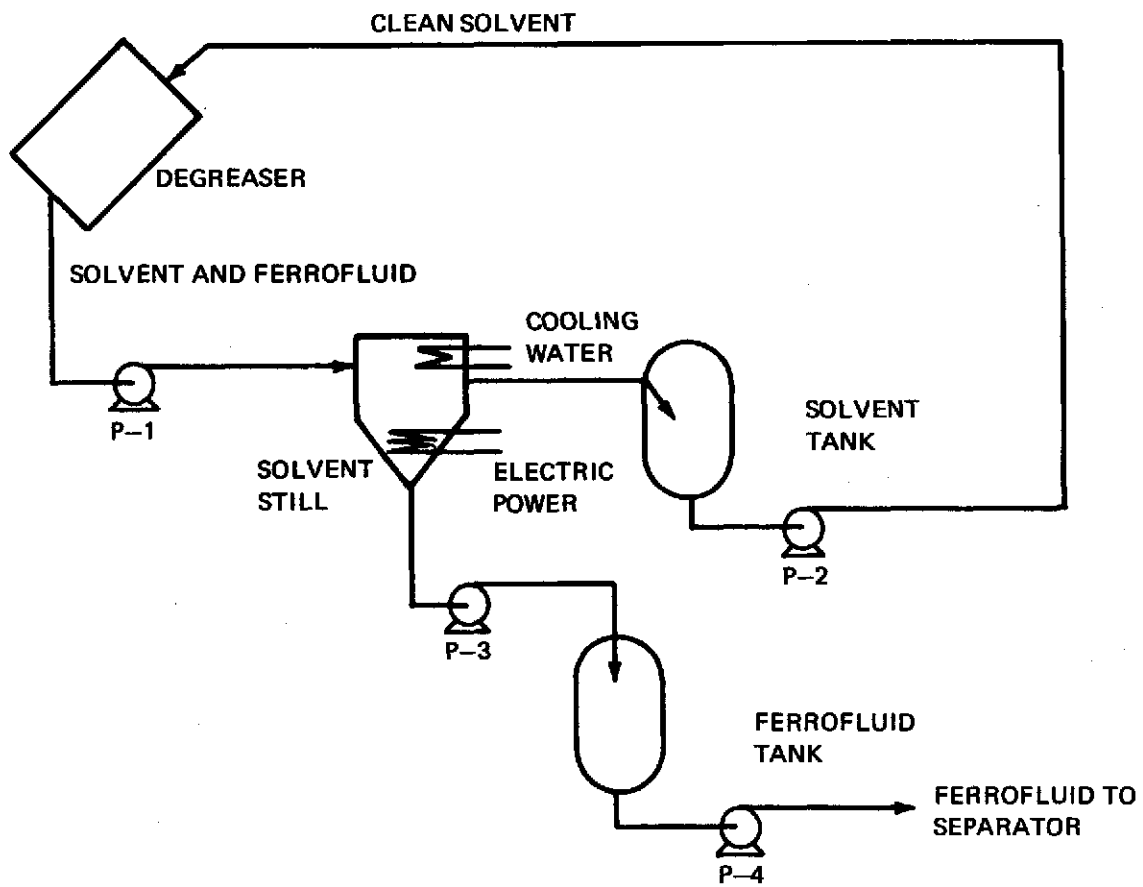
It will therefore be assumed that in a commercial operation with scrap handled automatically, and long running periods between separator cleaning, that the ferrofluid losses will be considerably lower. The specific estimate of ferrofluid loss that has been used up to now, one quart of about 2.7 pounds per ton will continue to be used. The losses of solvent are estimated to be about 1.5 gallons per ton of scrap. This is however a very rough estimate.

Figure 29 shows a schematic diagram of a ferrofluid recovery system proposed for commercial use, and its key operating parameters as a function of scrap processing rates. Table XIX lists the capacities of the various pumps and the storage tanks as a function of scrap degreasing rate.

TABLE XIX
SIZE OF SYSTEM COMPONENTS-SOLVENT RECOVERY

<u>Scrap Processing Rate (Tons/Hr.)</u>	<u>Pump Capacities (gpm)</u>				<u>Tank Volumes (Gallons)</u>	
	<u>P-1</u>	<u>P-2</u>	<u>P-3</u>	<u>P-4</u>	<u>Solvent</u>	<u>Ferrofluid</u>
1	1.54	1.46	0.08	0.08	500	100
2	3.08	2.92	0.16	0.16	1,000	200
5	7.70	7.30	0.40	0.40	2,500	500

The pumps were sized on the basis of using 88 gallons of solvent per ton of scrap and a ferrofluid carryover from the separator of 50 pounds of fluid per ton of scrap. The size of the solvent and ferrofluid tanks is somewhat arbitrary, but more than ample to supply the inventory of these fluids in the degreaser and separator, as well as the operating losses.



TONS SCRAP DEGREASED/HOUR	ELECTRIC POWER REQUIRED, kw	COOLING WATER REQUIRED, gal/hr
1.0	42.7	427
2.0	85.4	854
5.0	213	2130

83-1504

Figure 29 FERROFLUID RECOVERY SYSTEM

B. Basis for the Cost Estimates

1. Capital Cost

The capital cost of the plant will be estimated from the purchased cost of the major pieces of process equipment by multiplying the total purchased cost by a factor which takes into account the expenditures required to transform the purchased equipment into an operating plant. This is an accepted technique of estimating plant costs at the budget planning stage, and is accurate to within 15-20%. The specific technique of estimation is one developed by K.M. Guthrie and described in detail in the March 24, 1969 issue of Chemical Engineering. In this technique all cost elements of constructing the plant can be related to the purchased equipment costs, by multiplying the purchased equipment cost by different factors. These factors vary in some cases with the magnitude of the project and mix of liquid and solid handling equipment. In Appendix C, these factors are listed for the direct and indirect cost elements, assuming that the plant will cost less than \$1,000,000 and will be predominantly of the solids handling type.

The final relation for estimating the erected cost of the plant, from the purchased cost of the equipment is:

$$\text{Erected Cost} = 2.232 \times \text{Purchased Cost}$$

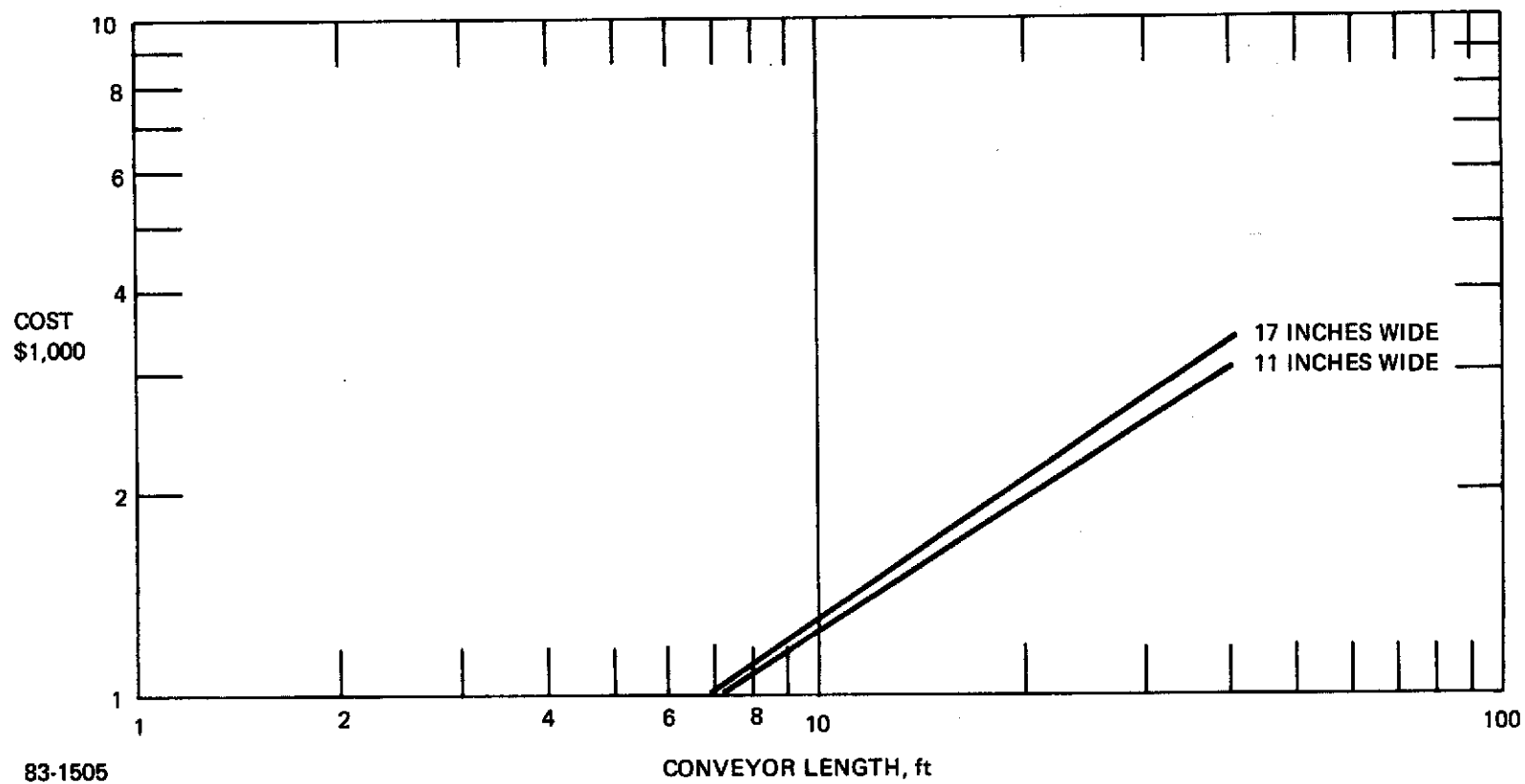
In the following sections, methods for estimating the purchased costs or FOB costs of the principal plant components are developed.

a. Magnet Costs

Two sizes of magnets and associated material handling equipment can be used in some of the plant design to be presented. The small magnet would be essentially identical to the magnet constructed under the present NASA contract. The larger magnet is designed to have 2.6 times the scrap processing capacity of the present magnet. The magnets are contrasted in detail in Appendix B. The present magnet was constructed under a sub-contract for \$17,500. It is estimated that duplicates of this magnet should be obtainable for \$15,000, reflecting a savings in engineering and other overhead costs which apply only to the first model. The large magnet would cost about \$23,400. The materials handling systems, or separators, would be essentially identical for the two magnets. The separator for the larger would be a stretched out version of the smaller one, with somewhat more powerful conveyor motors. On the basis of the experience gained in building the present separator we estimate that its duplicate should be obtainable for \$5,000, and that the larger version should be obtainable for \$6,000. Thus, the purchased costs of the duplicate of the present magnet-separator will be \$20,000 and that of the large magnet-separator \$29,400. The cost of rectifiers for powering the magnets is estimated to be \$50 per Kw.

b. Conveyor Costs

Two types of conveyors are used in the plant designs. For purely horizontal transport of scrap, vibratory conveyor are specified. The approximate costs of these conveyors were obtained from conveyor manufacturers and are plotted in Figure 30. These costs are accurate to about 10%. For non-horizontal transport of scrap, piano hinge conveyors are specified. These



83-1505

Figure 30 ESTIMATED PRICE OF VIBRATORY CONVEYORS

conveyors have 4 inch high cleats which enable them to elevate scrap at an angle of up to about 60°. These conveyors typically consist of a horizontal segment, followed by a rising section at an angle of 45°, and concluding with another horizontal segment. The cost of these conveyors is calculated from their total length and the number of bends (two for the above conveyors). A cost formula recommended by a manufacturer of such conveyors designed for scrap handling is presented in Table XX.

TABLE XX
COSTS OF PIANO HINGE CONVEYORS

<u>Component</u>	<u>Conveyor Width</u>		
	<u>18 Inches</u>	<u>24 Inches</u>	<u>36 Inches</u>
Drive and terminals	\$1, 300	\$1, 500	\$1, 730
Bend	300	350	400
Per Foot	109	125	144

The total purchased cost of a conveyor is obtained by adding the cost of the drive and terminals, the cost of the bends and the number of feet multiplied by the cost per foot. Thus a 24" wide conveyor having a total length of 10 feet and two bends would cost \$1,500 + 10 x \$125 or \$3,450.

c. Feed Bins

For transfer of stored scrap onto a conveyor, bins having a 45° conical bottom are used. In the experimental phase of the current program, a small bin of this type was used to feed the separator via a vibrating feeder. The system worked well and it is therefore proposed to employ it for the plant design. A typical configuration of two bins being filled by means of one elevating piano hinge conveyor and emptying onto a vibrating conveyor is illustrated in Figure 31. In order to save on conveyor costs one conveyor is positioned to fill these two bins by means of a rotating chute. This technique can be used to fill up to four bins by means of one conveyor.

The vibrating feeder presently being used costs \$300. It appears capable of handling over 3 tons of scrap per hour, and good feed rate control was obtained down to less than 500 pounds per hour. This type of feeder is therefore proposed for use in the plant designs. The cost of the feed bins is estimated from a correlation for flat top tanks presented in the Guthrie cost estimating paper, and updated to 1973. This correlation is shown in Figure 32.

d. Ferrofluid Recovery Module

The costs of the major pieces of equipment comprising the ferrofluid recovery module shown in Figure 29, were estimated by three different techniques. The costs of the pumps and storage tanks were estimated from published correlation, and are listed in Table XXI. The cost of the solvent recovery stills was estimated from the vendor quotes shown in Figure 33. Each

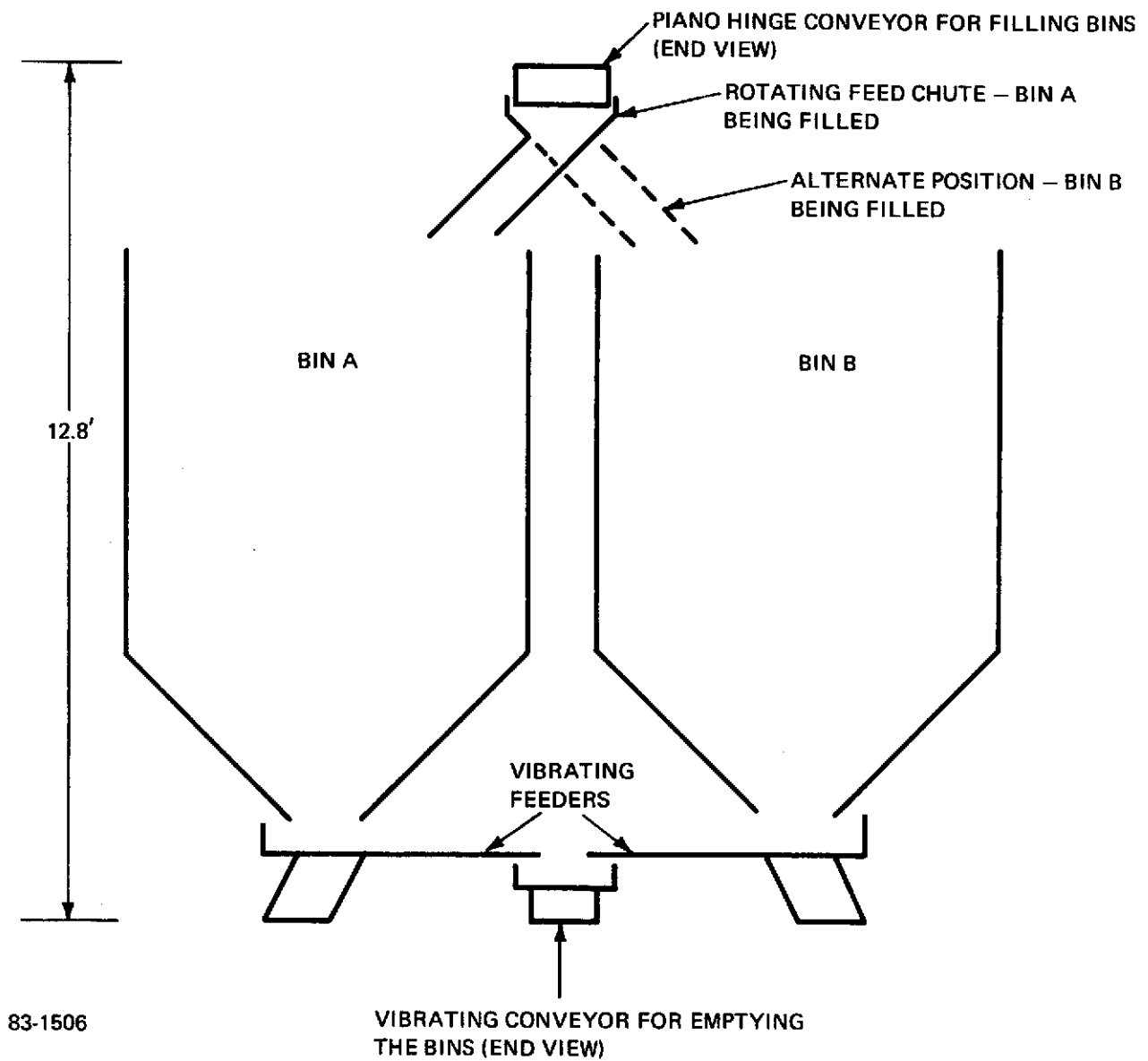
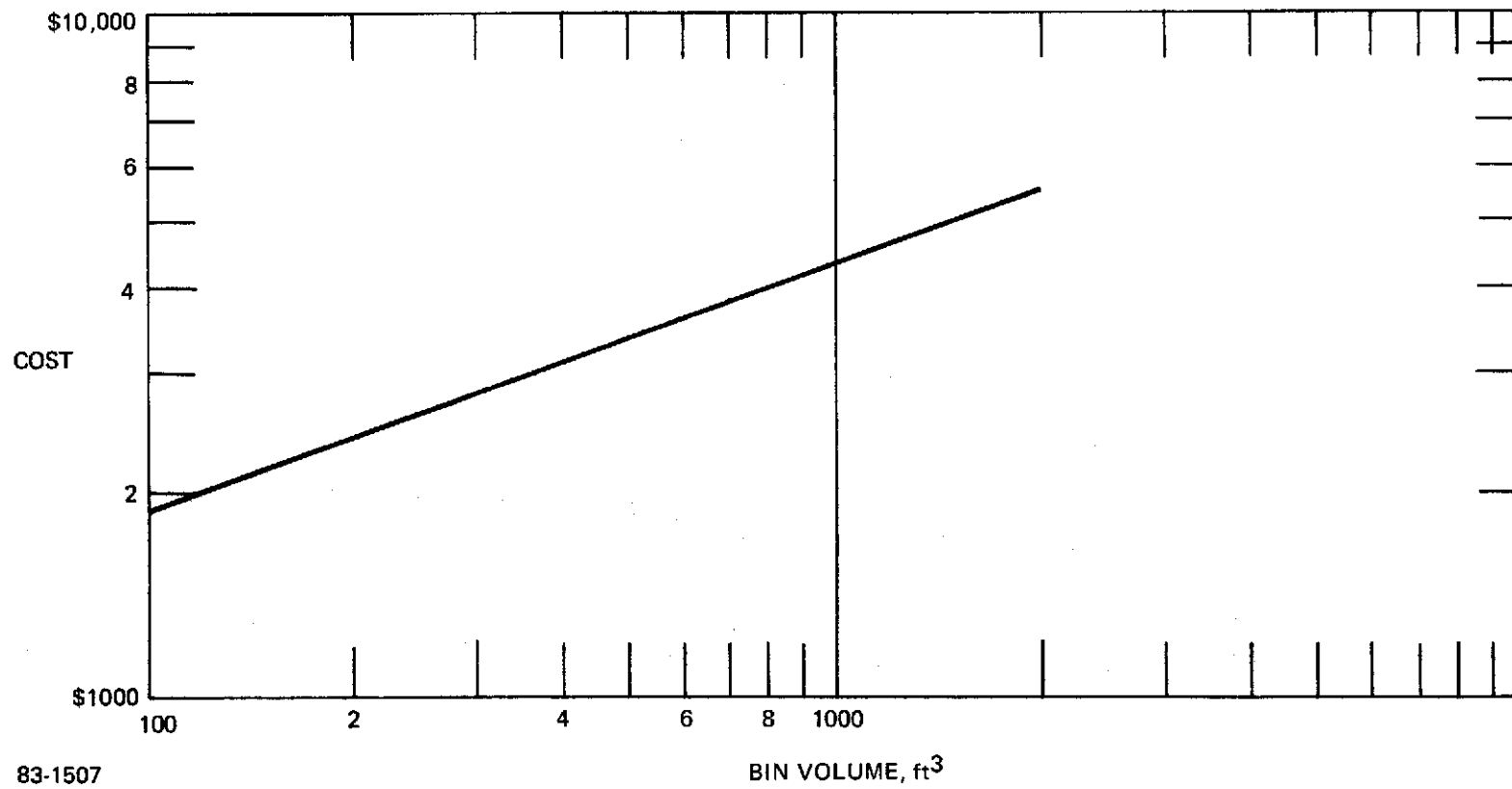


Figure 31 FEED BIN CONFIGURATION



83-1507

Figure 32 ESTIMATED PRICE OF FEED HOPPERS

datum point is a different quote. For estimation, the costs predicted by the correlation line shown in this figure were used. These costs are listed as a function of scrap processing rate in Table XXII. The sum of the pumps, tank and still costs which is the total equipment cost exclusive of the degreaser itself, are plotted in Figure 34. This figure will be used to estimate the cost of this portion of the ferrofluid recovery module for the plant designs.

TABLE XXI

FERROFLUID RECOVERY MODULE-COST OF PUMPS AND TANKS

(See Figure 29)

<u>Scrap Processing Rate</u> <u>(Tons/Hr.)</u>	<u>Pump Costs*</u>				<u>Tank Costs</u>	
	<u>P-1</u>	<u>P-2</u>	<u>P-3</u>	<u>P-4</u>	<u>Solvent</u>	<u>Ferrofluid</u>
1.0	\$390	\$390	\$200	\$200	\$ 850	\$100
2.0	440	440	200	200	1,200	200
5.0	500	500	200	200	2,100	350

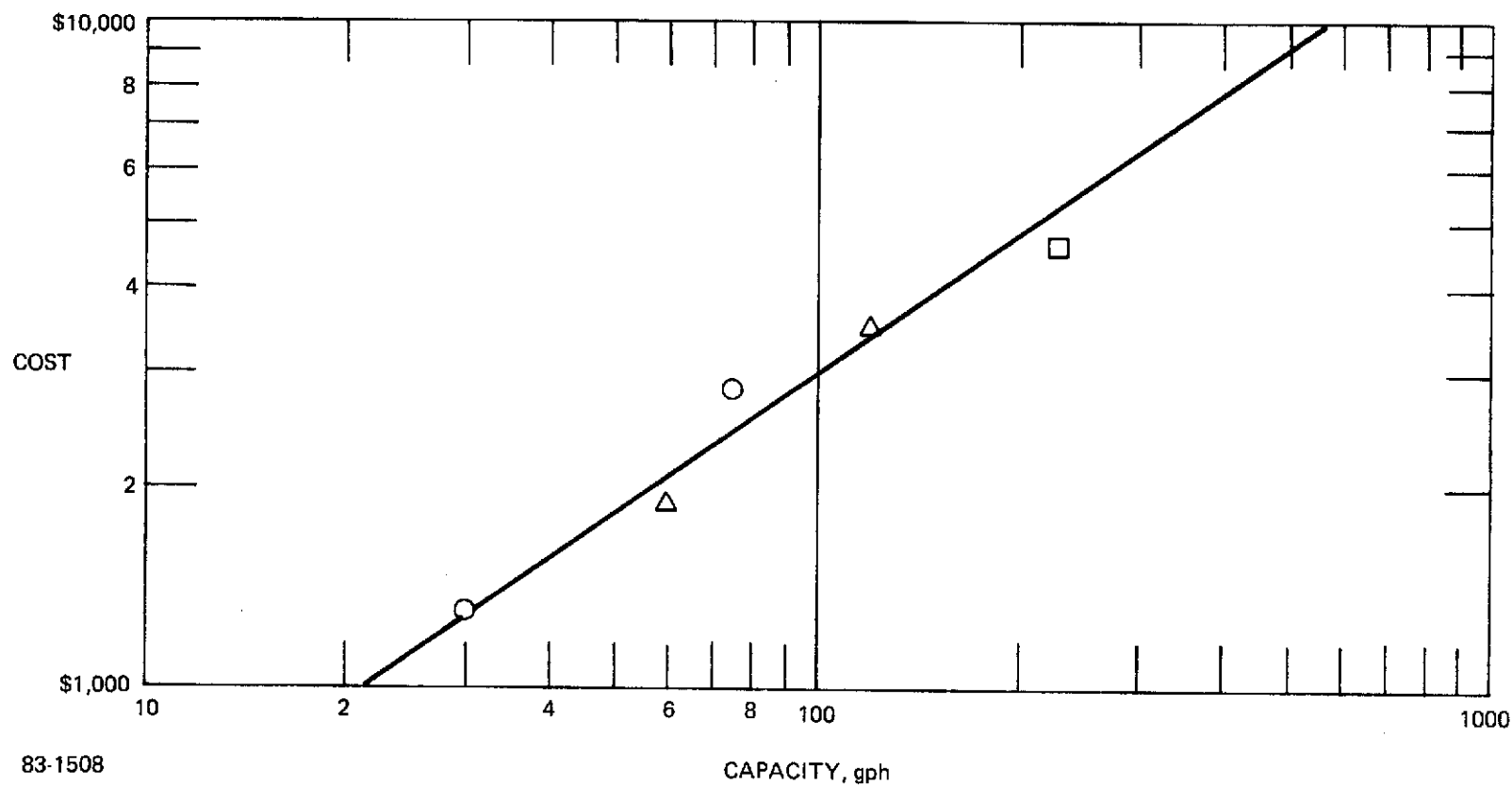
*Estimated From "How to estimate the costs of pilot plant equipment"
Chemical Engineering, February 9, 1970 and updated
to 1973.

The cost of the degreaser itself is known less accurately. Discussions with manufacturers indicate that a degreaser capable of processing up to about 2 tons of scrap per hour would cost \$15,000 after the prototype stage had been passed. The first prototype unit might cost somewhat more.

TABLE XXII

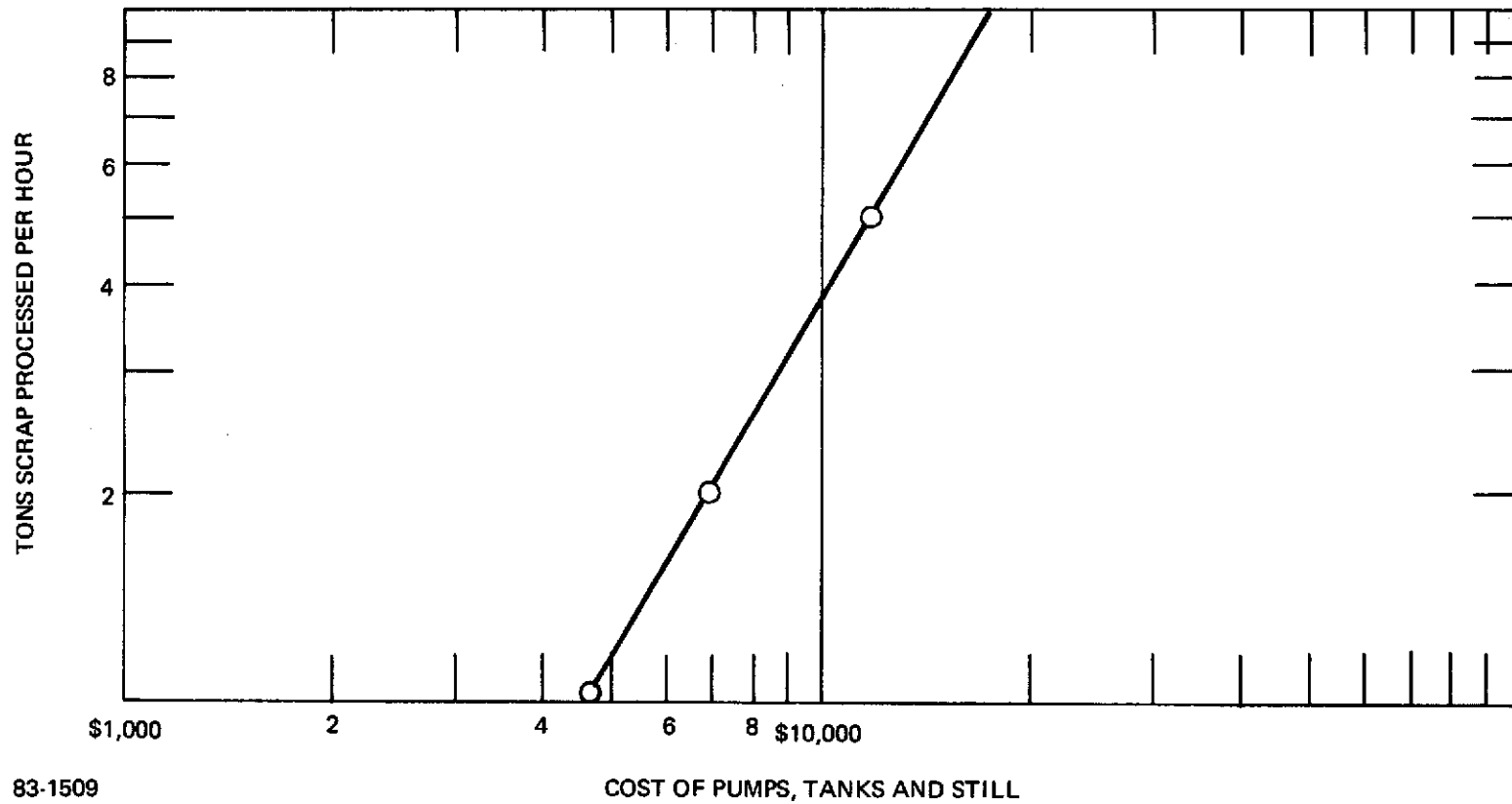
FERROFLUID RECOVERY MODULE-COST OF STILLS

<u>Scrap Processing Rate</u> <u>(Tons/Hr.)</u>	<u>Still Capacity</u> <u>gph</u>	<u>Still Cost</u>
1.0	88	\$2,700
2.0	176	4,400
5.0	440	8,300



83-1508

Figure 33 ESTIMATED PRICE OF SOLVENT RECOVERY STILLs



83-1509

Figure 34 ESTIMATED PRICE OF ENTIRE FERROFLUID RECOVERY MODULE

2. Operating Costs

The estimation of operating costs at this stage of process development is not as accurate as the estimation of capital costs, because of the lack of long term operating experience. Such operating factors as labor requirements, maintenance practices and losses of ferrofluid and solvent can only be roughly estimated. The following sections outline the assumptions made in estimating the principal operating costs.

a. Operating Labor

Three classes of operating labor are used at the following annual rates:

Foreman	-	\$12,000
Operators	-	9,000
Helpers	-	7,000

These labor rates are burdened at 81% to take into account supervision, payroll overhead and indirect costs. This labor burden is based on estimates made in an engineering feasibility study by the National Center for Resource Recovery of recovering aluminum and glass from municipal solid waste. It is felt that the municipal waste operation is sufficiently similar to auto scrap recovery for the labor overheads to be comparable.

b. Maintenance

Maintenance costs including both labor and materials are estimated to be 6% of capital costs. This "6%" figure is widely used to estimate maintenance costs in processing plants not subject to severe corrosion⁽¹³⁾. The use of this technique to calculate maintenance costs in scrap processing plants is clearly a very rough estimate. More accurate maintenance costs require actual operating experience.

c. Supplies

This category includes both ferrofluid and solvent makeup. Ferrofluid losses as previously mentioned are estimated to be 1 quart per ton of scrap. Avco projects that at a production rate of about 3,000 gallons per year, the cost of ferrofluid will be \$30 per gallon, corresponding to \$7.50 per ton of scrap. The loss of degreasing solvent, probably trichloroethane, is estimated to be 1.5 gallons per ton. This is a rough estimate, actual operating experience is required to generate more accurate values. At a cost of \$1.60 per gallon in 55 gallon drums, this amounts to \$2.50 per ton of scrap. If the solvent were bought in tank car lots, the price would be about \$1.30 per gallon, corresponding to \$1.95 per ton.

d. Utilities

It is assumed that the only energy source that will be available in electricity, which is charged at \$0.015 per Kwh. Were steam available for the solvent stills it would be a cheaper source of energy.

Cooling water for the magnets and the stills is charged at \$.10 per 1,000 gallons.

Another charge in this category is the cost of disposing of the non-metals, this cost is estimated to be \$6.00 per ton. If the shredder operator had ample land this cost would not apply. The unit costs for electricity, cooling water and non-metals removal vary considerably from locality to locality. Since the total of these costs is a small fraction of the total operating costs, deviations from the above unit costs will not introduce large cost differences.

e. Insurance

The following insurance costs are included:

Fire and business liability at	\$1.80 per \$1,000 of plant capital
Property tax at	\$15.00 per \$1,000 of plant capital
Unemployment compensation	\$2.50 per \$1,000 of plant payroll

3. Profitability

The profitability of the plant is determined by the sales price of the separated metals, the price that could have been obtained for them in the unseparated form, and the cost of separating them according to the following equations:

$$\text{Plant Profits} = \text{Added Value} - \text{Operating Costs},$$

where

$$\text{Added Value} = \text{Price of Separated Metals} - \text{Price of Unseparated Metals}$$

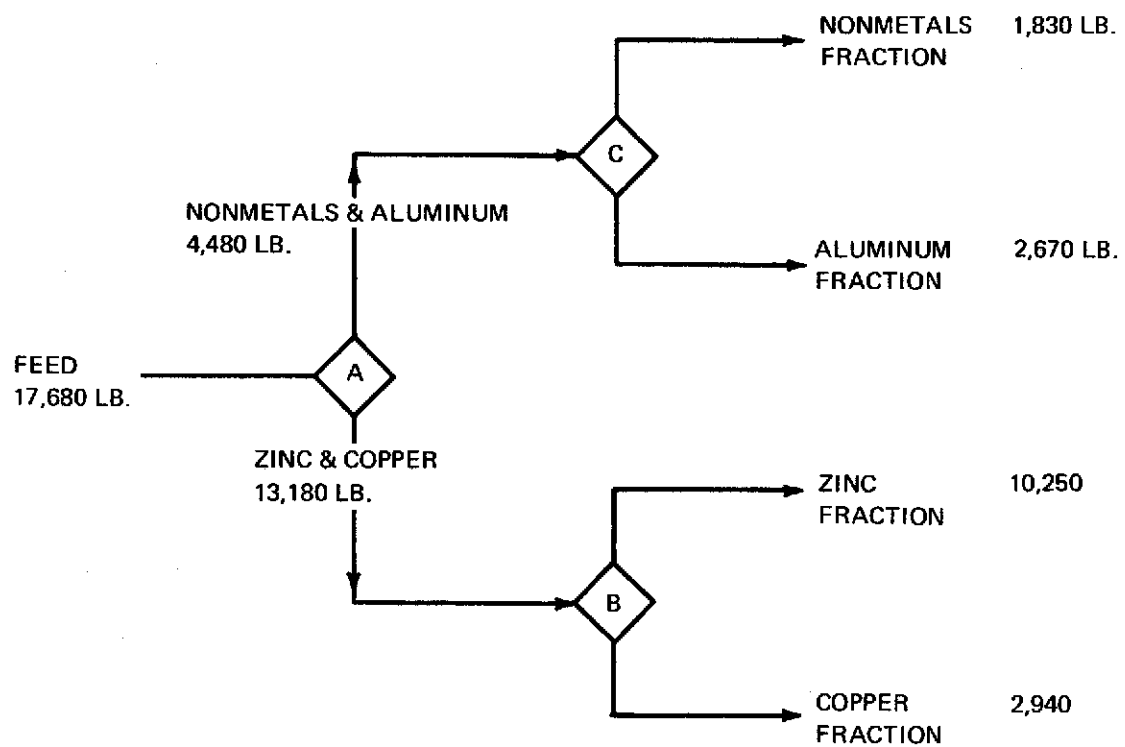
Table I presents the basis of Avco's estimate of the added value obtainable for the separated metals.

The measure of profitability used in this analysis is the payout time on invested capital. More sophisticated measures, reflecting more accurately the time value of money were felt to be inappropriate for a process at this stage of development.

C. Plant Design

1. Batch Plant

This plant is designed to process one ton of nonferrous metal per hour by using only one separator and one degreaser. This requires that intermediate products be stored for further processing. Consequently a rather large number of feed bins and conveyors is used. The cost of these bins and conveyors is however, lower than the cost of additional separators and degreasers required for continuous processing. In a later section a continuous plant which uses five separators and four degreasers for continuous processing at 5 tons per hour will be presented. Figure 35 shows the plant material balance for the plant and a schedule of separator operation. This schedule requires three changes in the apparent density of the ferrofluid pool per shift. There is, however, enough storage capacity in the system to allow these changes to be made only once every two shifts. Figure 36 shows a



SEPARATOR: LARGE TYPE

STAGE OF SEPARATION	SCHEDULE	OPERATING RATE
A	3.0 HOURS	84% OF CAPACITY
B	3.0 HOURS	65% OF CAPACITY
C	1.5 HOURS	63% OF CAPACITY

83-1510


Figure 35 EIGHT HOUR MATERIAL BALANCE – BATCH PLANT

NOTES: VIBRATORY FEEDERS ARE NOT SHOWN

HORIZONTAL CONVEYORS — CG } ARROWS SHOW DIRECTION
ELEVATING CONVEYORS — CR } OF MOTION

FEED BINS — B

ROTATING CHUTES AT END OF CONVEYORS SYMBOLIZED BY 

SCALE  25 FEET

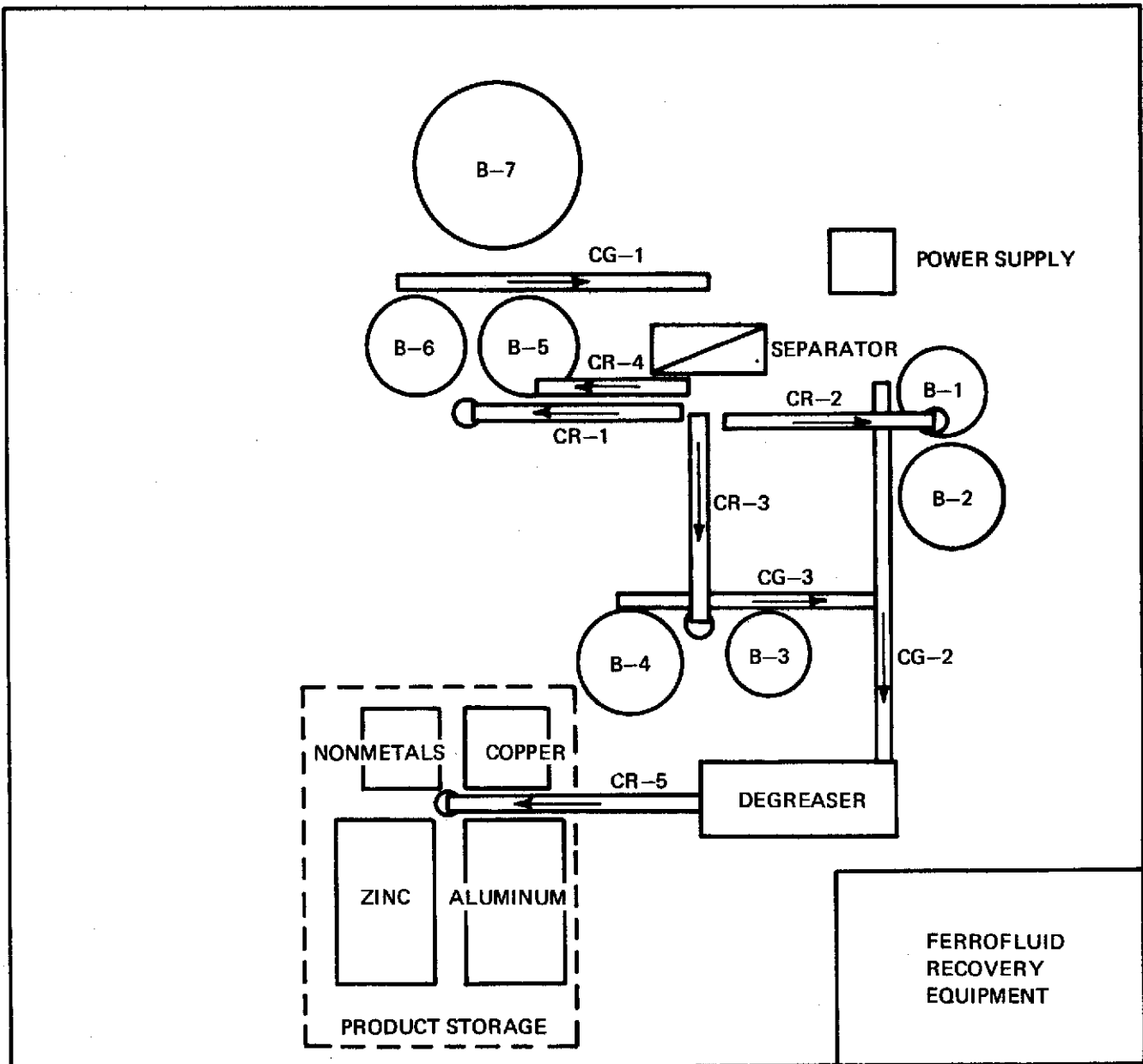


Figure 36 EQUIPMENT LAYOUT — BATCH PLANT

plan view of the proposed plant layout. The flow of materials through the plant may be understood with the aid of Tables XXIII and XXIV which describe the bins and the conveyors. The following description of material flow during Stage A of separation, which is the separation of the non-metals and aluminum from the denser metals, illustrates the functioning of the system.

TABLE XXIII
LIST OF FEED BINS - BATCH PLANT

<u>Bin</u>	<u>Stored Material</u>	<u>Volume (ft³)</u>	<u>Height Above Floor (ft)</u>	<u>Cost</u>
B-1	Non-metals wet with ferrofluid	100	12	\$ 1,900
B-2	Zinc wet with ferrofluid	200	12	2,400
B-3	Copper wet with ferrofluid	100	12	1,900
B-4	Aluminum wet with ferrofluid	200	12	2,400
B-5	Aluminum and non-metals wet with ferrofluid	150	10	2,000
B-6	Zinc and copper wet with ferrofluid	200	12	2,400
B-7	Scrap feed to process	500	14	<u>3,400</u>
TOTAL				\$16,400

The feed scrap is conveyed by CG-1 from B-7 to the separator. The floats, aluminum and non-metals are conveyed by CR-4 to B-5. The sinks, zinc and denser metals, are conveyed by CR-1 to B-6.

The degreasing of scrap is completely decoupled from the separations. The purified fractions contained in the in-process storage bins B-1, B-2, B-3 and B-4 may be conveyed to the degreaser in any order and without any fixed relation to the separations are going on concurrently.

The capital costs of the major pieces of equipment and the cost of the plant are given in Table XXV. The operating costs are listed in Table XXVI. In these economic analyses it is assumed that the plant is financed completely by equity capital without any debt. The resulting payout time on the invested capital is 2.8 years. This payout time, although adequate in many circumstances, can be improved when enough scrap is available to keep the plant operating for two or three shifts. Under these circumstances the capital cost remains constant, while most of the operating costs rise in proportion to the operating hours. In order to be prudent it has been assumed that the maintenance costs will also rise in proportion to the hours operated. The operating costs and profitability for 2 shift and 3 shift operation are given in Tables XXVII and XXVIII. The improved profitability produced by more effective plant utilization decreases the payout from 2.8 years for one shift operation to 1.6 years for two shift and down to 1.1 years for three shift operation.

TABLE XXIV
LIST OF CONVEYORS - BATCH PLANT

<u>Conveyor</u>	<u>Function</u>	<u>Lower Point ft</u>	<u>Upper Point ft</u>	<u>Horizontal Length ft</u>	<u>Rise ft</u>	<u>Cost</u>
CG-1	Convey scrap from B-5, B-6 and B-7 to separator	2	4	19	2	\$ 4,300
CG-2	Convey scrap from B-1, B-2 B-3 and B-4 to degreaser	2	2	23	0	2,400
CG-3	Convey scrap from B-3 and B-4 to CG-2	2.5	2.5	16	0	1,900
CR-1	Convey sinks (stage A) from separator to B-6	2	14	13	12	3,600
CR-2	Convey floats (stage B and C) from separator to B-1 and B-2	2	14	13	12	3,600
CR-3	Convey sinks (stage B and C) from separator to B-3 and B-4	2	14	13	12	3,600
CR-4	Convey floats (stage A) to B-5	2	10	10	8	3,000
CR-5	Convey degreased scrap to storage hoppers	6	12	16	6	<u>3,800</u>
						\$26,200

Note: CG conveyors are 17" wide
CR conveyors are 18" wide

TABLE XXV
CAPITAL COSTS - BATCH PLANT

<u>Item</u>	<u>Comments</u>	<u>Cost</u>	<u>Percent</u>
Magnet Separator	Large Type	\$ 29,400	8.22
Power Supply	60 Kw	3,000	0.84
Conveyors	Table XII	26,200	7.33
Feed Bins	Table XI	16,400	4.59
Degreaser	2 Tons Per Hour	15,000	4.20
Still and Ancillaries		<u>5,000</u>	<u>1.40</u>
	Total FOB Cost	\$ 95,000	26.57
	Plant Cost = $2.232 \times \$95,000 =$	\$212,000	59.30
	Electr. Substation	\$ 6,500	1.82
	Building 4900 ft ²	<u>\$ 79,400</u>	<u>22.21</u>
	TOTAL	\$297,900	83.33
	Contingency (20%)	<u>\$ 59,600</u>	<u>16.67</u>
	Total Capital Requirements	\$357,500	100.00

TABLE XXVI
OPERATING COSTS - BATCH PLANT
ONE SHIFT PER DAY

<u>Category</u>	<u>Comments</u>	<u>Annual Cost</u>	<u>Percent</u>
Labor	1. Operator at \$9,000	\$ 9,000	4.82
	2. Foreman at \$12,000	12,000	6.43
	3. Supervision, overhead and indirects	17,000	9.11
Maintenance	6% plant capital	\$ 21,500	11.52
Utilities	1. Electricity 126 Kw	\$ 3,300	1.77
	2. Water	1,000	0.54
	3. Dumping of refuse	1,300	0.70
Supplies	1. Ferrofluid 500 gal	\$ 15,000	8.03
	2. Solvent 3100 gal	5,000	2.68
Insurance		\$ 700	0.38
Property Tax		\$ 5,400	2.89
Feed Preparation	\$12 per ton	\$ 24,000	12.85
Depreciation	5 year straight line	<u>\$ 71,500</u>	<u>38.30</u>
		\$186,700	100.00

Added Value to Scrap at \$150/ton = \$300,000

Profit Before Taxes = \$113,300

Payout Time = $\frac{357,500}{71,500 + 113,300/2} = 2.8 \text{ Years}$

TABLE XXVII
OPERATING COSTS - BATCH PLANT
TWO SHIFTS PER DAY

<u>Category</u>	<u>Comments</u>	<u>Annual Costs</u>	<u>Percent</u>
Labor	1. Operators (2)	\$ 18,000	6.08
	2. Foreman (2)	24,000	8.11
	3. Supervision, etc.	34,000	11.49
Maintenance	12% of plant capital	\$ 43,000	14.53
Utilities	1. Electricity	\$ 6,600	2.23
	2. Water	2,000	0.68
	3. Dumping of refuse	2,600	0.88
Supplies	1. Ferrofluid	\$ 30,000	10.14
	2. Solvent	10,000	3.38
Insurance		\$ 800	0.27
Property Tax		\$ 5,400	1.82
Feed Preparation		\$ 48,000	16.22
Depreciation		<u>\$ 71,500</u>	<u>24.16</u>
		\$295,900	100.00

Added Value at \$150/Ton = \$600,000

Profit Before Taxes = \$304,100

Payout Time = $\frac{357,500}{71,500 + 304,100/2} = 1.6 \text{ Years}$

TABLE XXVIII
OPERATING COSTS - BATCH PLANT
THREE SHIFTS PER DAY

<u>Category</u>	<u>Comments</u>	<u>Annual Costs</u>	<u>Perce</u>
Labor	1. Operators (3)	\$ 27,000	6.
	2. Foreman (3)	36,000	8.
	3. Supervision, etc.	51,000	12.
Maintenance	18% of plant capital	\$ 64,500	15.
Utilities	1. Electricity	\$ 9,900	2.
	2. Water	3,000	0.
	3. Dumping of refuse	3,900	0.
Supplies	1. Ferrofluid	\$ 45,000	11.
	2. Solvent	15,000	3.
Insurance		\$ 900	0.2
Property Tax		\$ 5,400	1.3
Feed Preparation		\$ 72,000	17.7
Depreciation		<u>\$ 71,500</u>	<u>17.5</u>
		\$405,100	100.0

Added Value to Scrap at \$150/Ton = \$900,000

Profit Before Taxes = \$494,900

Payout Time = $\frac{357,500}{71,500 + 494,900/2} = 1.1 \text{ Years}$

2. Continuous Plant

This plant is designed to process larger quantities of scrap than can be conveniently processed by means of a batch plant. Specifically, 5 tons per hour, 20 hours per day for 250 days per year, or a total of 25,000 tons per year. This quantity of material is most conveniently processed in a continuous system, separated products from Stage A are continuously fed to the separators of Stage B and Stage C. The four separated products from Stage B and C are continuously fed to four degreasers.

The operating schedule is based on three $6 \frac{2}{3}$ hour operating shifts per day. These short shifts are specified to allow time for maintenance between the conclusion of one shift and the start of the next. If it should turn out that less maintenance is required, then the plant could be run for more hours and its productivity would rise accordingly.

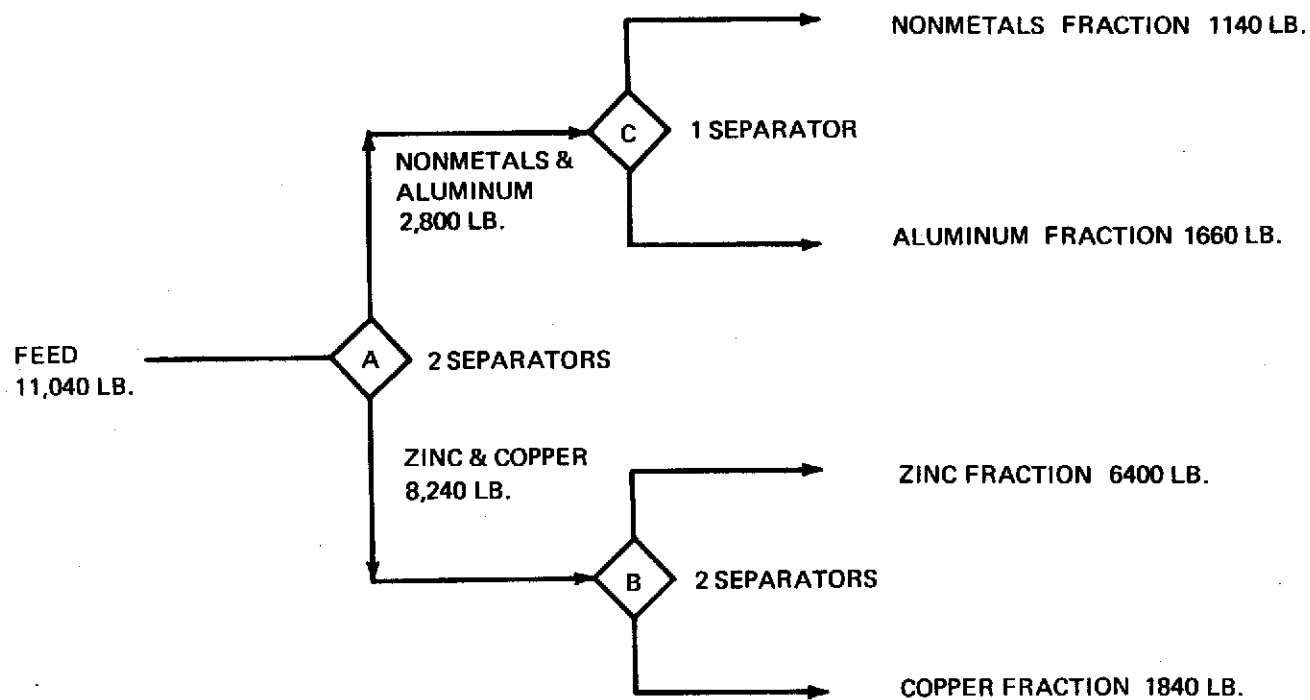
In order to reduce labor costs, no materials handling operator is used on one shift. This savings can be realized by having the operator on the preceeding shift empty the product bins so that they can accommodate the entire output of the succeeding shift. Similarly, one shift is run without a foreman. The foreman of the preceeding shift being available to start-up the succeeding shift.

A one hour material balance for this plant is shown in Figure 37, and a plan view of the plant layout is shown in Figure 38. The two large separators that carry out the Stage A separation in parallel and the two that carry out the Stage B separation are rather under-utilized. Some capital savings would be obtained by using a small and a large separator for each stage. It was felt that the additional complexity of adjusting feed rates to each separator was not worth the possible savings. The degreaser sizes are more closely matched to the size of the stream being treated in order to reduce these costs. The cost of the degreasers was assumed to still be \$7,500 per ton per hour. The plant conveyors are described in Table XXIX. The plant capital costs are given in Table XXX and the operating costs are given in Table XXXI. As in the analysis of the batch plant it has been assumed that the plant is financed completely by equity capital. The resulting payout time on the invested capital is 0.6 year.

The principal reason that this payout is better than for the batch plant is that the capital equipment is more thoroughly utilized and the labor requirements per ton are lower. For example, the smallest sized commercially available conveyors that can handle scrap 2-3 inches in size are oversized in capacity for the batch plant, but of proper size for the continuous plant.

D. Discussion

The recovery of nonferrous metals from automobile scrap by ferrofluid levitation promises to be a profitable process. The profitability as measured by payout time on invested capital runs from 2.8 years for a plant processing 2000 tons of scrap per year to 0.6 year for a plant processing 25,000 tons per year. The former plant has sufficient capacity to process the nonferrous scrap from 300 shredded automobiles per day. The latter plant can process the nonferrous metals from 3,750 cars per day.



STAGE OF
SEPARATION

NO. OF SEPARATORS
(LARGE)

OPERATING RATE

A

2

78% OF CAPACITY

B

2

61% OF CAPACITY

C

1

60% OF CAPACITY

83-1512

Figure 37 ONE HOUR MATERIAL BALANCE — CONTINUOUS PLANT

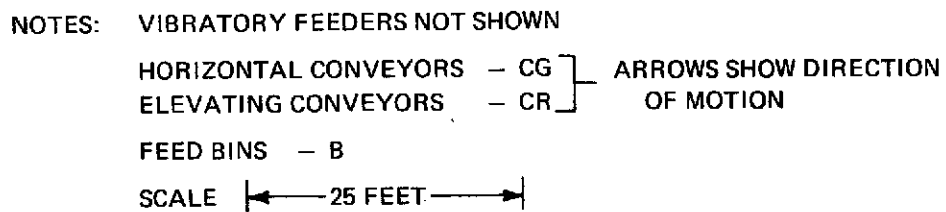


Figure 38 EQUIPMENT LAYOUT – CONTINUOUS PLANT

TABLE XXIX

LIST OF CONVEYORS - CONTINUOUS PLANT

<u>Conveyor</u>	<u>Function</u>	<u>Width (In.)</u>	<u>Lower Point (Ft.)</u>	<u>Upper Point (Ft.)</u>	<u>Horizontal Length (Ft.)</u>	<u>Rise (Ft.)</u>	<u>Cost</u>
CR-1	Convey Scrap from Feed	18	2	6	10	4	\$ 3,200
CR-2	Bins to Stage A Separators	18	2	6	10	4	3,200
CR-3	Convey Non-metals from Degreaser to Storage	18	2	12	14	10	3,400
CR-4	Convey Aluminum from Degreaser to Storage	18	2	12	14	10	3,400
CR-5	Convey Zinc from Degreaser to Storage	24	2	12	14	10	4,500
CR-6	Convey Copper from Degreaser to Storage	18	2	12	14	10	3,400
CG-1	Convey Floats from Stage A to Stage C Separator	11	2.5	2.5	18	0	2,000
CG-2	Convey Zinc from Stage B Separator to Degreaser	17	2.5	2.5	24	0	2,700
CG-3	Convey Copper from CG-4 and 5 to Degreaser	11	2	2	24	0	2,500
CG-4	Convey Copper from	11	2.5	2.5	6	0	1,000
CG-5	Stage B Separators to CG-3	11	2.5	2.5	6	0	1,000
CG-6	Convey Non-metals from Stage C Separator to Degreaser	11	2.5	2.5	8	0	1,100
							<u>\$31,400</u>

TABLE XXX
CAPITAL COSTS - CONTINUOUS PLANT

<u>Item</u>	<u>Comments</u>	<u>Cost</u>	<u>Percent</u>
Magnet-Separators	Large Type	\$147,000	15.90
Conveyors	Table XVI	31,400	3.40
Feed Bins	2 Bins 1,000 ft ³ each	8,600	9.30
Power Supply	140 Kw	7,000	0.76
Degreasers		40,000	4.33
Still and Ancillaries		<u>11,800</u>	<u>12.76</u>
	Total FOB Cost	\$245,800	26.58
<hr/>			
	Plant Cost = 2.232 x 245,800 =	\$548,600	59.26
Electrical Substation		\$ 20,000	2.16
Building	12,000 ft ²	<u>\$202,000</u>	<u>21.84</u>
	Total	\$770,600	83.34
	Contingency (20%)	<u>\$154,800</u>	<u>16.74</u>
	Total Capital Requirements	\$924,700	100.00

TABLE XXXI
OPERATING COSTS - CONTINUOUS PLANT
THREE SHIFTS PER DAY

<u>Category</u>	<u>Comments</u>	<u>Cost</u>	<u>Percent</u>
Labor	1. Separation Operators - 3 at \$9,000	\$ 27,000	2.4
	2. Degreasing Operators - 3 at \$9,000	27,000	2.4
	3. Materials Handling Operators - 2 at \$7,000	14,000	1.2
	4. Foreman - 2 at \$12,000	24,000	2.1
	5. Supervision, etc.	74,500	6.6
Maintenance	18% Plant Capital	\$ 166,500	14.8
Utilities	1. Electricity 300 Kw	\$ 22,500	2.0
	2. Water	3,000	0.2
	3. Disposal of Refuse	15,000	1.3
Supplies	1. Ferrofluid 6250 gal	\$ 187,500	16.6
	2. Solvent 39,000 gal	62,500	5.5
Insurance		\$ 2,000	0.18
Property Tax		\$ 14,000	1.25
Feed Preparation	\$12/Ton	\$ 300,000	26.68
Depreciation	5 Year Straight Line	\$ 184,900	16.44
		\$1,124,400	100.00

Added Value to Scrap at \$150/Ton = \$3,750,000

Profit Before Taxes = \$2,625,000

Payout Time = $\frac{924,700}{184,900 + 2,625,000/2} = 0.6 \text{ Years}$

The largest automobile shredders currently operating can process about 1,200 cars per day. Accordingly this large plant could be a central processing plant for a number of shredders. Because the large plant is more profitable than the smaller one, a tendency may develop for a number of small shredder plants to process their nonferrous metals in such a central plant. This tendency would be particularly strong in densely populated areas with a concentration of small shredders. Large plants, shredding about 1,000 cars per day, could process their nonferrous metals on a small, batch plant by operating it for three shifts per day. The profitability of this operation, while not as good as that of a central processing plant, is very high and promises to be attractive to operators of large shredder plants.

The attractiveness of nonferrous metal separation for the shredder operator who has only enough metal for one shift of operation (2,000 tons per year from 300 cars per day), might be increased if the plant were partly financed by borrowed capital. This assumes of course that the small shredder operator could obtain this capital at a reasonable interest rate, probably no higher than about 10%.

The above considerations suggest that the ferrofluid levitation process for nonferrous metal separation will be very attractive for large and medium shredder operators who have between 4,000 and 6,000 tons of metal to process per year. Small shredder operators will probably find it more attractive to use a central processing plant, or to finance the plant by borrowed capital.

E. Ecological Considerations

It is estimated that by 1975 about ten million automobiles will be shredded annually in the United States. The resulting scrap will contain about 44,000 tons of aluminum alloys, 196,000 tons of zinc alloys and 25,000 tons of copper alloys. The recovery of this material and its recycle would have important ecological benefits to the country. An important direct ecological benefit would be a reduction in electrical energy requirements. The refining of metals from ores is an energy intensive process. By replacing virgin metals with recycled ores, a substantial saving in the Nation's energy requirements results, with attendant reductions in the ecological side effects of electricity production. An estimate of these savings is shown in Table XXXII. The total energy savings of five billion Kwh are about equivalent to the energy consumption of a city of 900,000 people.

By reducing the need for virgin metals the ecologically harmful side effects of mining and refining are reduced. The refining of zinc and copper ores is attended by troublesome sulfur dioxide emissions, and that of aluminum reduction by fluoride emissions. This is an indirect but important ecological benefit of recycling scrap metals.

The high potential profitability of this process has an important direct ecological benefit by encouraging the transportation of abandoned automobiles to shredder operators. Because the shredder operators will be able to recover between \$6 and \$11 more per car, at a substantial profit, their demand for cars will rise. They will therefore pay more for junk cars, which will in turn be an incentive for auto wreckers to procure more cars. This will hopefully induce them to transport abandoned cars from locations, from which it has up to now been economically impossible to do so.

TABLE XXXII
POTENTIAL ENERGY SAVINGS IN 1975
DUE TO RECOVERY OF NONFERROUS METALS

<u>Metal</u>	<u>Tons Recovered</u>	<u>Energy to* Win from Ores (Million Kwh)</u>	<u>Energy Savings (Million Kwh)</u>
Aluminum	49,000	2,500	2,400
Zinc	196,000	2,600	2,300
Copper	25,000	340	<u>300</u>
			5,000

*Estimates based on ORNL-NSF Environmental Program Report ORNL-NSF-EP-24, "Energy Expenditures Associated with the Production and Recycle of Metals"

The ferrofluid levitation process of scrap recovery and separation has virtually no harmful side effects on the environment. It of course uses electrical power, but its operation as shown above, results on a large net decrease in national energy requirements. The modest water requirements of the process are solely for cooling, there is accordingly no by-product water pollution. There is of course a small amount of thermal pollution. In view however of the large ecological benefits of recycling scrap metals, this ecological disadvantage is almost inconsequential.

IV. CONCLUSIONS AND RECOMMENDATIONS

The results achieved in the execution of this program permit us to conclude that the recovery of relatively pure aluminum alloy and zinc alloy fractions from shredded automobile scrap is technically feasible by the ferrofluid levitation process. In addition an enriched copper alloy fraction is also recoverable. The specific conclusion on which the economic analysis of the process were carried out are:

1. The magnet design and construction met the objective of generating a constant apparent density of at least 8 g/cm^3 in a suitable ferrofluid.
2. The removal of ferrofluid from separated scrap by solvent washing and the recovery of the ferrofluid by boiling away the solvent was achieved with acceptable losses.
3. The present separator can carry out the various separation of nonferrous metal recovery at rates of between 1800 and 3000 pounds per hour.

Based on these conclusions and engineering estimates, projections were made for the economics of nonferrous metal recovery on an industrial scale. It was concluded that the process would be profitable for shredder operators handling more than about 300 cars per day. Payout time on invested capital ranged from about 3 years to less than a year, with increasing throughput. It therefore appears that the process can be introduced into the automobile shredding industry. The public benefits of the widespread recovery of nonferrous metals by this process would be:

1. Increased incentives for recovering abandoned cars, thus lessening environmental pollution.
2. Increased recycling of metals with an attendant reduction in national energy requirements.
3. Decreased needs to import nonferrous metals, which contributes to the solution of the balance of payments problem.

Furthermore, the process would not produce any by-product pollution problems. In order to achieve these benefits the process must of course achieve a rapid and wide penetration of the industry. Because the car scrapping industry consists of many relatively small firms with limited risk capital, the introduction requires the construction of a full scale plant to demonstrate unequivocally the profitability and the workability of the process under industrial constitution.

The first recommendation is therefore to construct and operate a demonstration plant at an automobile shredder, as a means of introducing the process effectively to the industry.

The results achieved on automobile scrap appear applicable to the recovery of nonferrous metals from municipal solid waste (MSW). The supply of nonferrous metals in MSW waste is considerably larger than in car scrap, but it is present in a much lower concentration. In order to determine what processing changes are required for this stream it is recommended that a program be undertaken to study the recovery of nonferrous metals from MSW, using the separator constructed under the current program.

V. REFERENCES

1. Papell, S.S. and Faber, O.C. Jr., "Zero and Reduced Gravity Simulation on a Magnetic Colloid Pool Boiling System", NASA-TN-D-3288 (February, 1966).
2. Papell, S.S. and Faber, O.C. Jr., "On the Influence of Non-Uniform Magnetic Fields on Ferromagnetic Colloidal Sols", NASA-TN-D-4676, (August, 1968).
3. Braetner, H. and Grunner, R., "Conditions for the Appearance of Ferromagnetism in Real Gases", Z. Naturforsch., 23a, 648 (1968).
4. Nakagawa, Y., "Magnetic Susceptibility of Liquid Alloys", J. Phys. Soc., Japan, 14, 1372 (1959).
5. Busch, G. and Guentherodt, H.J., "Ferromagnetic Behavior of Liquid Alloys", Phys. Letters, 27A, 110 (1968).
6. Neuringer, J.L. and Rosensweig, R.E., "Ferrohydrodynamics", The Physics of Fluids, 27, 1927-1937 (1964).
7. Kaiser, R. and Rosensweig, R.E., "Study of Ferromagnetic Liquid", NASA-CR-1407 (August, 1969).
8. Rosensweig, R.E., "Means for and Method of Moving Objects by Ferrohydrodynamics", U.S. Patent 3,488,531 (January 6, 1970).
9. A Study to Identify Opportunities for Increased Solid Waste Utilization, Prepared for National Association of Secondary Material Industries, Inc., by Battelle Columbus Laboratories, Columbus, Ohio, June, 1972.
10. Newell, Scott, "Technology and Economics of Large Shredding Machines", Proceedings of the Third Mineral Waste Utilization Symposium, ITT Research Institute, Chicago, Illinois, March, 1972.
11. Automobile Disposal, A National Problem, U.S. Department of the Interior, Bureau of Mines, Washington, D.C., 1967.
12. Where Shredders are Located, Institute of Scrap Iron and Steel, Inc., Washington, D.C., March, 1971.
13. Chemical Engineering Plant Design by Frank C. Vilbrandt and Charles E. Dryden, McGraw-Hill Book Company, 1959.

APPENDIX A
THEORETICAL ESTIMATE OF SEPARATION RATE IN
FERROFLUID SINK-FLOAT SEPARATOR

1. Motion of a Weakly-Magnetic Body in a Magnetized Ferrofluid

The purpose of this analysis is to develop approximate relations for predicting the trajectory of weakly-magnetic bodies immersed in a ferrofluid, with the ultimate objective of estimating separation rates in a scrap separator in which a vertical magnetic field gradient acts in the direction of gravity. The equation of motion in the vertical direction is then given by:

$$\rho_s v \frac{dy}{dt} + C_D \frac{dy}{dt} = F_b \quad (A1)$$

v - volume of body

ρ_s - density of body

y - distance in vertical direction

t - time

C_D - drag coefficient

F_b - body force

For the approximate results desired it is permissible to specialize the analysis to spheres moving at Reynold's numbers low enough for Stokes Law to apply. Under these conditions;

$$C_D = 3\pi \eta d \quad (A2)$$

d - diameter of sphere

η - viscosity of ferrofluid

The body force is given by:

$$F_b = v (\rho_s - \rho_f) g - v (M_f - M_s) G \quad (A3)$$

g - acceleration of gravity

ρ_f - physical density of ferrofluid

M_f - magnetic dipole moment per unit volume of the ferrofluid

M_s - magnetic dipole moment per unit volume of the sphere

G - imposed vertical magnetic field gradient acting in the direction of gravity

The "apparent" densities of the ferrofluid and the solids are defined as:

$$\rho_{af} = \rho_f + \frac{M_f G}{g} \quad (A4a)$$

$$\rho_{as} = \rho_s + M_s \frac{G}{g} \quad (A4b)$$

The body force relation (3) may therefore be rewritten as:

$$F_b = v (\rho_{as} - \rho_{af}) g \quad (A5)$$

For the initial conditions of interest;

$$y = 0, \frac{dy}{dt} = 0 \text{ at } t = 0;$$

the integral of Equation 1 is:

$$y = \frac{F_b}{C_D} \left[t + \frac{e^{-\frac{C_D t}{\rho v}} - 1}{\left(\frac{C_D}{\rho v}\right)} \right] \quad (A6)$$

$$\frac{F_b}{C_D} = \frac{d^2}{18 \eta} (\rho_{as} - \rho_{af}) g \quad (A7)$$

$$\frac{C_D}{\rho v} = \frac{18 \eta}{\rho d^2} \quad (A8)$$

For small values of the variable $\frac{C_D t}{\rho v}$, equation (6) reduces to:

$$y = \frac{\rho_{as} - \rho_{af}}{\rho_s} g \frac{t^2}{2} \quad (A9)$$

This equation describes the motion of the sphere, for small values of time, when effects of viscosity are small. It shows, as expected, that for $\rho_{af} < \rho_{as}$, the object will move downward, the positive direction; and for $\rho_{af} > \rho_{as}$ it will move upward. This equation can be simplified further, when ρ_{as} is only slightly larger than ρ_s , to the following forms:

$$y = \left(1 - \frac{\rho_{af}}{\rho_{as}}\right) g \frac{t^2}{2} \quad (A9a)$$

The time required to traverse a distance y is obtained by inverting Equation (9a) as:

$$t = \sqrt{\frac{2y}{\left(1 - \frac{\rho_{af}}{\rho_{as}}\right) g}} \quad (A10)$$

This equation may be used to estimate the residence time of scrap in a ferrofluid separator since the condition $C_D t / \rho v < 1$ obtains over most sets of operating conditions.

For example, in a separator having a total height of 20 cm, with the scrap being introduced in the mid-plane, the largest value of y is 10 cm. The viscosity of the ferrofluid is about 0.05 poise. For the separation of zinc from copper, $\rho_{as} = 8.9$ and ρ_{af} will be about 7.9. Therefore, the value of $C_D t / \rho v$ at the outlet of the separator is obtained by combining Equations (8) and (10), as:

$$\frac{C_D t}{\rho v} = \frac{1.8 \times 0.5}{8.9 d^2} \sqrt{\frac{20}{0.11 \times 980}} = \frac{0.043}{d^2}$$

Thus, for d greater than 4.7 mm (3/16"), the value of $C_D t / \rho v < 0.2$, and equations (9) and (10) are useful approximations. Since scrap produced by hammer-milling shredded automobiles is generally larger than this, these equations may be used to calculate approximate times for this type of scrap in a separator.

2. Estimate of Separation Rates in a Levitation Separator

The ferrofluid volume in which separation takes place is illustrated schematically in Figure A-1. The feed is shown being introduced at the mid-plane, with the products being removed at the top and bottom. The volumetric transfer rate of scrap from the mid-plane to the end planes is given by:

$$Q = A y \epsilon / t \quad (A11)$$

A - horizontal cross-sectional area of separator

ϵ - volume fraction of separator occupied by scrap

t - transit time from mid-plane to top or bottom planes as given by Equation 10

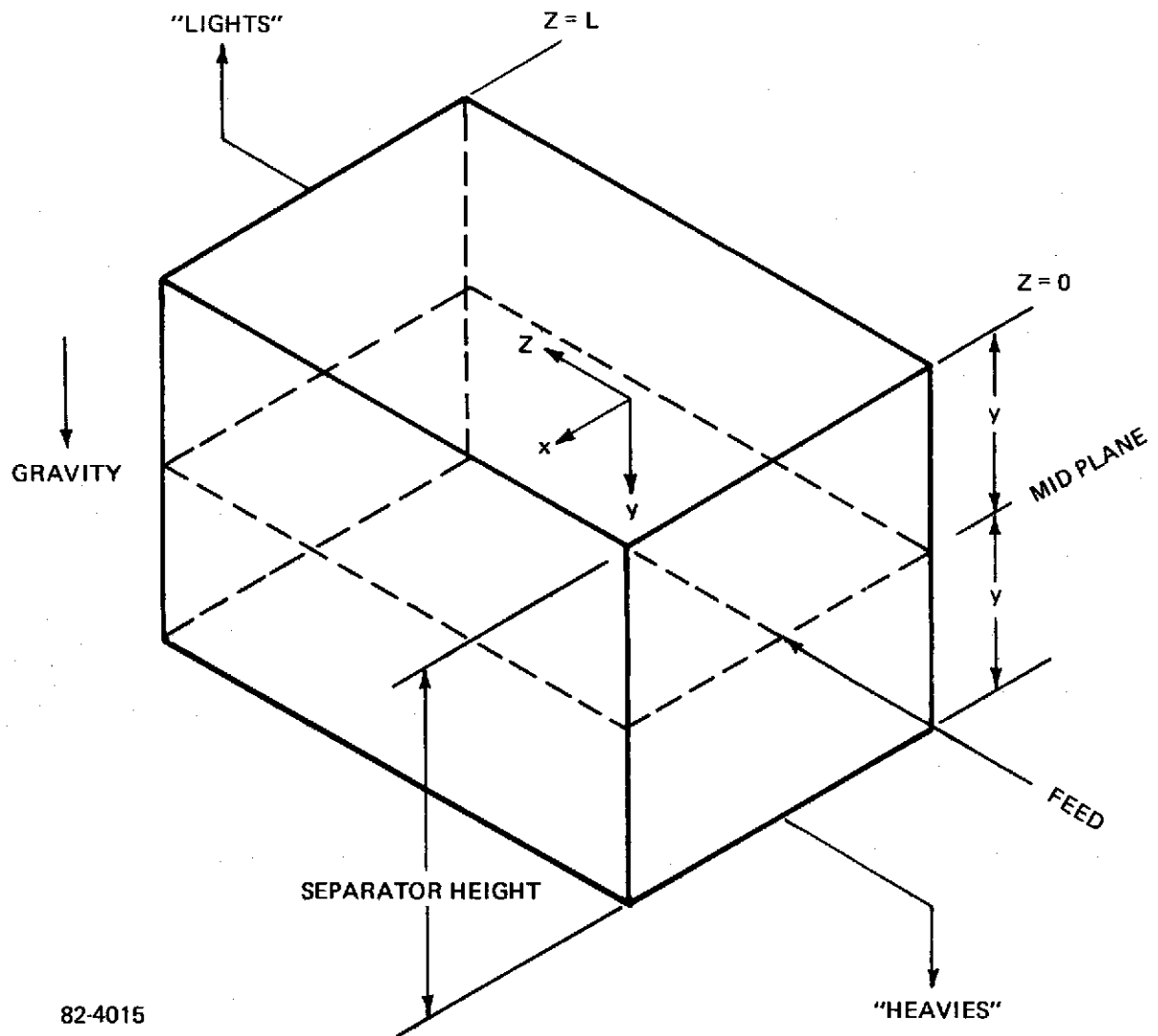


Figure A-1 SCHEMATIC OF SEPARATOR

When separating scrap composed of roughly equal volumes of light and heavy materials it is plausible to set ρ_{af} so that both types of scrap have roughly equal transit times through the separator. This value of ρ_{af} is calculated by equating these transit times as given by Equation (10) for the light and heavy components:

$$\rho_{af} = \frac{2}{\frac{1}{\rho_{al}} + \frac{1}{\rho_{ah}}} \quad (A12)$$

and

$$1 - \frac{\rho_{af}}{\rho_{ah}} = \frac{\rho_{ah} - \rho_{al}}{\rho_{ah} + \rho_{al}} \quad (A13)$$

ρ_{al} - apparent density of the light component

ρ_{ah} - apparent density of the heavy component

It is apparent that in order to prevent interference, even interlocking, between the rising light component and the falling heavy component, the feed rate, Q , should be low enough, so that ϵ , as calculated from Equation (11) is much less than the solid fraction of loosely piled scrap.

The volume fraction of metal in loosely piled scrap may vary from as high as 0.60, for very compact, uniform material to perhaps 0.15 for regranulated metal turnings.

For the purposes of estimation it will be assumed that the maximum value of at which the interference is tolerable, is 0.01. For spherical scrap, this corresponds to an average interparticle distance of 2 sphere diameters. Using this value of ϵ in the combined equations (11) and (13) one obtains:

$$Q^* = 1.00 \sqrt{\frac{y}{(1 - \frac{\rho_{af}}{\rho_{as}}) g}} \quad (A14)$$

Q^* - volume of metal passing in one direction through separator per 100 cm² of horizontal cross-section.

For the separation of zinc from copper,

$$1 - \frac{\rho_{af}}{\rho_{as}} = 0.11$$

Using $y = 10 \text{ cm}$

$$\begin{aligned} Q^* &= 23.4 \text{ cm}^2/\text{sec} \\ &= 1650 \text{ lb/hr of copper} \\ &= 1320 \text{ lb/hr of zinc} \end{aligned}$$

When more than two components are present in the mixture to be separated equation (14) is still applicable to every component. If ρ_{af} is set to the value given by equation (12), intermediate between ρ_{ah} and ρ_{al} , then all components with a density greater than ρ_{ah} will sink more rapidly than component h, and all components with a density lower than ρ_{al} will float more rapidly than component l. Consequently, if the value of t corresponding to l is used in equation (11), the value of Q^* so calculated will be a conservative estimate of the capacity of the separator.

3. Scale-Up of Separator Length (Z)

In the previous analysis of separation rates it is assumed that the scrap pieces introduced through the "feed" plane ($Z = 0$) are distributed along the mid-plane of the separator volume up to $Z = L$ (Figure A-1). To achieve this distribution the scrap pieces must be introduced into the ferrofluid volume with a horizontal velocity component which is sufficiently high to overcome the viscous resistance encountered in reaching $Z = L$.

This velocity (V_o) can be calculated by solving Equation (1) under the following specialized conditions:

$$F_b = 0$$

At

$$t = 0; \quad Z = 0 \quad \frac{dZ}{dt} = V_o$$

$$\frac{dZ}{dt} = 0 \quad \text{when } Z = L$$

The resulting equation for V_o is:

$$V_o = \frac{18 \eta L}{d^2 \rho_s} \tag{A15}$$

For a ferrofluid having the following properties:

$$\eta = 0.05 \text{ poise}$$

$$\rho = 1.2 \text{ g/cm}^3$$

and for scrap pieces of density 2.7 (aluminum), larger than 5 mm, the minimum velocity is:

$$V_o = 1.33 L$$

In the present separator L is 20 cm, the required velocity is therefore 27 cm/sec or 52 feet per minute. For scrap of higher density, the velocity would be lower as predicted by Equation (15).

To construct a separator having twice the capacity of the present one, by doubling its length to 40 cm, the velocity of feed introduction would have to be correspondingly doubled to about 104 feet per minute. Such velocities can be routinely obtained by introducing the scrap by means of a horizontal conveyor or by sliding it down an inclined chute.

APPENDIX B
MAGNET DESIGN

1. Pole Piece Shape

The design of poles to yield a constant gradient field in the direction of gravity is based on a rectangular hyperboloid, shown in Figure B-1. The poles extend indefinitely in both the +Z and -Z directions.

The magnetic field between the poles and the mirror plate is given by:

$$\underline{H} = \Gamma x \hat{j} + \Gamma y \hat{i} \quad (B1)$$

Γ is the magnetic field gradient along the y axis. The y component of the magnetic field gradient is:

$$\frac{\partial H}{\partial y} = \frac{\Gamma}{\sqrt{1 + \left(\frac{x}{y}\right)^2}} \quad (B2)$$

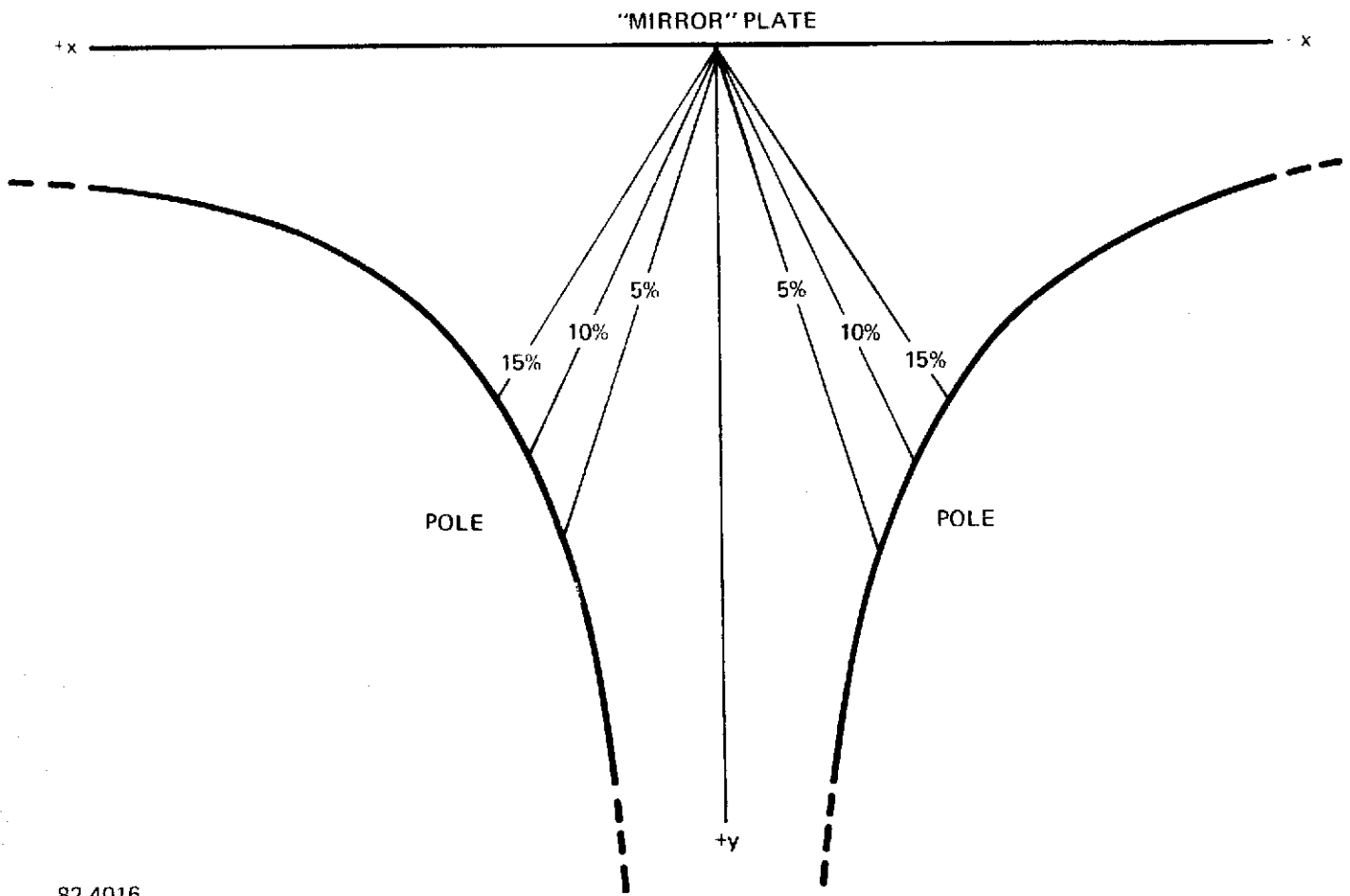
This gradient component has its maximum value, Γ , along the y axis. It has lesser, constant values along straight lines passing through the origin. Three sets of these straight lines along which the gradient is lower by 5%, 10% and 15% than its value along the y axis, are shown in Figure B-1.

The construction of a magnet based on infinitely large poles is of course impractical. A modified finite pole design which maintains the gradient accuracy of the ideal pole, within the sector bounded by the 10% accuracy lines has been developed by Avco. It is shown in Figures B-2 and B-3.

2. Motion of Objects Within the Working Volume

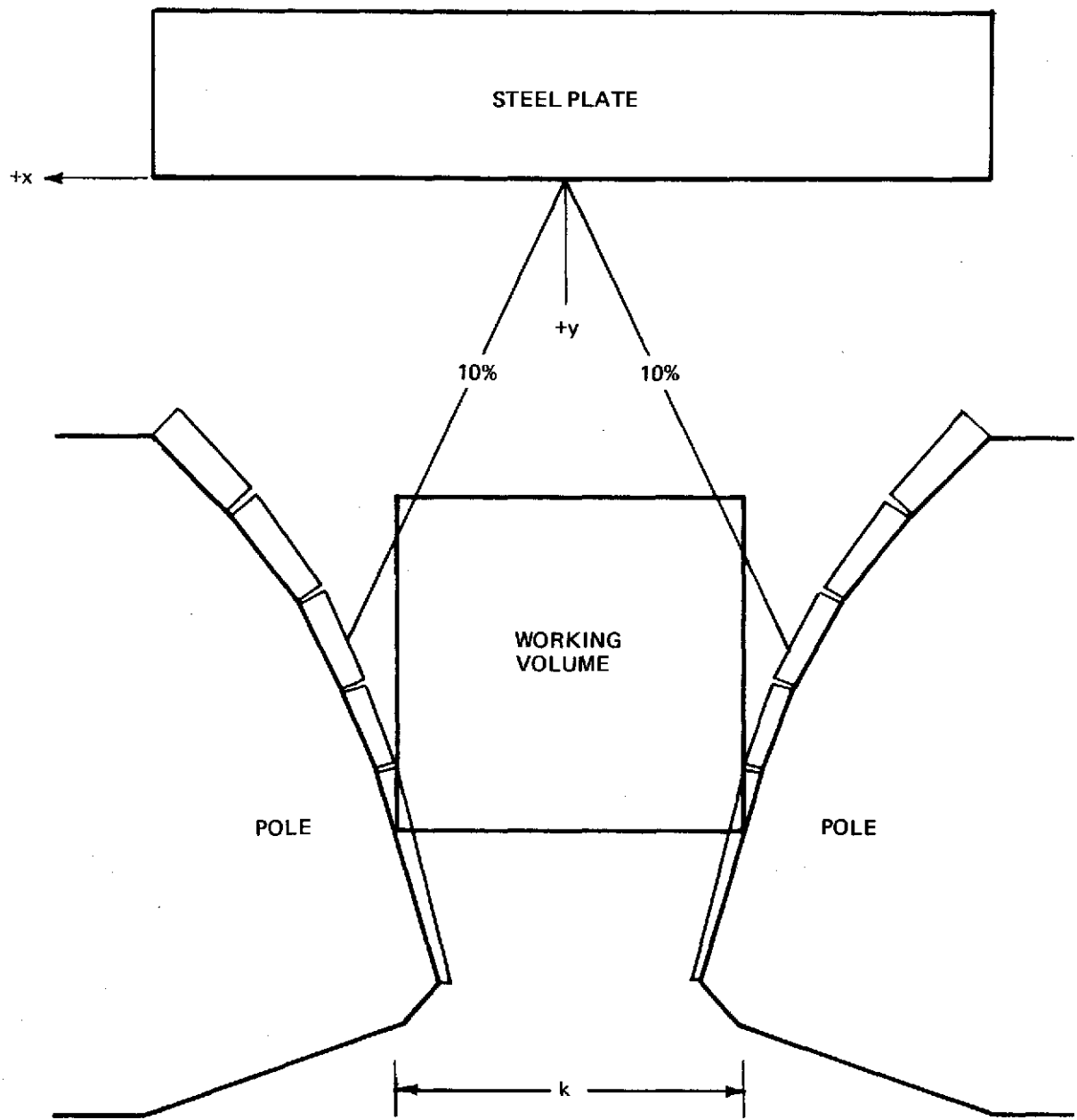
An object introduced into a ferrofluid pool within the working volume experiences both vertical and horizontal magnetic forces. The effect of the vertical magnetic forces, which determine whether an object sinks or floats has been discussed in Appendix A. The horizontal forces are produced by a magnetic field gradient pointing from the axis of the working volume toward the poles. The magnitude of this gradient is

$$\frac{\partial H}{\partial x} = \frac{\Gamma}{\sqrt{1 + \left(\frac{y}{x}\right)^2}} \quad (B3)$$



82-4016

Figure B-1 HYPERBOLIC POLES



82-4017

Figure B-2 CONSTANT GRADIENT POLES (FRONT VIEW)

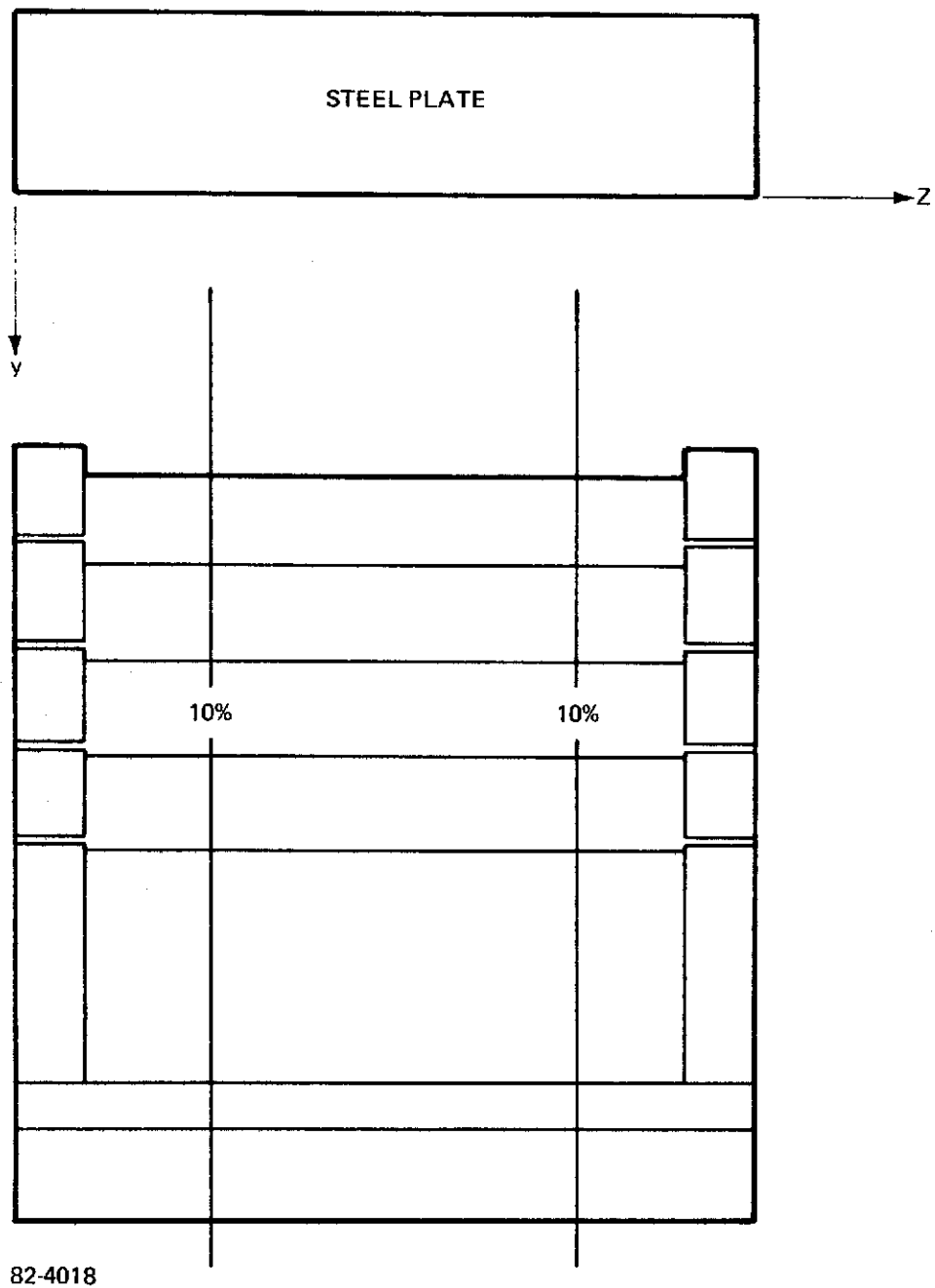


Figure B-3 CONSTANT GRADIENT POLE (SIDE VIEW)

These forces move non-magnetic objects from the periphery of the working volume (the poles) toward the axis. Equation (2) shows that the vertical gradient and consequently the ferrofluid's apparent density become more and more constant as the axis is approached. Therefore the movement of scrap toward the axis brings it into a region where high accuracy separation is possible. For example, it is possible to separate metals differing in density by considerably less than 10%, even though the vertical gradient at the upper corners of the working volume is about 10% lower than the vertical gradient on the axis.

3. Yoke and Coil Design

Since in auto scrap separation, very high magnetic fields are not required, a "C" yoke is adequate. A magnet design based on such a yoke is illustrated in Figures B-4 and B-5.

The approximate weight of steel required for this magnet is given by:

$$W_s = 2 \rho_{St} hz (g + 2h + 2l) \quad (B4)$$

ρ_{St} - density of steel

The weight of copper in both coils is given by:

$$W_c = 4 \rho_c \lambda \text{ tl} [z + 2t + h] \quad (B4a)$$

λ - volume fraction of coil occupied by copper, typically 0.45

ρ_c - density of copper

The power dissipated in both coils (8) is given by:

$$P = \rho_e J^2 V_c \quad (B5)$$

ρ_e - electrical resistivity of copper, 2×10^{-6}

J - current density in conductor

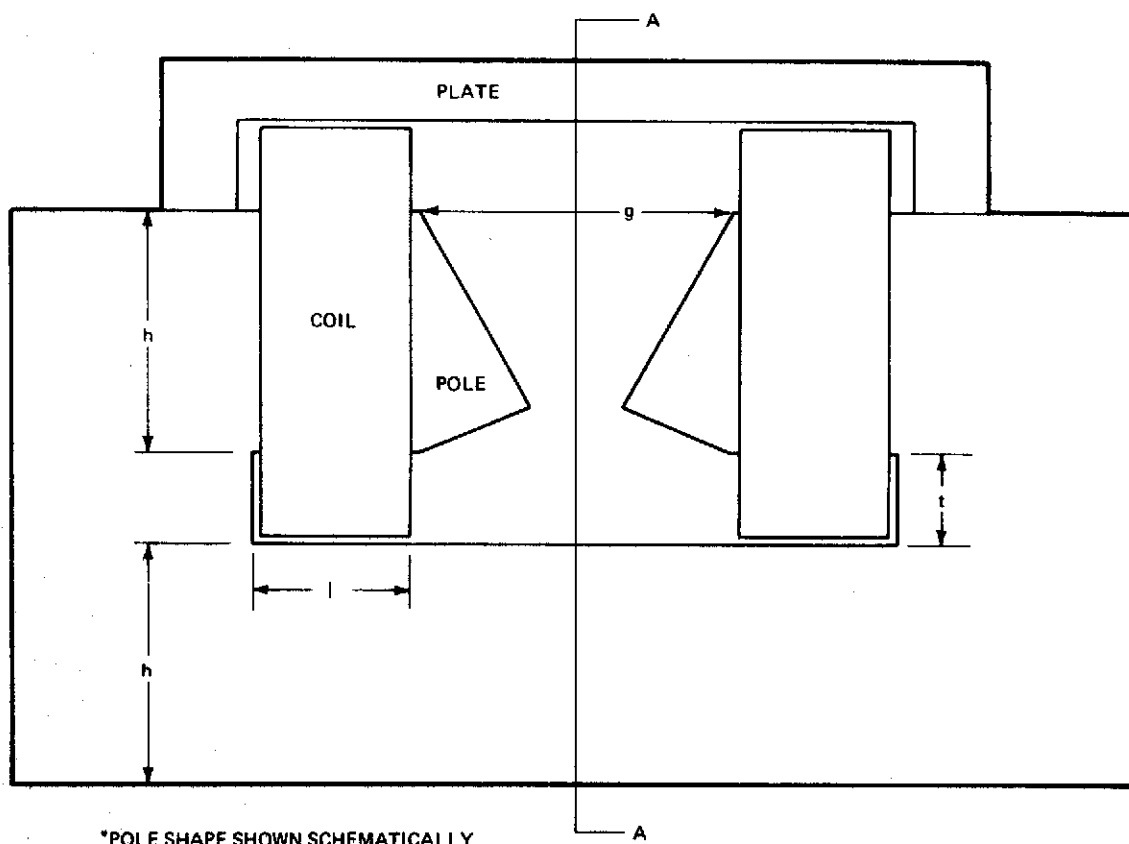
V_c - volume of copper

The current density is related to the number of ampere turns (NI) in both coils by:

$$J = \frac{NI}{\lambda 2 \text{ lt}} \quad (B6)$$

On combining equations (4), (5), and (6), one obtains;

$$P = \frac{\rho_e}{\lambda} (NI)^2 \frac{z + 2t + h}{\text{lt}} \quad (B7)$$



82-4019

Figure B-4 CONSTANT GRADIENT MAGNET (FRONT VIEW)

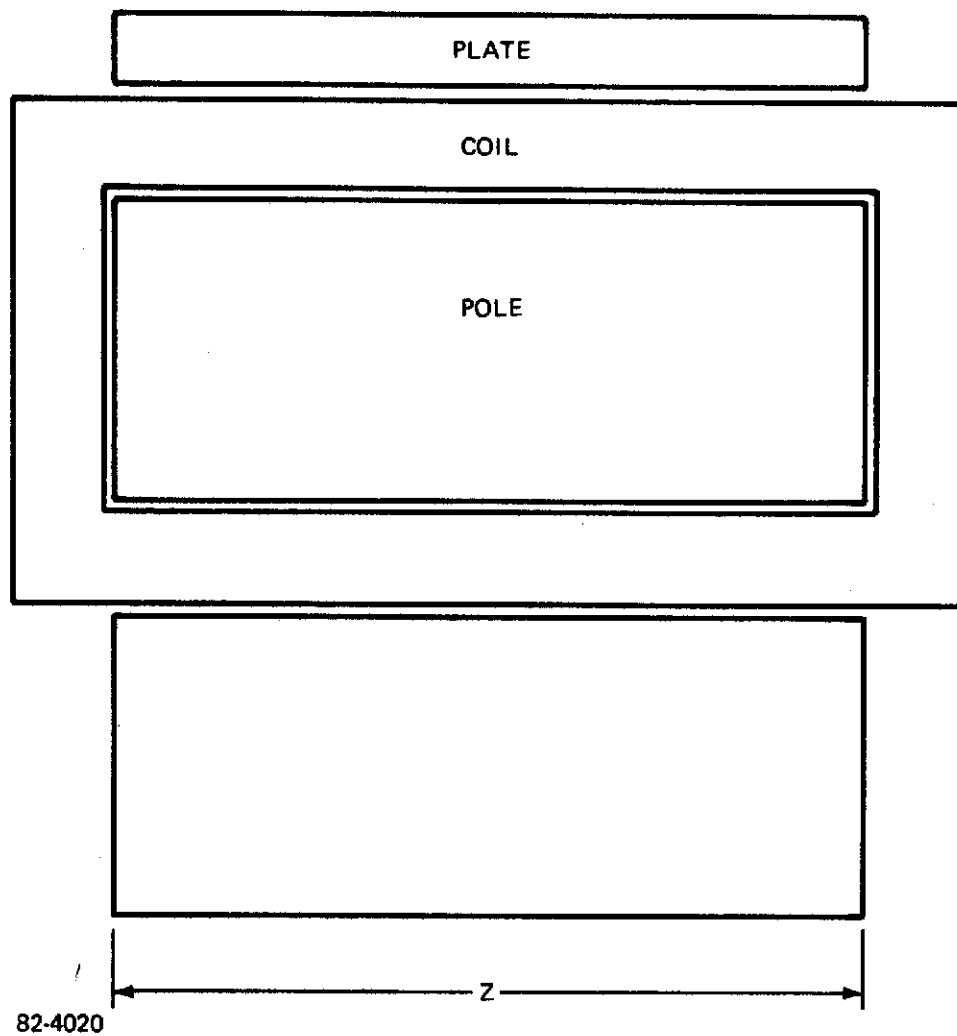


Figure B-5 CONSTANT GRADIENT MAGNET (SIDE VIEW ALONG SECTION A-A)

The number of ampere turns required to power the coils depends on the gradient desired, the shape of the pole pieces and the saturation of the yoke. For the pole pieces illustrated in Figure B-2, when the yoke is unsaturated the dependence is obtainable by the application of Ampere's Law, and, is approximately;

$$NI = \frac{\Gamma k^2}{0.2} \quad (B8)$$

k - width of working volume (Figure B-2)

For the present separator this relation holds up to about a gradient of 150 gauss per centimeter. Above this value the empirically determined relation between I and Γ is used (Figure 13).

4. Application to Specific Magnets

The present magnet and a magnet designed to accommodate a ferrofluid pool twice as long, are contrasted in Table B-1.

TABLE B-1
MAGNET CHARACTERISTICS
Physical Dimensions (Figures B-4 and B-5)

<u>Dimension</u>	<u>Present Inches</u>	<u>Magnet Centimeters</u>	<u>Proposed Inches</u>	<u>Magnet Centimeters</u>
g	21	53.3	21	53.3
Z	16	40.6	30	76.2
h	16	40.6	16	40.6
t	5	12.7	5	12.7
	10	25.4	10	25.4
Length (g + 2 + 2h)	73	185.0	73	185.0

<u>Weights</u>				
	<u>Pounds</u>	<u>Kilograms</u>	<u>Pounds</u>	<u>Kilograms</u>
Steel	10,500	4,760	19,700	8,950
Copper	1,340	610	1,800	820

The power requirements of the present magnet can be calculated from Equation (7) and the measured relation between current and gradient which was referred to above. These power requirements are plotted in Figure B-6. It is expected that the proposed larger magnet will start exhibiting saturation of the yoke at higher values of the current than the small magnet, because the large magnet has relatively less leakage flux. In order to obtain a conservative estimate of the electrical power requirements it will be assumed however, that the form of the Γ vs I curves for this magnet will be the same as for the small magnet. The power requirements of the large magnet are also shown in Figure B-6. This figure also shows a plot of the apparent density of the ferrofluid used in the course of this work, against the magnetic field gradient, which makes it possible to calculate the power requirements as a function of apparent density. This relation depends however on the ferrofluid used; other ferrofluids require a different curve.

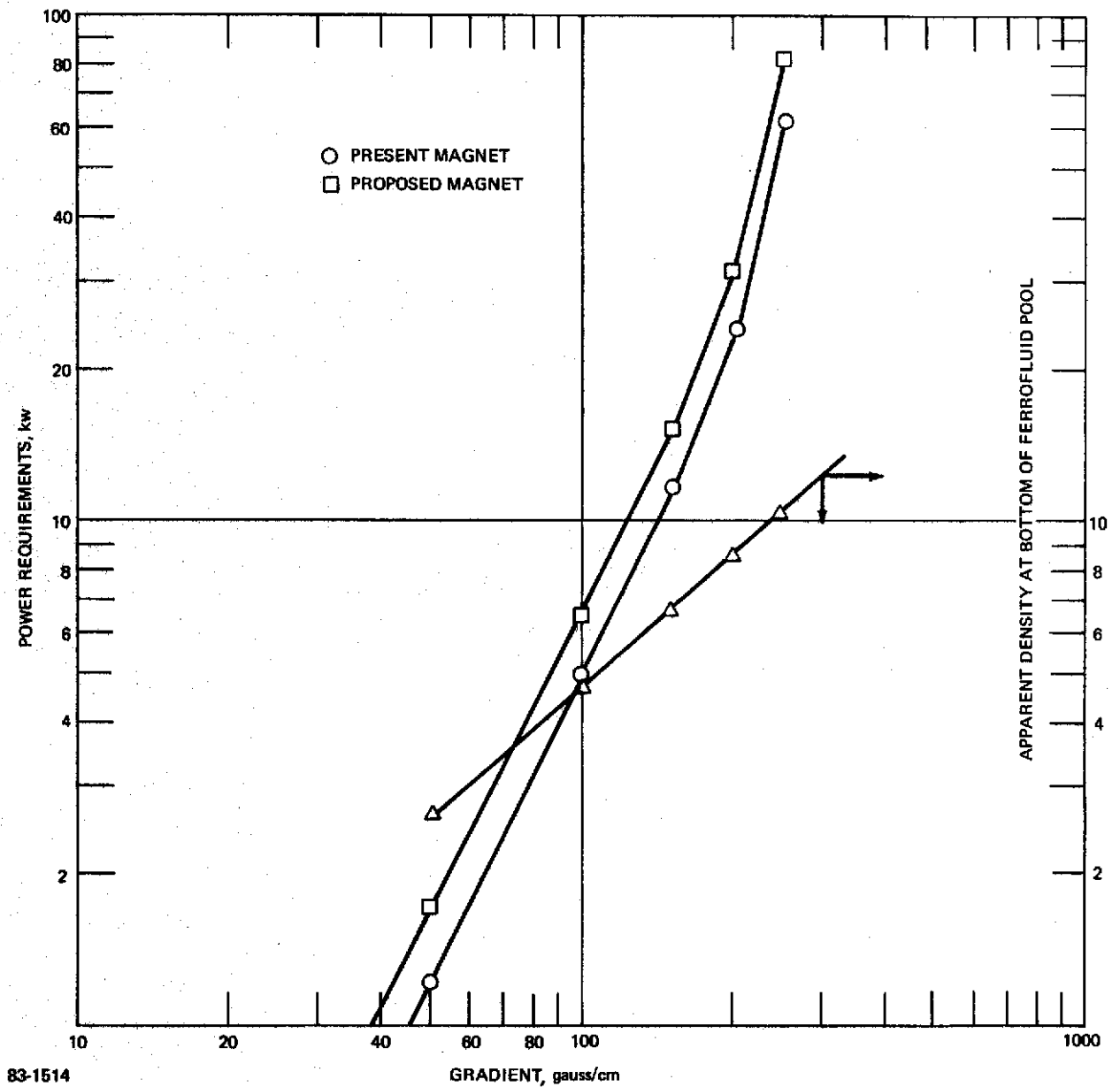


Figure B-6 POWER REQUIREMENTS OF MAGNETS

APPENDIX C
FACTORS FOR ESTIMATING PLANT CAPITAL COSTS

These factors are derived from K. M. Guthrie's article, "Capital Cost Estimating" in the March 24, 1969 issue of Chemical Engineering.

Symbols: F.O.B. Equipment Cost - E
Auxiliary Construction Materials - m
Construction Labor - L
Total Material (m&E) - M

The indirect cost factors in Guthrie's method must be corrected for the size of the project, the L/M ratio and mix of solid and liquid handling equipment. In making these estimates, it has been assumed that the cost of the plant will be less than \$1,000,000 and that it will be a predominantly solids handling type.

The total of the direct cost elements in Table C-I is 1.613E, and the total of the indirect cost elements in Table C-II is 0.619E. The total cost of a plant is therefore equal to the sum of these, or 2.232 times the F.O.B. cost of the major pieces of process equipment.

The cost of buildings to house a plant is not included in the above costs. In Guthrie's method it is calculated from the plant area, and a general classification of the type of plant it is. Table C-III shows these cost elements per square foot of plant, adjust to 1973 costs from Guthrie's 1968 cost base.

As a check on the general validity of applying this cost estimating method to scrap plants, a comparison was made of the ratio of certain cost elements as predicted by Guthrie to the same ratios as calculated by a much more detailed engineering study of solid waste recycling. This study of the cost of recycling valuable components from shredded municipal solid waste was undertaken by the National Center for Resource Recovery, Inc., and published as "Materials Recovery System - Engineering Feasibility Study" in December, 1972.

The comparison of critical cost ratios is shown in Table C-IV. The close agreement between the cost ratios gives credence to the validity of using Guthrie's cost estimating method for scrap processing plants.

TABLE C-I
DIRECT COST ELEMENTS

F.O.B. Equipment Cost (E)	1.000E
Construction Labor (L)	<u>0.343E</u>
Sub-Total	1.343E

Auxiliary Construction Materials:

Concrete	0.085E
Steel	0.005E
Piping	0.015E
Electricity and Instruments	0.160E
Paint	<u>0.005E</u>
Sub-Total (m)	0.270E

Total Direct Costs	1.613E
--------------------	--------

$$L/M = 0.267$$

TABLE C-II
INDIRECT COST ELEMENTS

Freight and Taxes	0.1020E
Construction Overheads	
Fringe Benefits	0.0306E
Labor Burden	0.0454E
Field Supervision	0.0368E
Temporary Facilities	0.0184E
Construction Equipment	0.0306E
Small Tools	0.0071E
Miscellaneous	<u>0.0366E</u>
Sub-Total	0.2060E
Engineering Costs	
Project Engineering	0.0236E
Process Engineering	0.0079E
Design and Drafting	0.0452E
Procurement	0.0049E
Home Office Construction	0.0029E
Office Indirects	<u>0.0865E</u>
Sub-Total	0.1710E
Engineering Fee	<u>0.1400E</u>
Total Indirect Costs	0.6190E

TABLE C-III
PLANT BUILDING COSTS

<u>Element</u>	<u>Cost (\$/ft²)</u>
<u>Direct Costs</u>	
Building Shell	\$ 5.01
Lights	2.15
Heating and Ventilation	1.84
Plumbing	2.09
Fire Prevention	<u>1.35</u>
Sub-Total	\$12.44
<u>Indirect Costs</u>	<u>\$ 3.73</u>
Total	\$16.17

TABLE C-IV

COMPARISON OF COST RATIOS DERIVED BY TWO COST ESTIMATING METHODS

<u>Cost Ratio</u>	<u>Guthrie Method</u>	<u>NCRR Study</u>
m/E	0.270	0.230
L/E	0.343	0.341
<u>Engineering</u>		
M + L	0.109	0.100
<u>Contractor Overhead</u>		
M + L	0.178	0.196